DISSERTATION

SILICA BIOGEOCHEMISTRY ACROSS A GRASSLAND CLIMOSEQUENCE

Submitted by

Steve W. Blecker

Soil and Crop Sciences

In partial fulfillment of the requirements

for the Degree of Doctor of Philosophy

Colorado State University

Fort Collins, Colorado

Fall 2005

COLORADO STATE UNIVERSITY

July 8, 2005

WE HEREBY RECOMMEND THAT THE DISSERTATION PREPARED UNDER OUR SUPERVISION BY STEVE W. BLECKER ENTITLED SILICA BIOGEOCHEMISTRY ACROSS A GRASSLAND CLIMOSEQUENCE BE ACCEPTED AS FULFILLING IN PART REQUIREMENTS FOR THE DEGREE OF DOCTOR OF PHILOSOPHY.

Committee on Graduate Work

Advisor

Department Head

ABSTRACT OF DISSERTATION

SILICA BIOGEOCHEMISTRY ACROSS A GRASSLAND CLIMOSEQUENCE

The importance of primary mineral dissolution and formation of secondary minerals has been recognized as an important control on silica concentrations and fluxes in soil solutions and stream waters. Such reactions are important in understanding such earth surface processes as soil development, soil buffering against acid deposition and regulation of atmospheric carbon dioxide. Links between terrestrial and marine systems are also important in terms of Si, where Si-based diatoms play a large role in marine primary productivity. Assessments of the controls on silica export from the terrestrial environment tend to ignore the role of plant silica cycling and biogenic silica storage in soils and vegetation, assuming that mineral weathering reactions alone controls this flux. Most weathering studies have occurred in forested ecosystems; though weathering in grasslands is typically less intense, they cover up to 40% of the earth's land surface and may play an important role in global Si biogeochemistry.

To this end, I employed a mass balance study of Si pools and fluxes along a grassland climosequence in the Central Great Plains. In general, shortgrass systems tend to have greater pools of soil biogenic Si than tallgrass systems though the plants in shortgrass systems add less Si to the soil annually. Though biologically mediated Si accounts for only a few percent of the total Si in these systems, I believe that this Si is far

more labile than mineral Si. Although these grassland systems are less weathered than temperate and tropical forests, biological Si cycling appears to impact mineral weathering to a greater extent as compared to forested systems.

To date, the biological fractionation of Ge during plant Si uptake has been deduced from studies of plants in situ, where isolation of source Si is difficult at best. I provide more solid evidence regarding the magnitude and direction of biologic Ge fractionation through a controlled greenhouse study, where source Ge/Si values are more easily isolated. Fractionation differences among grassland species were similar, with those species grown in a nutrient solution fractionating against Ge by roughly 82%, and those grown in different soil mediums fractionating against Ge by approximately 53%. However, the differences between these two groups (nutrient solution vs. soil grown vegetation) and differences between leaf and stem Ge/Si values point to potentially different uptake mechanisms in Ge compared to Si. Biologic Ge fractionation could be the result of differences in reactivity and speciation, as well as Ge toxicity and kinetically driven fractionation resulting from differences in molecular weight between Ge and Si.

As Ge behaves as a pseudo isotope of Si, differences in Ge/Si ratios among major pools in terrestrial systems allows for the potential use of Ge/Si as a tracer of silicate weathering and Si flux in these systems, and can provide a valuable tool for studying weathering processes and Si cycling in terrestrial and marine systems. Trends of Ge sequestration in secondary minerals, and depletion in both biologic and aquatic pools were similar in direction to those of tropical systems but less in terms of magnitude. Overlap in Ge/Si ratios among the pools examined (plant, soil, stream) in the less

intensely weathered grassland ecosystems confounds the utility of this particular isotopic tool in elucidating weathering relationships.

This initial extensive look at grassland Si biogeochemistry provides promise in studying fluxes of terrestrial Si, though a combination of more intensive catchment scale studies and/or additional tools to Si mass balance and Ge/Si ratios will be necessary to clarify the complexities associated mineral weathering and the Si biogeochemistry in terrestrial systems.

Steve Blecker
Soil and Crop Sciences Department
Colorado State University
Fort Collins, CO 80523
Fall 2005

ACKNOWLEDGEMENTS

So many people were instrumental in making this project happen, it's hard to know where to start. I thank the LTER program for the funding behind this research and specifically the SGS and KONZA sites for the access, The Nature Conservancy of Colorado, Kansas and Missouri for allowing me to sample in some of the last tracts of remnant prairies in the Great Plains, and Rebecca McCulley for putting me in touch with right people to gain access to those sites. I appreciate the suggestions by committee members Oliver Chadwick and Sally Sutton for helping me 'think outside the box' in terms of Ge geochemistry. Thanks also to Wendy Harrison and Sally Sutton for help with XRD analysis. The Ge geochemistry would not have happened but for the long hours put in by Stagg King at Cornell, and special thanks to Lou Derry for the insights and conversation. Thanks to Cherie, Jorin, Carol, and all those other students who've passed through NREL over the years, making this a great place to work. April Shelhon and Allie Grow were a great help in the lab and the greenhouse. Dan, I really appreciate your expertise in the lab and patience with my many forays to the field. Caroline, your support for this work and being there for all the other projects over the years has been great to say the least, thank you. Mom, Dad it was and always is comforting to know you're there to support me through thick and thin. Colleen thanks for your friendship and your help with the field sampling. Pat thanks for your inspiration. Laura and Iris, you

were there back when this whole thing started almost 10 years ago (ok it was a different project) but still, I haven't forgotten your support and encouragement, nor will I ever, thank you. Gene, your inexhaustible enthusiasm, expertise, and guidance will always be immensely appreciated. Thanks for introducing me to silica; I look forward to future collaboration. Jim, first off thanks for running SEM-EDS on those samples, every bit of data helps (especially if I can pawn off the work on someone else). But far more important to me through this whole process though has been your friendship, you da man. Lisa, I'm not sure how you managed to put up with me through all of this; I'm pretty sure this was harder on you than me. Your persistence, support and love were of great comfort and support.

TABLE OF CONTENTS

Chapter I: INTRODUCTION

Background

Impetus for this research was fueled by decades of laboratory and field studies designed to further our understanding of the influence of plants on soil formation and the critical plant and soil interactions that mitigate biogeochemical functioning of terrestrial ecosystems. Study of plant-soil interactions and their impact on mineral weathering has taken on many forms, details of which are provided in extensive reviews (e.g. Drever 1994 and Kelly et al. 1998). Plants impact mineral weathering through a number of biogeochemical processes, such as the production of weathering agents (e.g. CO_2, organic acids, and ligands; Berner 1992), cation biocycling (Johnson-Maynard et al. 2005), production of biogenic minerals (Kelly et al. 1998), and physical processes that increase soil stability and soil-water residence time. The significance of these interactions has been debated for decades, with numerous studies providing evidence that plants increase weathering rates by varying orders of magnitude (e.g. Lovering 1959, Drever 1994, Brady et al. 1999, Moulton et al. 2000, Hilsinger et al. 2001, Wilson 2004). Studies across larger temporal and spatial scales have examined the influence of plant-soil interactions on such areas as long-term regulation of atmospheric CO_2 (e.g. Berner 1992, Chadwick et al. 1994), and the relationship between atmospheric CO_2 and marine net primary productivity or NPP (Mortlock et al. 1991, Froelich et al. 1992).

One of the focal points of these interactions involves the terrestrially ubiquitous compound silica (SiO_2). The importance of primary mineral dissolution and buffering provided by secondary mineral formation has long been recognized as a key control of silica concentrations and flux in soil solutions and stream waters (e.g. Drever and Zobrist 1992, Likens and Bormann 1995, Swistock et al. 1997, White et al. 1998, Gaillardet et al. 1999). The influence of watershed-scale impacts by plants on mineral weathering is occasionally hinted at (e.g. Taylor and Velbel 1991, Schulz and White 1999, Schmitt et al. 2003), or in some instances focused on in studies of plant uptake and cycling on silica activity and mineral stability (Bartoli 1983, Lucas et al. 1993, Alexandre et al. 1997, Markewitz and Richter 1998, Meunier et al. 1999), but typically not included in complete mass balance studies. In addition, the aforementioned catchment-scale weathering studies are typically conducted in forested ecosystems, while contributions of less intensely weathered ecosystems remain largely unknown.

With these points in mind, another driving force that helped shape the experimental design of my study was brought out by Kelly et al. (1998), who discussed current knowledge and gaps in the research of soil and plant interactions: lack of studies in climatically diverse settings; reliable means of linking nutrient content of biological components to nutrient provenance; quantitative understanding between vegetation and hydrologic cycles; and lack of information regarding the relationship between NPP, internal nutrient cycling and soil mineral weathering therein.

The Great Plains of North America is an ideal system for assessing the biogeochemical behavior of grassland ecosystems. These ecosystems are graminoid-dominated with woody species rare, sub-dominant or co-dominant. Moreover fire, large grazers and climatic extremes (droughts) were important to their evolution, and remain key drivers of ecological patterns and processes across precipitation and productivity gradients. Grasslands of North America are relatively young ecosystems, first arising 5-7 million years ago, with many of the present vegetation associations arising less than 10,000 yrs ago (Wright 1970; Stebbins 1981; Axelrod 1985; Coughenour 1985).

Given this backdrop, I became interested in the relationship between soils and plants within grassland ecosystems and the relative importance of grasslands to the global biogeochemical silica cycle. I decided to conduct a detailed study of the biogeochemistry of Si in different grassland ecosystems distributed across a Great Plains climosequence (Jenny 1941) that spanned a moisture gradient from the semi-arid shortgrass steppe of eastern Colorado to the humid remnant tallgrass prairie of western Missouri. Relatively level landscape positions sustaining 10 to 30 ky soils formed in sedimentary residuum and loess comprised the field setting for this study.

Research objectives and hypotheses

Using a state factor approach (Jenny 1941), a combination of geochemical, mineralogical and mass balance techniques were applied to examine the 1) biogeochemistry of Si in grassland ecosystems, 2) the impact of plants on mineral weathering, and 3) associated linkages between less intensely weathered terrestrial and aquatic systems on a catchment-

level scale. Sampling and characterization of the major ecosystem pools (soil, vegetation, stream water), were carried out to study potential variations that weathering intensity and above ground net primary productivity (ANPP) have on Si biogeochemistry in grassland ecosystems and how grassland data compare to the accumulated data from temperate and tropical forests.

To meet the objectives of this work I generated the following questions to guide my research:

1) What are the quantities of biogenic Si stored in both the annual biomass and soils within and among grassland ecosystems as a function of climate and grassland type?

2) What is the chemical behavior of biogenic Si in the soil matrix with regard to solubility and weatherability in each grassland system?

3) Does experimental evidence support results derived from the field evidence with regards to the biologic fractionation of Ge versus Si?

4) Does the biogenic Si in grassland plants carry a unique Ge/Si fingerprint as a function of climate and biotic community?

Work in temperate and tropical ecosystems by Bartoli (1983), Lucas et al. (1993), Alexandre et al. (1997), and Meunier et al. (1999) have emphasized the role of plants in the biogeochemical Si cycle through intriguing, yet incomplete, Si mass balance studies. Measurement of plant uptake, storage and return of Si to the soil were conducted in varying levels of completeness, but have generally not encompassed the totality of Si pools and fluxes in a given system. I set out to employ a more complete mass balance analysis in a relatively unstudied ecosystem to compare how the biogenic cycling of Si varies within a grassland climosequence as well as between grassland and forest

ecosystems. To this end, I measured (**bold**) or estimated (*italic*) the biogeochemical Si pools and fluxes as depicted in Figure 1.1.

The following hypotheses will be tested in Chapter 2 of this dissertation, addressing questions 1 and 2.

H1: Grassland ecosystems mobilize and store higher proportions of biogenic silica per unit biomass than forested ecosystems.

H2: The rates of biogeochemical cycling of biogenic silica in temperate grassland ecosystems are controlled, in part, by the impacts of precipitation and Annual Net Primary Production.

A host of studies have related the importance of Si to plant structure, function, growth and development (e.g. Raven 1983, Sangster et al. 2001). Examining Ge and Si uptake by grasses in the controlled conditions afforded by a greenhouse, where an individual Si source can be isolated (in terms of its Ge/Si signature), I set out to take a more definitive look at the magnitude and direction of biologic Ge fractionation and compare that data to what has thus far been inferred in field studies (Derry et al. 2005; Chapter 4). Such information should increase the utility of Ge/Si ratios as a tool in the study of terrestrial weathering and biogeochemical Si cycling.

The following hypothesis will be tested in Chapter 3 of this dissertation, addressing question 3.

H3: Plants fractionate against Ge compared to Si during monogermanic/silicic acid uptake.

The few weathering studies employing Ge/Si ratios in terrestrial systems (Murnane and Stallard 1990, Froelich et al. 1992, Filippelli 2000, Kurtz et al. 2002, Derry et al. 2005) have been carried out in tropical and temperate forested systems, and show promise for understanding mineral weathering processes and Si fluxes. Applying this tool in other ecosystems will test the versatility and utility of Ge/Si ratios in less intensely weathered systems. To this end, I measured Ge/Si ratios for the pools (soil, plant, water) sampled in Chapter 2 as an attempt at further quantifying biogeochemical Si cycling and weathering in grassland systems.

The following hypothesis will be tested in Chapter 4 of this dissertation, addressing question 4.

H4: The export of dissolved silica from grasslands in streams (and ultimately to the oceans) is proximally controlled by the dynamics of biogenic silica rather than mineral weathering reactions.

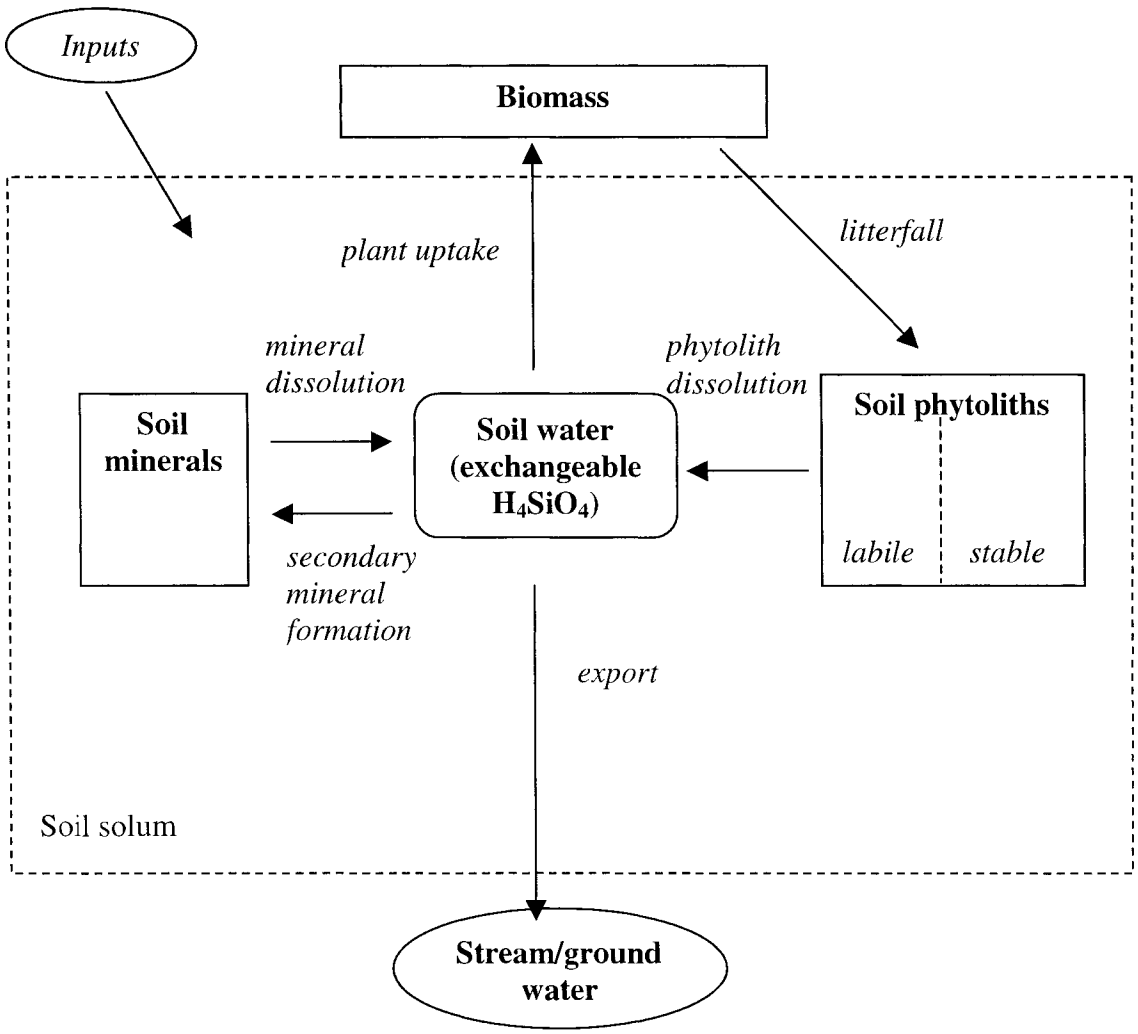

Figure 1.1 Conceptual model of the terrestrial Si biogeochemical cycle. (**bold** = measured, *italic* = estimated).

References

Alexandre A., Meunier J.D., Colin F., and Koud J.M. 1997. Plant impact on the biogeochemical cycle of silicon and related weathering processes. Geochim. Cosmochim. Acta 61:677-682.

Axelrod D.I. 1985. Rise of the grassland biome, Central North America. Botanical Review 51:163.201.

Bartoli F. 1983. The biogechemical cycle of silica in two temperate forest ecosystems. Environ. Biogeochem. Ecol. Bull. 35:469-476.

Berner R.A. 1992. Weathering. Plants and the long term carbon cycle. Geochim. Cosmochim. Acta 56:3225-3231.

Brady P.V., Dorn R.I., Brazel A.J., Clark J., Moore R.B., and Glidewell T. 1999. Direct measurement of the combined effects of lichen, rainfall, and temperature on silicate weathering. Geochim. Cosmochim. Acta 63:3293-3300.

Chadwick O.A., Kelly E.F., Merritts D.M., and Amundson R.G. 1994. Carbon dioxide consumption during soil development. Biogeochemistry 24:115-127.

Coughenour M.B. 1985. Graminoid responses to grazing by large herbivores – Adaptations, exaptations, and interacting processes. Annals of the Missouri Botanical Garden 72:852-863.

Derry L.A, Kurtz A.C., Ziegler K. and Chadwick, O.A. 2005. Biological control of terrestrial silica cycling and export fluxes to watersheds. Nature 433:728-730.

Drever J.I. 1994. Effect of plants on chemical weathering rates. Geochim. Cosmochim. Acta 58:2325-2332.

Drever J.I. and Zobrist J. 1992. Chemical weathering of silicate rocks as a function of elevation in the southern Swiss Alps. Geochim. Cosmochim. Acta 56:3209-3216.

Filippelli G.M., Carnahan J.W., Derry D.A., and Kurtz A. 2000. Terrestrial paleorecords of Ge/Si cycling derived from lake diatoms. Chemical Geology 168:9-26.

Froelich P.N., Blanc V., Mortlock R.A., Chillrud S.N., Dunstan W., Udomkit A., and Peng T.H. 1992. River fluxes of dissolved silica to the ocean were higher during glacials: Ge/Si in diatoms, rivers and oceans. Paleoceanography 7:739-767.

Gaillardet J., Dupre B., Louvat P., Allegre C.J. 1999. Global silicate weathering and CO_2 consumption rates deduced from the chemistry of large rivers. Chemical Geology 159:3-30.

Hilsinger P., Barros O.N.F., Benedeti M.F., Noack Y., and Callot G. 2001. Plant-induced weathering of a basaltic rock: Experimental evidence. Geochim. Cosmochim. Acta 65:137-152.

Jenny, H. 1941. Factors of soil formation; a system of quantitative pedology. McGraw-Hill, New York. 281p.

Johnson-Maynard J.L., Graham R.C., Shouse P.J., and Quideau S.A. 2005. Base cation and silicon biogeochemistry under pine and scrub oak monocultures: implications for weathering rates. Geoderma 126:353-365.

Kelly E.F., Chadwick O.A., and Hilinski T.E. 1998. The effect of plants on mineral weathering. Biogeochemistry 42:21-53.

Kurtz A.C., Derry L.A., and Chadwick, O.A. 2002. Germanium-silicon fractionation in the weathering environment. Geochim. Cosmochim. Acta 66:1525-1537.

Likens G.E. and Bormann F.H. 1995. Biogeochemistry of a forested ecosystem. Springer-Verlag, New York. 159 p.

Lovering T.S. 1959. Significance of accumulator plants in rock weathering. Bull. Geol. Soc. Am. 70:781-800.

Lucas Y., Luizao F.J., Chauvel A., Rouiller J., and Nahon D. 1993. The relationship between the biological activity of the rain forest and the mineral composition of the soils. Science 260:521-523.

Markewitz D. and Richter D.D. 1998. The *bio* in aluminum and silicon geochemistry. Biogeochemistry 42:235-252.

Meunier J.D., Colin F., and Alarcon C. 1999. Biogenic silica storage in soils. Geology 27:835-838.

Moulton K.L., West J., and Berner R.A. 2000. Solute Flux and mineral mass balance approaches to the quantification of plant effects on silicate weathering. Amer. J. of Sci. 300:539-570.

Mortlock R.A., Charles C.D., Froelich P.N., Zibello M.A., Saltzman J., Hays J.D., and Burckle L.H. 1991. Evidence of lower productivity in the Antarctic Ocean during the last glaciation. Nature 351:220-223.

Murnane R.J. and Stallard R.F. 1990. Germanium and silicon in rivers of the Orinoco drainage basin. Nature 344:749-752

Raven J.A. 1983. The transport and function of silicon in plants. Biol. Rev. 58:179-207.

Sangster A.G, Hodson M.J., and Tubb H.J. 2001. Silicon deposition in higher plants. *In* Datnoff L.E., Snyder G.H, and Korndorfer G.H. (eds.) Silicon in Agriculture. Elsevier, New York. p. 85-114.

Schmitt A.D., Chabauz F., and Stille P. 2003. The calcium riverine and hydrothermal isotopic fluxes and the oceanic calcium mass balance. Earth and Planetary Sci. Letters 213:503-518.

Schulz M.S. and White A.F. 1999. Chemical weathering in a tropical watershed, Luquillo Mountains, Puerto Rico III: Quartz dissolution rates. Geochim. Cosmochim. Acta 63:337-350.

Stebbins G.L. 1981. Coevolution of grasses and herbivores. Annals of the Missouri Botanical Garden. 68:75-86.

Swistock B.R., Edwards P.J., Wood F. and DeWalle D.R. 1997. Comparison of methods for calculating annual solute exports from six forested Appalachian watersheds. Hydrological Processes 11:655-669.

Taylor A.B. and Velbel M.A. 1991. Geochemical mass balances and weathering rates in forested watersheds of the southern Blue Ridge. 2. Effects of botanical uptake terms. Geoderma 51:29-50.

White A.F., Blum A.E., Schulz M.S., Vivit D.V., Stonestrom D.A., Larsen M., Murphy S.F., and Ebrel D. 1998. Chemical weathering in a tropical watershed, Luquillo Mountains, Puerto Rico: I. Long-term versus short-term weathering fluxes. Geochim. Cosmochim. Acta 62:209-226.

Wilson M.J. 2004. Weathering of the primary rock-forming minerals: processes, products and rates. Clay Minerals 39:233-266

Wright H.E. 1970. Vegetational history of the central plains. *In* W. Dort, and J.K. Jones (eds). Pleistocene and recent environments of the Central Great Plains. University of Kansas Press. Lawrence, KS. p. 157-172.

CHAPTER II: SILICA BIOGEOCHEMISTRY ACROSS A GRASSLAND CLIMOSEQUENCE

Introduction

Silicon is the most abundant element in the earth's crust after oxygen, plays a key role in earth surface processes, and is an important nutrient and structural component of marine and terrestrial organisms. Understanding the fate and mobility of SiO_2 (silica) in terrestrial systems is critical to understanding soil development (Kelly et al. 1998), buffering capacity against acidic deposition (Drever 1994), and long-term regulation of atmospheric carbon dioxide (Berner 1992, Chadwick et al. 1994). The importance of primary mineral dissolution and formation of secondary minerals has been recognized as a primary control on silica concentrations and fluxes in soil solutions and stream waters (White and Blum 1995, Gaillardet et al. 1999). Most assessments of the controls on silica export from the terrestrial environment have largely ignored the role of biogenic silica stored in soils and vegetation, assuming that mineral weathering reactions alone control this flux (e.g. Berner 1995, White et al. 1998). However, several pivotal papers have stressed the importance of plant uptake and cycling on silica activity and mineral stability in soils subjected to high amounts of chemical weathering (Lucas et al. 1993, Alexandre et al. 1997, Markewitz and Richter 1998, Meunier et al. 1999).

Plants extract silica from the soil as monosilicic acid, transport it via the transpiration stream, and transform the soluble silica into opal that is stored in cell walls, cell luminas, and intercellular spaces near evaporating surfaces (Jones and Handreck 1967, Raven 1983, Sangster and Hodson 1992, Epstein 1999). These structural features form amorphous silica bodies known as phytoliths, which have unique morphological features that can be diagnostic of plant species (Piperno 1988). Phytoliths are present in most plants, ranging in concentration from 0.5% or less in most dicotyledons, 1-3% in typical dryland grasses, and up to 10-15% in some wetland plant species. Species within the latter two groups often actively transpire Si against the concentration gradient (Epstein 1994). This plant, or biogenic silica, is cycled back into the soil upon death and decomposition of the plants. Phytolith abundance and distribution in the soil is regulated by the balance between plant production and the degree of chemical weathering (Alexandre et al. 1997), soil mineralogy (Dahlgren et al. 1993), and bioclimatic conditions (Kelly et al. 1993). Phytolith stability in the soil environment plays a key role on the impact that biogenic Si has on the overall terrestrial Si cycle. In terms of solubility, phytoliths are generally grouped with amorphous silica ($10^{-2.74}$), a solubility product intermediate to silica glass ($10^{-2.71}$), and quartz ($10^{-4.00}$; Lindsay 1979).

Growing evidence exists suggesting that plants play a major role in controlling silica storage in, and export from, terrestrial environments. Both the literature and current understanding of silica production and cycling focus primarily on forested ecosystems. Lucas et al. (1993) reported that silica inputs from vegetation in a Congo rainforest study was 4 times greater than the silica that was leached from the system. This process has

maintained a soil mineralogical profile that is more siliceous (kaolinitic) in the upper horizons compared to more aluminous (gibbsitic) lower horizons, which contrasts with expected geochemical model predictions. In another tropical forest setting, Alexandre et al. (1997) calculated that the relatively small pool of more soluble biogenic silica (phytoliths) released twice the silica to the soil compared to the much higher pool of less soluble mineral silicates. Meunier et al. (1999) notes that a significant portion of silica dissolved from parent rock can be stored in the soil as phytoliths, thus slowing the transfer of silica from soils to surface and ground waters. Therefore, quartz and silicate mineral dissolution do not always control dissolved silica concentrations of surficial waters in systems with high rates of biologic silica turnover. In temperate forest systems, where biogenic silica turnover can be much lower than the tropics, Markewitz and Richter (1998) demonstrated that the greater biogenic silica sink could increase silica released by silicate mineral weathering by upwards of 82%. They also point out that omission of biotic uptake and accumulation can create up to 4 fold errors in estimates of mineral weathering rates. Bartoli (1983) concluded that biogenic Si cycling is an important control on mineral weathering in deciduous forest systems, where 85% of soluble silica was derived from biogenic silica, compared to only 15% in coniferous forest systems.

These studies in forest ecosystems have illustrated that omitting the biological cycling of Si in mass balance weathering studies can critically underestimate the role of vegetation on mineral weathering. Conley's (2002) review of global Si biogeochemistry highlights the need for greater understanding of terrestrial Si, particularly in grassland ecosystems,

where biogeochemical data is lacking. Grassland phytoliths and their paleoenvironmental significance have been studied for decades (e.g. Wilding and Drees 1971, Kelly et al. 1993, Blinnikov et al. 2002), but their role in the overall terrestrial biogeochemical Si cycle has not been quantified. If grassland ecosystems are a particularly large and active reservoir of biogenic silica, the global expansion of grasslands during the late Neogene (Axelrod 1985, Stromberg 2004) could have had important consequences for both marine and terrestrial Si cycles, and perhaps the global carbon cycle. Despite the potential significance of grasslands for the global silica (and carbon) cycle, the biogeochemical behavior and residence time of biogenic Si in terrestrial grassland ecosystems is largely unknown.

The objectives of this chapter are fourfold: First, to determine the quantities of biogenic Si stored in the annual biomass within and among temperate grassland ecosystems as a function of climate and grassland type; second, to determine the quantities and distribution of biogenic Si within and among soils of temperate grassland ecosystems; third, to determine the range in biogeochemical behavior (turnover) of biogenic Si in the soils formed under grassland vegetation; fourth, to estimate the potential significance of grasslands in mobilizing silica from terrestrial ecosystems.

Methods

Study Area/Sampling Design

A climosequence (Jenny 1941) spanning a precipitation gradient of approximately 350 - 1100 mm (Table 2.1) in the Central Great Plains was sampled in order to utilize estimates of annual net primary production (ANPP) data measured by McCulley and Burke (2004). The climosequence was extended into western Missouri and additional sites within the sequence were sampled in order to further examine variability of Si cycling in grassland ecosystems. Figure 2.1 provides a site location diagram with major grasslands types, and study site abbreviations. Table 2.1 provides a description of basic site characteristics including vegetation, soil, and ownership. Appendix I provides more detailed soils descriptions for the pedons sampled across the climosequence.

To minimize the influence of slope and aspect across the sampling gradient, relatively flat upland sites were selected; two in shortgrass (SGS and ARIK), three in mixedgrass (SV, HAYS and WILSON) and two in tallgrass (KONZA and WKT) communities. Two pedons were sampled at the Shortgrass Steppe LTER in order to examine smaller scale spatial variability (SGS-A and SGS-B). SGS-A is located approximately 1 km from SGS-B, the former having a greater fluvial component (Blecker et al. 1997). Soils are derived from residual sedimentary rock and loess (Mason et al. 2003; Roberts et al. 2003) and range from drier (Aridic Argiustoll) to wetter (Typic Hapludoll) Mollisols across the gradient. Given the geomorphic history along the gradient and radiocarbon dates I have estimated soil age at 10-30 ky (Blecker et al. 1997; Oviatt 1998). Land use was held

constant (moderate grazing) and plant communities varied with mean annual precipitation (MAP). In terms of plant species, blue grama (*Bouteloua gracilis*) and buffalograss (*Buchloe dactyloides*) dominate the shortgrass sites (SGS-A, SGS-B, ARIK), *Bouteloua gracilis, Buchloe dactyloides,* fescue (*Festuca sp.*) the drier mixedgrass sites (SVR and HAYS), little bluestem (*Schizachyrium scoparium*) and big bluestem (*Andropogon gerardii*) the wetter mixedgrass site (WILSON), and *Andropogon gerardii* the tall grass sites (KONZA and WKT).

Field Methods

To quantify the degree of chemical weathering along the precipitation gradient, soils were sampled to the C horizon (SGS-A, SGS-B, ARIK, SVR, HAYS) or bedrock (WILSON, KONZA, WKT) during the summer of 2003. Pedons were described and sampled by genetic horizon (Soil Survey Staff, 1992). Approximately 1 kg of soil was sampled from each horizon. To examine soil phytolith variability, two additional surface horizon samples were taken in a random direction three meters from each pedon. Where possible, soil peds were taken back to the lab for bulk density analysis. For plant phytolith study, samples of the major grass, shrub and forb species at each site were taken adjacent to the soil sampling area. To examine yearly and seasonal variability in plant Si concentration, live (green) and dead (brown) plant samples from consecutive years (2002-2003) were sampled. The ANPP data was taken from McCulley and Burke (2004), except for the WILSON and WKT sites, where ANPP was measured using $0.25m^2$ quadrats.

Water samples were taken near each sample site periodically from Spring 2003 through Spring 2004 to examine temporal and spatial variability in dissolved Si inputs (precipitation) and outputs (groundwater, stream water). It is important to note that natural water values are dissolved Si and do not include particulate Si. Likens and Bormann (1995) estimated 25% particulate and 75% dissolved Si in stream water measurements within the Hubbard Brook experimental forest. Treguer et al. (1995) noted that particulate Si comprises only about 5% of the total terrestrial Si load delivered to the oceans. To supplement the water samples, publicly available USGS hydrologic data for discharge and water chemistry was used. Stream, rain, and ground water were collected in acid-rinsed LDPE bottles, filtered through 0.4um polycarbonate filters and stored in acid-washed LDPE bottles prior to analysis.

Analytical Methods

Total carbon and nitrogen were analyzed on oven-dried <2-mm subsamples of ground soil using a LECO-1000 CHN analyzer (LECO Corporation, St. Joseph MI). Inorganic carbon was measured by pressure-calcimeter method (Sherrod et al., 2002). Organic carbon was determined by subtracting inorganic carbon from total carbon. Soil texture was determined on a subsample of <2-mm unground soil by hydrometer method (Gee and Bauder 1986). Soil bulk density was determined by a combination of core and clod method (Blake and Hartge 1986), where soil structure and consistency determined which method was used. Oven-dried, ball-mill pulverized soil and rock samples were submitted to SGS Mineral Services of Toronto, Canada for total elemental analysis. Samples were ashed at 500°C to remove organic matter, fused with Li-metaborate, dissolved in dilute

HNO_3 and analyzed by inductively coupled plasma atomic emission spectroscopy (Hossner 1996). Results are reported on ash-free samples. Internal standards, blind standards and duplicates were analyzed for quality control.

Soil phytoliths were extracted by heavy liquid floatation from sand and silt fractions, and cleaned with dilute hydrochloric acid, hydrogen peroxide, and deionized water in a method adapted from Piperno (1988), Kelly (1990), and Parr (2002). Oven-dried (105 °C), 2-mm sieved soils were treated with sodium acetate (buffered at pH 5 with acetic acid) to remove carbonates, and 30% hydrogen peroxide to remove organic matter. After rinsing with deionized water, 5% sodium hexametaphosphate was added and the sample was shaken overnight. Sand was separated from the silt and clay fraction by wet sieving through a 53 μm screen. Silt was separated from clay by centrifugation and gravity sedimentation. The sand and silt fractions were then rinsed with deionized water, dried overnight and stored in plastic bottles. To obtain phytoliths, a subsample (2-5g) of either sand or silt was placed in a 50-ml plastic centrifuge tube along with cadmium iodide/potassium iodide (specific gravity of 2.30 g cm^{-3}). The samples were thoroughly stirred and then centrifuged at 2000 rpm for 10 min. Phytoliths were removed by pipet from the surface and stored in a separate container. Additional stirring and centrifugation was repeated until negligible yield was obtained. Samples were rinsed of the heavy liquid with deionized water. Small amounts of clay obtained during the separation were removed by shaking the phytolith sample in 5% sodium hexametaphosphate overnight, allowing the phytolith to settle, and siphoning off the suspended clays. Phytoliths were further cleaned in separate steps with 10% hydrochloric acid and 30% hydrogen

peroxide. Samples were collected on a 0.2 μm polycarbonate filter, dried overnight, and stored in plastic vials. Subsamples of the soil phytoliths were mounted in immersion oil with a refractive index of 1.51 and examined under light microscope as well as a dissecting scope to ensure that samples were not contaminated with other minerals. X-ray diffraction anaylsis of random phytolith samples corroborated the lack of contamination. The lack of correlation (r^2 = 0.001; p = 0.79) between sediment used in the extraction and phytolith recovered also supports the purity of the soil phytoliths. Known amounts of diatomaceous earth (with a density similar to that of phytoliths) were used to check the recovery rates of the procedure, both alone (94% recovery) and spiked with silt-sized material known to contain negligible phytolith (96% recovery), suggesting minimal contamination from non-phytolith material. Soil phytolith data was converted to a mass/volume basis by incorporating bulk density, pedon thickness, and percent soil phytolith by weight to arrive at g/cm^2 of phytolith per site. This value was then converted to soil phytolith content on a watershed scale in terms of kg Si/ha assuming 10 % soil phytolith water concentration and 5% concentration of elements other than SiO_2 (Bartoli and Wilding, 1980; Bartoli 1985; Drees et al. 1989). The upper 50cm of each pedon was used in order to: 1) affect an equivalent comparison among all the sites, and 2) compare the grassland data to those data reported in forest ecosystems. Given the sharp decline in soil phytolith content with depth (Figure 2.3), this approach is reasonable, except for SGS-A, where relatively high soil phytolith content throughout the profile may be due to the fluvial influence of the site, rather than a buried soil, as the soil organic carbon remains low with depth.

Plant samples were cleaned to remove soil contamination, dry ashed, then treated to remove non-siliceous material in a method adapted from Piperno (1988), Kelly (1990), and Parr et al. (2001). A 5-10 g sample of oven-dried (55-60 °C) plant material was cut into 2-3 cm lengths, washed in a mixture of 5% sodium hexametaphosphate, 10% hydrochloric acid and deionized water. After thorough rinsing, the sample was washed in 70% ethanol, and rinsed again with deionized water. After drying again at 55-60 °C, a subsample of the cleaned plant material was weighed into a Ni crucible. The sample was ashed at 500 °C for 1 hour, allowed to cool in a desiccator and weighed. The ash was washed in warm, 10% hydrochloric acid, rinsed with deionized water, washed in hot 30% hydrogen peroxide, filtered through a 0.20 μm filter, and rinsed thoroughly with deionized water. After drying at 55-60 °C, the sample was allowed to cool in a desiccator, weighed, and stored in a plastic vial. Average plant Si values by site were determined by converting cleaned plant phytolith contents to % Si dry weight, assuming a 10% mean water concentration (Bartoli and Wilding 1980; Bartoli 1985), and a 5% concentration of other elements (Drees et al. 1989), which amounted to an average plant phytolith Si concentration of 39.7% dry weight.

Soil water samples were prepared by bringing soil samples to near saturation with deionized water (Lajtha et al. 1999). After equilibrating for 72 hr, the samples were filtered through Whatman 40 filter paper and filtered again through a 0.22 μm polycarbonate membrane. Sample aliquots of soil water, stream water and precipitation were analyzed for Si concentration using a blue silicomolybdous acid method and read on a spectrophotometer at 812 nm (Mortlock and Froelich 1989).

To determine the impact of atmospheric inputs of Si to these systems, Si concentrations were directly measured via precipitation or estimated in the case of dust. Monthly rainfall samples taken from April through September 2003 near the SGS sites were analyzed for Si concentration, and averaged 0.003 mg Si/L or 0.03 kg Si ha/yr over the period studied. Applying this concentration throughout the study gradient, the maximum amount of Si added to the wettest site (WKT) would be approximately 0.1 kg Si ha/yr. An estimate of annual dust influx rates and the Si concentration of that dust were used to estimate eolian Si inputs. Mahowald et al. (1999) estimated dust deposition rates in the Central Great Plains at approximately 2 to 10 kg/ha/yr, a range that spans current to the last glacial maximum approximately 12 ky. Combining the average of this influx rate with a typical Great Plains loess composition of 20% clay and 80% silt (Roberts et al. 2003), and an average Si concentration of 34% for clay and 77% for silt as measured from surface horizons of the current study, I calculated an annual dry deposition rate of roughly 2 kg Si/ha/yr.

Results

Plant biogenic Si

Dominant grass species at each of the sites along the gradient were measured for plant Si concentration. *Bouteloua gracilis, Buchloe dactyloides, Aristada longiseta, Carex sp., Agropyron smithii* at the shortgrass sites ranged from 2.4-3.0 % Si on a dry weight basis; *Bouteloua gracilis, Buchloe dactyloides, Festuca sp.,* and *Schizachyrium scoparium* at the mixedgrass sites ranged from 2.2-3.6 % Si; and *Andropogon gerardii* at the tallgrass

sites ranged from 1.7-2.1 % Si. The widest range in values is associated with the mixedgrass sites, which also happen to have the widest range in ANPP within a given grassland type. A slight though statistically non-significant decrease in plant Si with increasing ANPP (Figure 2.2) was noted and may be due to differences in plant physiology (e.g. differences in transpiration stress) or soluble Si in the soil. Fredlund and Tieszen (1994) noted a species difference between *Bouteloua gracilis* (7.5% phytolith content) and *Andropogon gerardii* (2.5% phytolith content) from a Great Plains field study. Plant Si values from the current study are in line with values for grasses (approximately 1-3%) reported in other studies (Piperno 1988, Epstein 1999, Ma et al. 2001). Though forbs tend to accumulate less Si on a dry weight basis (with dominant forb species averaging 0.24% Si for the shortgrass, 0.20% for the mixedgrass, and 0.29% Si for the tallgrass sites), their contribution to ANPP in grassland ecosystems is significant enough that a measure of just grasses would tend to overestimate biomass Si. For example, estimates from previous LTER studies at SGS and Konza (unpublished data from the respective LTER websites) reported a contribution of forbs to total ANPP of approximately 11% and 23% respectively. When calculating plant Si on a watershed scale (kg Si/ha), differences in ANPP along the climosequence overshadow differences in plant Si concentration among the sites.

Soil biogenic Si

Soils contain roughly 1,000 times more biogenic Si than the plant biomass when viewing these grassland systems as a whole (Table 2.2). Figure 2.3 shows the depth distribution for soil organic C and soil phytolith contents grouped by grassland system. In general,

both parameters exhibit similar trends typical of plant-mediated constituents, with maximum accumulation near the surface and a fairly sharp decrease with depth; however, differences between SOC and soil phytoliths among the different grassland systems are evident. Whereas SOC and annual input of Si though litterfall (Table 2.2) increase with increasing precipitation (i.e. from short to tallgrass), soil phytoliths do not show a similar trend. On average the greatest accumulation of soil phytoliths are found in the mixed grass sites (48.5 x 10^3 kg Si/ha; 1.8% of total soil Si), followed by shortgrass (31.5 x 10^3 kg Si/ha; 1.5% of total soil Si) and tallgrass sites (15.3 x 10^3 kg Si/ha; 0.9% of total soil Si). The weight percentage of total soil Si is derived from the soil phytolith and soil mineral Si numbers from Table 2.2. Assuming differences in phytolith solubility are minor, the balance between weathering intensity and litterfall inputs are the most likely explanation for this trend. Shortgrass systems experience the lowest weathering intensity and receive the least amount of annual plant Si; whereas on the other end of the spectrum, the relatively large annual inputs of plant Si associated with tallgrass systems may be offset by greater weathering intensity. The large variability of soil phytolith content within the mixed grass sites may be due to differences among plant communities and parent material. The Wilson site, though falling within the mixed grass zone geographically, actually resembles a tallgrass site in terms of species composition, SOC and soil phytolith stocks. The low soil phytolith content may also reflect parent material composition, as the soil at this site is fairly shallow to limestone. Higher pH generally increases phytolith solubility (Fraysse et al. 2004).

Soil Mineral Si

Soil mineral Si was split into two pools: <2μm (clay) and 2μm - 2mm (silt and sand). From X-ray diffraction analysis, quartz and feldspar were found to dominate the sand and silt size fraction, with smectite, illite and kaolinite comprising the majority of the clay fraction. Increasing clay content (clay = 0.0029(MAP) +0.705, r^2 = 0.872, p = 0.006; excluding the Wah-Kon-Tah site, which has a much lower clay content due to the more resistant sandstone parent material), and decreasing carbonate content (carbonate = $12.952e^{-0.0127(MAP)}$, r^2 = 0.952, p = 0.05) excluding the Wilson site, which formed in relatively shallow limestone) along the climosequence reveal expected trends in these parameters when regressed with MAP. As mentioned previously, differences in mineral Si among the study sites are a reflection of climate and parent material, with slightly more total soil Si found in more resistant parent materials (e.g. Arikaree and WKT). Not surprising, mineral Si dominates the overall Si pool in the soil, comprising 96 to 99% of the total soil Si across the climosequence. Magnitude alone, however, does not tell the whole story of the reactivity of both the mineral and biogenic Si pools in the overall terrestrial biogeochemical Si cycle.

As a means of examining weathering and Si flux along the climosequence, open-mass transport functions were calculated using the equations 2.1 and 2.2 (Egli and Fitze 2000).

$$\tau_{j,w} = [\rho_w C_{j,w}/\rho_p C_{j,p} (\varepsilon_{i,w} + 1)] - 1 \qquad (2.1)$$

where;

$\tau_{j,w}$ = open-system mass transport function for element **j**
ρ_w = bulk density of soil
ρ_p = bulk density of parent material
$C_{j,p}$ = concentration of element **j** in the parent material
$C_{j,w}$ = concentration of element **j** in the soil

$$\varepsilon_{i,w} = (\rho_p C_{i,p} / \rho_w C_{i,w}) - 1 \qquad (2.2)$$

$\varepsilon_{i,w}$ = strain; volumetric change during weathering compared to volume of initial parent material
$C_{j,p}$ = concentration of immobile element **i** in soil
$C_{j,w}$ = concentration of immobile element **i** in the parent material

Results of these calculations are graphed in figure 2.4 for Si and 2.5 for Al. Titanium was selected as the immobile element for these calculations, based on transported mass fraction vs. strain comparisons with zirconium (another relatively immobile element) for the sampled horizons (Chadwick et al. 1990). Limitations to this approach include selection of representative parent material and elemental additions from sources other than the parent material, such as atmospheric input. Minor fluctuations in Si and Al relative to the parent material were observed throughout the climosequence, the major exception being Wah-Kon-Tah (possibly due to a combination of weathering, soil depth and parent material). However, atmospheric input (a variable requiring further study)

cannot be ruled out as a partial explanation for maintaining an elemental balance relative to the parent material (i.e. it is difficult to quantify the impact of eolian additions versus weathering losses and flux). Surficial losses of Al across the weathering gradient provide another potential line of evidence of weathering and illuvial transport in these systems. Greater surficial losses of Al compared to Si across the climosequence may be the result of greater Si biocycling supporting higher surficial Si concentrations.

External Inputs and Outputs

Given the minor input of precipitation derived Si, this component was omitted from the atmospheric input component, and was based solely on the dust input estimation of 2 kg Si/ha/yr. For comparison with previous studies of Si cycling, atmospheric inputs were estimated at <1 to 1.5 kg Si/ha/yr (Alexandre et al. 1997 and Bartoli 1983, respectively), and either ignored or comprised a very small portion of the overall Si cycle. The slightly higher values estimated for this study seem reasonable given the drier climate associated with grassland systems compared to forests. Estimation errors are likely to have a minor impact, as this input is a minor component in the terrestrial biogeochemical Si cycle.

Table 2.2 provides a look at the Si exports estimated for each site along the climosequence. Average stream water Si concentration tended to decrease slightly (shortgrass sites: 10.4 mg Si/L, n=4 watersheds; mixedgrass sites: 8.3 mg Si/L, n=3 watersheds; tallgrass sites: 5.2 mg Si/L, n=5 watersheds; data is taken from the current study and unpublished USGS data available on the internet) with increasing precipitation along the gradient. Greater stream discharge associated with wetter sites led to substantial increases in Si output along the gradient (Si export = 0.0149(MAP) – 6.569; $r^2 = 0.935$, p

= 0.0002). Groundwater exports of Si are assumed to be minor or accounted for by the stream water.

Discussion

Distribution and behavior of biogenic Si in grasslands

Table 2.2 and Figure 2.6 display the trend of plant mediated Si across the grassland climosequence. As mentioned previously, grasses in the shortgrass systems tend to have higher plant Si concentration on a dry weight basis than grasses of tallgrass systems. However, tallgrass systems realize greater annual Si input through litterfall, as the greater ANPP associated with tallgrass sites offsets lower plant Si concentration (litterfall = 30.945ln(ANPP) – 185.26; r^2 = 0.872, p = 0.01). The large variability in litterfall apparent at some of the sites along the climosequence is not necessarily peculiar to that particular grassland type and is at least partially due to sampling bias (i.e. greater variability in ANPP during the years sampled; McCulley and Burke 2004). Such variability in ANPP is directly related to variability in MAP. Conversely, soil biogenic Si pools tend to decrease across the gradient (soil biogenic Si = -37.32ln(ANPP) + 271.56, r^2 = 0.445, p = 0.10), even though the trend isn't as prominent as that seen with litterfall, largely due to the variability within the mixedgrass ecosystems. Part of this variability can be explained by the difference in plant communities between the driest (Smokey Valley = lowest ANPP) and wettest (Wilson = highest ANPP) sites within the mixed grass communities. The general trend in decreasing soil phytolith content is likely driven by the increased weathering intensity along the gradient. As mentioned previously, soil biogenic Si as a percentage by weight of the total Si pool is quite small, but this small

pool of more soluble biogenic Si likely undergoes faster turnover than the larger more stable pool of mineral derived Si (Alexandre et al. 1997).

Figure 2.7 displays the relationship between soil organic carbon and soil phytoliths across the grassland climosequence for all horizons sampled. In general, soil phytoliths tend to accumulate to a greater extent in soils of drier sites (i.e. short- and mixedgrass, where MAP < 600 mm). Soil organic carbon accumulates to a greater extent at the wetter sites (i.e. tallgrass where MAP > 600 mm). Such a distribution profile illustrates that both translocation and dissolution of the soil phytoliths are likely occurring in the soil (Bartoli and Souchier 1978, Piperno 1988, Alexandre et al. 1997). If translocation were the only process, the annual influx and soil phytolith pool would provide an estimate of the soil age (approximately 100-1,200 years across the climosequence of the current study). Radiocarbon dates (Blecker et al. 1997) and morphological properties of the soil across the climosequence imply that phytolith dissolution has occurred, as this age range is too young for these soils.

Stabile vs. Labile soil phytolith pools

Phytolith solubility

Existing studies of plant phytolith solubility, though useful, are generally laboratory based, and given the various extraction methods and propensity for greater dissolution rates under lab conditions compared to the field, should be interpreted with caution. Bartoli and Wilding (1980) found that plant phytolith solubility increased with increasing Si/Al ratio, surface area and water content. Although based on relatively few samples,

solubility tended to decrease in the order of grass>deciduous>coniferous species, owing primarily to the differences in composition. In a later study, Bartoli (1985) reported lower phytolith surface Si/Al ratios compared to the whole phytolith and again showed that plant phytoliths of deciduous and graminoid plants (*Festuca sp.*) are more soluble than those of coniferous plants. More recently, Fraysse et al. (2004) reported bamboo phytolith dissolution rates intermediate between quartz and vitreous silica. With a minimum dissolution at pH 3, the authors reported a linear increase in phytolith solubility with increasing pH (approximately two orders of magnitude greater at pH 9 than pH 3). Phytoliths isolated from the soil fraction tend to have greater Al concentration, less water and surface area and consequently are less soluble than plant phytoliths (Bartoli and Wilding 1980).

Approaches for estimating phytolith dissolution

Different approaches of varying complexity have been used to estimate the annual input of biogenic Si to the soluble Si pool through phytolith dissolution. Bartoli (1983) used biogenic silica mean residence time and soil profile distribution of phytoliths to estimate phytolith solubility in studies of silicon biogeochemistry in temperate forests. Meunier et al. (1999) estimated phytolith solubility by examining the radiocarbon age of material above and below the horizon of maximum phytolith accumulation, along with a comparison of the annual plant input of biogenic silica and the soil biogenic silica pool to determine a soil phytolith mean residence time. Given the similarity in trends between soil organic carbon and soil phytolith with depth, and a detailed study of phytolith

morphology, Alexandre et al. (1997) proposed that soil phytolith stability behaves in a similar manner to that of soil organic carbon, both having a labile pool that decreases rapidly with depth, and a more stable pool that maintains a more constant concentration throughout the profile. Composition of phytoliths deeper in the profile would likely be those more resistant, translocated phytoliths.

Phytolith mean residence time (MRT)

Related to dissolution rate, and important in the calculation of phytolith dissolution in the current study, is the mean residence time or turnover of soil phytoliths. Alexandre et al. (1994) used qualitative observation (degree of pitting and presence/absence of different types depending on occurrence in different parts of the leaf of phytoliths in plants and litter) to estimate a mean residence time in the litter of between 6-18 months. Bartoli and Souchier (1978) estimated phytolith turnover times of 0.5 to 2.4 y in plants, 2 to 10 y in the litter, and 1 to 300 y in the soil, with coniferous forests having slower turnover times than deciduous forests.

Using the ratio of soil phytolith pool (kg Si/ha) / litterfall Si input (kg Si/ha/yr), I estimated turnover times for soil phytoliths across the climosequence, finding a relatively strong trend of faster turnover with increasing ANPP (turnover time = -797.97ln(ANPP) + 6832; r^2=0.825, p = 0.003). Average turnover rates for soil phytoliths at the shortgrass sites were 1150 y, mixed grass sites 725 y, and tallgrass sites 200 y (Figure 2.8). Tallgrass systems were most comparable to the forest systems, as the application of this equation to Alexandre et al. (1997) gives an average MRT of approximately 280 yr.

Current approach for estimating phytolith dissolution

Silicon flux associated with phytolith dissolution has been estimated based on data from previous studies and the phytolith distribution found in the grasslands systems. Regressing phytolith dissolution against phytolith turnover from data in forest systems (Bartoli 1983, Alexandre et al. 1997, Meunier et al. 1999), the following equation was used to estimate phytolith dissolution in terms of stable and labile phytolith pools in grassland systems: phytolith dissolution (%) = -0.0921 ln(turnover) + 1.3264; $r^2 = 0.778$, $p = 0.08$. Applying an equation derived from forest systems to grasslands may overestimate phytolith dissolution rates, as weathering intensity does not necessarily follow the same pattern. However, in the context of the overall biogeochemical Si cycle, a conservative estimate downplays the impact of plant Si cycling on mineral weathering. Also, the differences in weathering may be offset somewhat by differences in phytolith solubility between forest and grassland plant species as mentioned previously.

Comparisons between grasslands and forest – phytolith distribution and behavior

Analyzing litterfall inputs of biomass Si and soil phytolith Si provides a framework for comparing biogenic Si cycling between grasslands and forests. Additions of biogenic Si to the soil are primarily a function of plant Si concentration, ANPP, and litterfall. In general, greater total ANPP and aboveground Si storage in forest systems are offset by the greater annual litterfall associated with grassland systems, which near 100% for grasslands compared to roughly 5-10% for forests. Tropical forests and mixed- tallgrass systems are quite similar in terms of annual biogenic Si inputs to the soil, the former

having a range of 41-67 kg Si/ha/yr; (Lucas et al. 1993, Alexandre et al. 1997, Meunier et al. 1999) and the latter 58-75 kg Si/ha/yr. The deciduous forest site (22 kg Si/ha/yr; Bartoli 1983) is comparable to the shortgrass systems (23 - 26 kg Si/ha/yr); the lowest annual Si additions are associated with the coniferous forest (4.5 kg Si/ha/yr; Bartoli 1983).

Despite differences in phytolith dynamics between forests and grasslands, as well as differences in ecosystem parameters such as MAP, ANPP, and parent material, stores of soil phytoliths in these systems are remarkably similar. The range of soil phytolith Si pools found in tropical forests (19 x 10^3 kg Si/ha for Alexandre et al., 1997 and 170 x 10^3 kg Si/ha for Meunier et al., 1999) is comparable to those of the grasslands (Table 2.2). The deciduous (0.45 x10^3 kg Si/ha) and coniferous (1.4 x 10^3 kg Si/ha) forests from Bartoli (1983) are roughly an order of magnitude less, reflecting the lower plant Si concentration, lower litterfall inputs and possibly greater weathering intensity compared to the grasslands; differences that may help explain the similarities in soil phytolith pools among these disparate ecosystems. Differences in phytolith solubility among the plant species might also explain this trend. Given the relative similarities in biogenic Si distribution between grasslands and forests (aside from aboveground storage), a discussion of phytolith impact on mineral weathering follows.

Phytolith impact on mineral weathering

Researchers have long recognized that plants can increase chemical weathering rates in soils by increasing rhizosphere acidity, cation biocycling, altering soil physical properties

that impact mineral/water interaction time, and biogenic mineral production (Lovering 1959, Berner 1992, Drever 1994). Table 2.3 (populated by data from Table 2.2) presents a closer look at the impact of plants on mineral weathering in terms of potential mineral dissolution (in units of kg Si/ha/yr) along the grassland climosequence of the current study, compared to forested ecosystems from previous studies. The input-output mass balance approach (column 1) is a relatively simple means of estimating the relative degree of weathering in a system, the difference between the two accounting for element accrual or loss. A net ecosystem loss in Si occurs when the Si output (stream water Si concentrations) exceed Si inputs (atmospheric dust deposition). Applied to the current study, this relationship shows the expected impact of climate on weathering; where mineral dissolution = -0.0149(MAP) + 8.5688; $r^2 = 0.922$, $p = 0.0004$. Not until the tallgrass systems does Si show a net watershed level export, as eolian inputs of Si in the drier sites exceed the Si lost to stream water (assuming that groundwater Si ultimately winds up in streams). Table 2.3 shows that Si exports in tallgrass approaches those found in forested ecosystems.

Comparing elemental inputs and outputs typically excludes information about internal cycling of elements and the impact of biogenic cycling on weathering. When plant cycling of Si is included, the impact on mineral dissolution is potentially much greater, as indicated by the calculated increase in Si released by mineral dissolution. As the annual dissolution of soil phytoliths is not sufficient to meet the annual plant uptake of Si, the additional Si (assuming the inputs and outputs are relatively constant over time) would be supplied from mineral dissolution. Although not as strong as the input-output trend, there

is a noticeable positive relationship along the weathering gradient (mineral dissolution = -0.0228(MAP) – 4.380; $r^2 = 0.497$, $p = 0.05$), where internal plant cycling increases the amount of Si released through mineral dissolution. A threshold of plant Si concentration and ANPP may exist that helps explain the similarity in mixed and tallgrass systems and their greater impact on mineral dissolution over shortgrass sites.

Even though overall weathering is greater in forested ecosystems (as seen in the greater stream outputs of dissolved Si), the impact of plant Si cycling on mineral weathering in grasslands is potentially greater. Grasses tend to accumulate more Si on a dry weight basis and turnover just as much Si if not more on an annual basis, offsetting the greater overall ANPP seen in forested systems. The main exception to this trend exists in the bamboo forest (Meunier et al. 1999), which combines the greater ANPP of a forest with the higher Si uptake and litterfall associated with grassland systems, bamboo being a member of the graminoid family.

Column 3 of Table 2.3 further refines the impact of plant Si cycling by removing the input and output fluxes. The impact of grassland systems on mineral dissolution changes slightly, with mixedgrass > tallgrass > shortgrass. Of further interest is the two-fold increase in mineral dissolution of grasslands over forests (excluding the bamboo forest; grassland average of -12.7 kg Si/ha/yr (n=7) vs. forest average of -6.5 kg Si/ha/yr (n=4)). This result suggests that Si biocycling may be a more important factor on mineral weathering in grasslands (drier systems) compared to forests (wetter systems), where climate driven weathering overshadows weathering associated with Si biocycling.

A key Si pathway not included in this calculation is secondary mineral formation (see Figure 2.9). This pathway would further deplete the stock of soluble Si available for plant uptake, theoretically increasing the amount of Si released through primary mineral dissolution in order to maintain the calculated rates of plant Si uptake. As weathering intensity and thus clay formation should increase along the climosequence, this impact would be greater along the climosequence as well.

Conclusions

Phytolith distribution in grasslands is similar to that of soil organic carbon and is driven largely by ANPP and weathering. In grasslands systems, plant Si concentration tends to decrease as MAP increases. Across the grassland climosequence, soil phytolith pools tend to decrease with increasing MAP, even though annual phytolith inputs through litterfall increase. From the perspective of an ecosystem scale Si mass balance, biogenic Si cycling should enhance mineral dissolution, as phytolith dissolution alone is not sufficient to meet annual plant Si uptake. Despite the lesser weathering intensity and productivity generally associated with grasslands when compared to forests, biocycling of Si on a watershed scale is comparable between these ecosystems and should be accounted for at the watershed scale as well as globally.

Table 2.1 Characteristics for the 7 sites comprising the Great Plains climosequence (SGS – Shortgrass Steppe Long-Term Ecological Research (LTER) site, ARIK – Arikaree River Ranch, owned by The Nature Conservancy (TNC), SV – Smokey Valley River Ranch owned by the TNC, HAYS – Hays Range Area, owned by Ft. Hays State University, WILSON – owned by Wilson Lake State Park, KONZA – Konza Prairie Research Natural Area and LTER site, WKT – Wah-Kon-Tah Natural Area owned by TNC, MAP = mean annual precipitation, MAT = mean annual temperature.

	SGS Shortgrass Steppe - LTER	ARIK Arikaree – TNC	SV Smokey Valley – TNC	HAYS Ft. Hays State Univ.	WILSON Wilson Lake State Park	KONZA Konza Prairie – LTER	WKT Wah-Kon-Tah - TNC
Latitude	40° 51.99 N	39° 45.02 N	38° 53.11 N	38° 52.44 N	38° 56.33 N	39° 05.48 N	37° 53.52 N
Longitude	104° 41.47 W	102° 28.68 W	100° 57.63 W	99° 23.15 W	98° 40.40 W	96° 34.12 W	93° 58.58 W
Elevation (m)	1,650	1,220	879	610	536	406	287
MAP[1] (mm)	344	462	502	575	650	884	1110
MAT[1] (°C)	9.3	9.7	10.8	11.9	12.3	12.7	13.1
Vegetation type	shortgrass steppe	shortgrass steppe	mixedgrass	mixedgrass	mixedgrass	tallgrass	tallgrass
Soil subgroup	Aridic Argiustoll	Aridic Argiustoll	Typic Argiustoll	Typic Argiustoll	Typic Calciustoll	Udic Argiustoll	Typic Hapludoll

[1] U.S. Dept. of Commerce, U.S. Monthly Climate Normals, 1971-2000

Table 2.2 – Silicon distribution in terms of pools and fluxes across the climosequence. Errors listed represent ± 1 standard error of the mean. Soil phytolith and soil mineral Si are from the top 50 cm.

Pools (kg Si/ha)	SGS	Arik	Smokey Valley	Hays	Wilson	Konza	WKT
Biomass	29 ± 9	25 ± 16	66 ± 36	70 ± 27	64 ± 9	83 ± 18	72 ± 9
Soil phytoliths (x 10^3)	32 ± 2.6	31 ± 1.8	67 ± 2.9	30 ± 2.4	8 ± 0.4	18 ± 2.2	20 ± 1.7
Soil Minerals (x 10^6) 2μm to 2mm	1.76 ± 0.25	1.92 ± 0.35	1.53 ± 0.25	1.48 ± 0.35	1.29 ± 0.15	1.39 ± 0.35	1.94 ± 0.35
Soil Minerals (x 10^6) < 2μm	0.31 ± 0.05	0.28 ± 0.05	0.34 ± 0.05	0.40 ± 0.05	0.49 ± 0.05	0.56 ± 0.10	0.23 ± 0.05

Fluxes (kg Si/ha/yr)	SGS	Arik	Smokey Valley	Hays	Wilson	Konza	WKT
Input	2 ± 1	2 ± 1	2 ± 1	2 ± 1	2 ± 1	2 ± 1	2 ± 1
Litterfall	26 ± 10	23 ± 16	59 ± 36	63 ± 27	58 ± 9	75 ± 18	65 ± 9
Labile phytoliths	16 ± 6	15 ± 10	40 ± 24	48 ± 21	50 ± 8	61 ± 15	52 ± 7
Stable phytoliths	10 ± 4	8 ± 6	19 ± 12	15 ± 6	8 ± 1	14 ± 3	13 ± 2
Mineral dissolution	-7.5 ± 11	-6.8 ± 17	-18.8 ± 37	-15.7 ± 28	-7.3 ± 10	-18.3 ± 22	-22.8 ± 14
Secondary mineral formation	n.d.	n.d.	n.d.	n.d.	n.d.	n.d.	n.d.
Stream/ground water	0.2 ± .03	0.5 ± .03	0.3 ± .05	1.5 ± .40	1.7 ± .48	6.3 ± 2.7	11.0 ± 3.8

n.d. = not determined

Table 2.3 – Comparison of the impact of Si biocycling on mineral dissolution of Si between grassland and forest ecosystems.

	---------- Mineral Dissolution (kg Si/ha/yr) ----------		
	w/o plant Si cycling (inputs-outputs) *column 1*	*w/ plant Si cycling* (input + phytolith dissolution) - (output + plant uptake) *column 2*	phytolith dissolution – plant uptake *column 3*
Grasslands			
SGS	1.8	-7.5	-9.3
Arikaree	1.5	-6.8	-8.3
Smokey Valley	1.7	-18.8	-20.5
Hays	0.5	-15.7	-16.2
Wilson	0.3	-7.3	-7.0
Konza	-4.3	-18.3	-14.0
Wah-Kon-Tah	-9.0	-22.8	-13.8
Forests			
Deciduous[1]	-4.5	-10.5	-6.0
Coniferous[1]	-24.5	-28.5	-4.0
Tropical-congo[2]	-15.0	-20.0	-5.0
Tropical-amazon[3]	-10.0	-21.0	-11.0
Tropical-bamboo[4]	-15.0	-41.0	-26.0

[1]Bartoli 1983, [2]Lucas et al. 1993, [3]Alexandre et al. 1997,[4] Meunier et al. 1999.

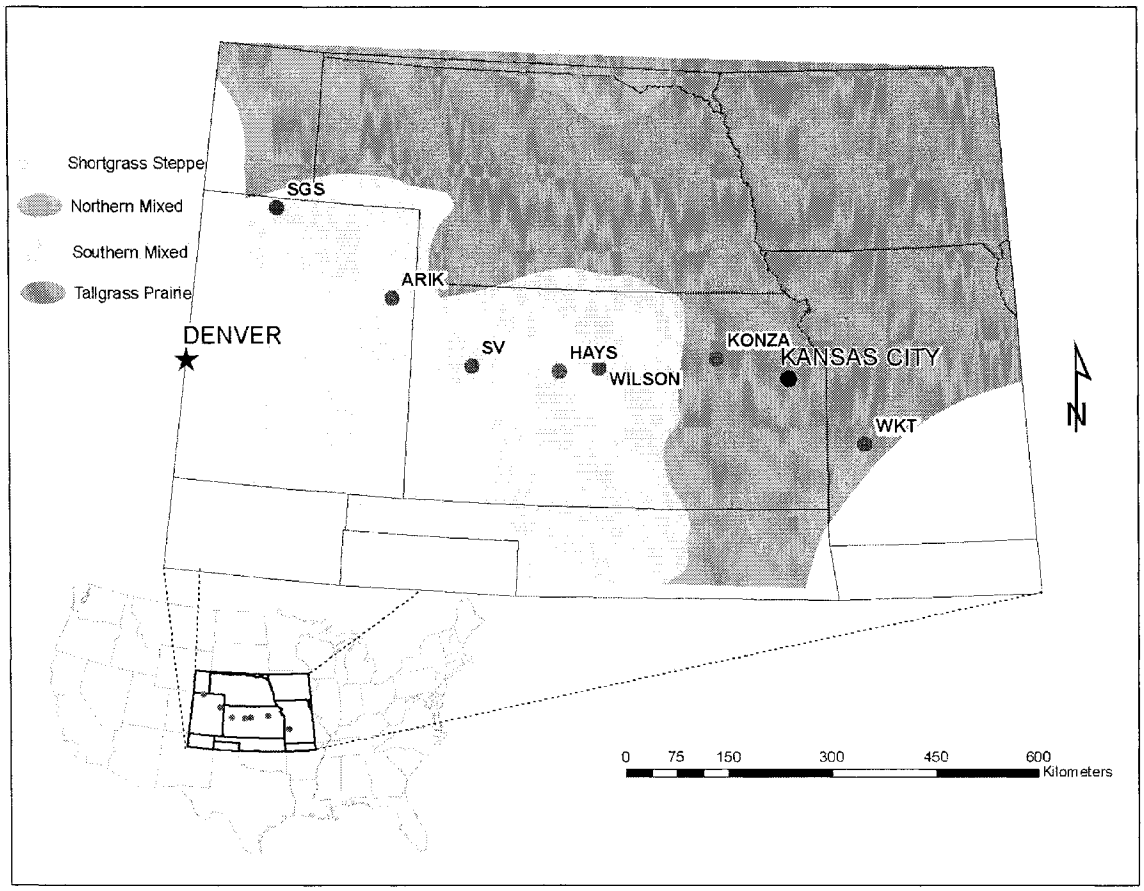

Figure 2.1 Location map for field sites located along the Great Plains climosequence.

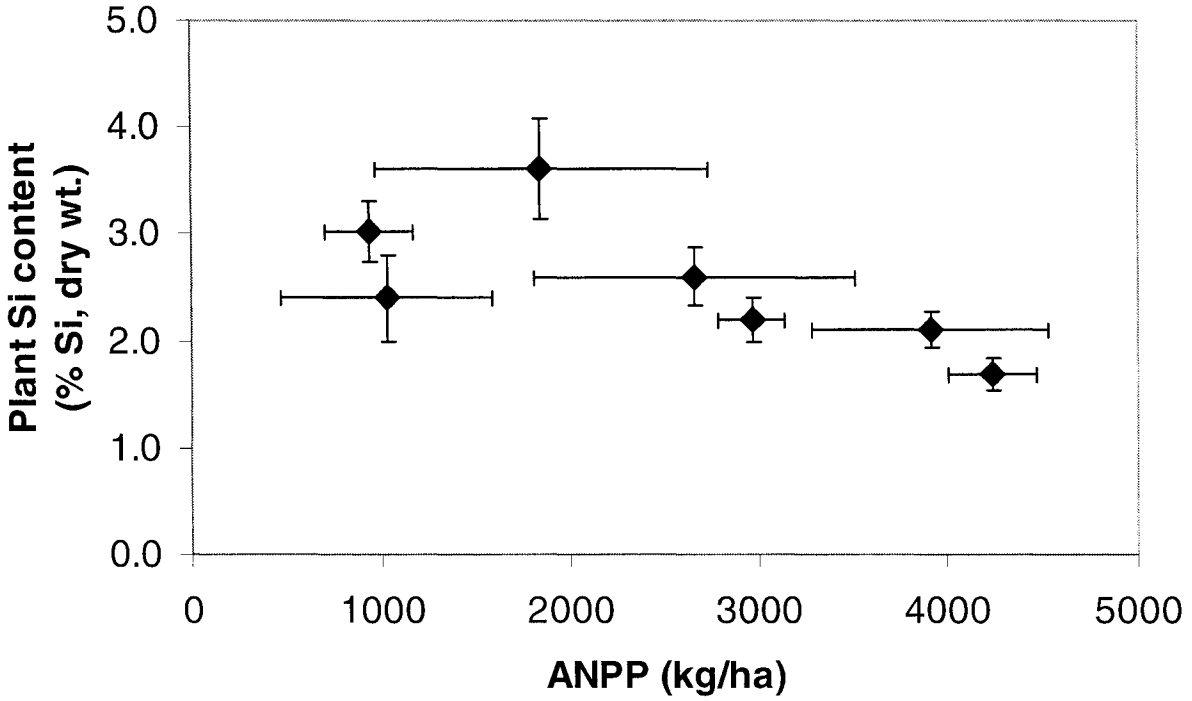

Figure 2.2 – Mean plant Si concentration (on a % dry weight basis) for the major grass species at each of the 7 climosequence sites (± 1 S.E.M). Plant Si concentration = -0.0018 (ANPP) + 3.704; $r^2 = 0.592$, $p = 0.08$.

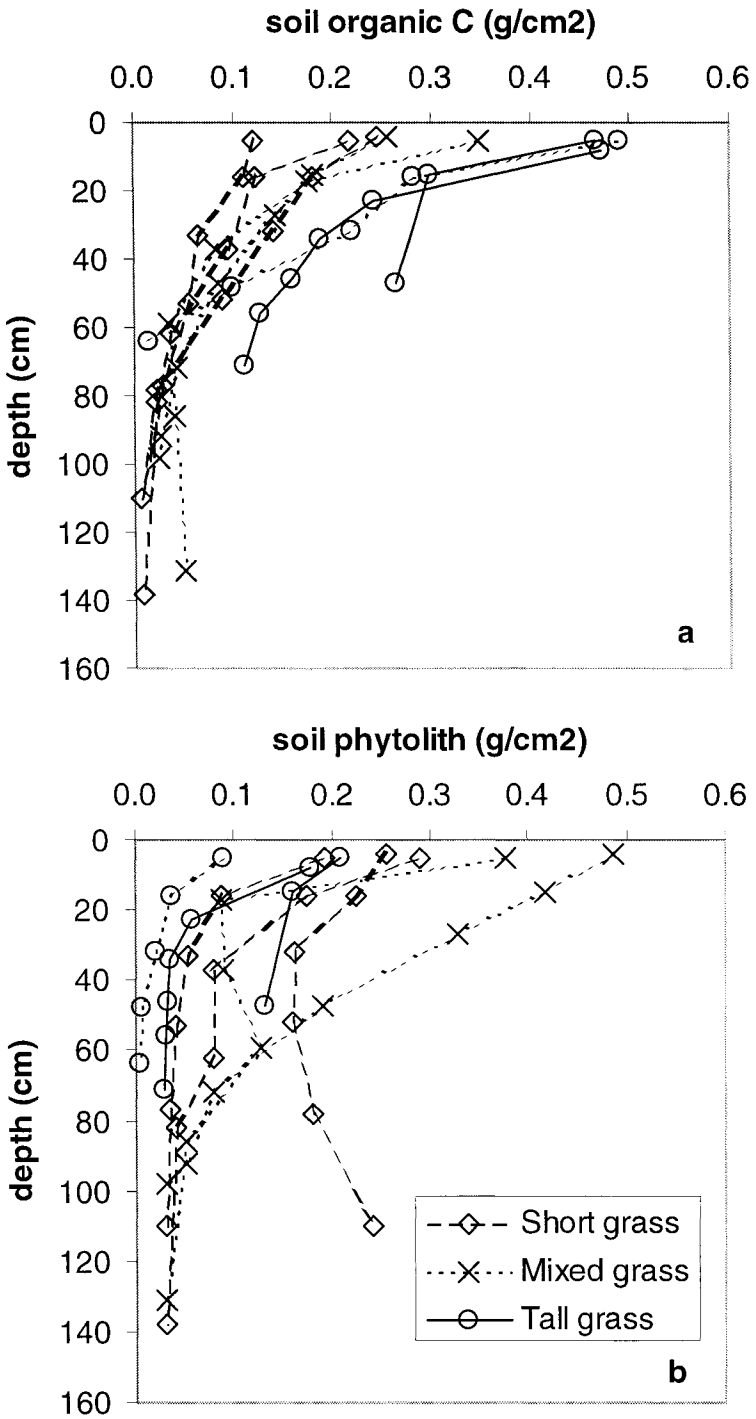

Figure 2.3 – (a) Soil organic carbon depth profiles for the short-, mixed- and tallgrass sites. (b) Soil phytolith depth profiles for the short-, mixed- and tallgrass sites.

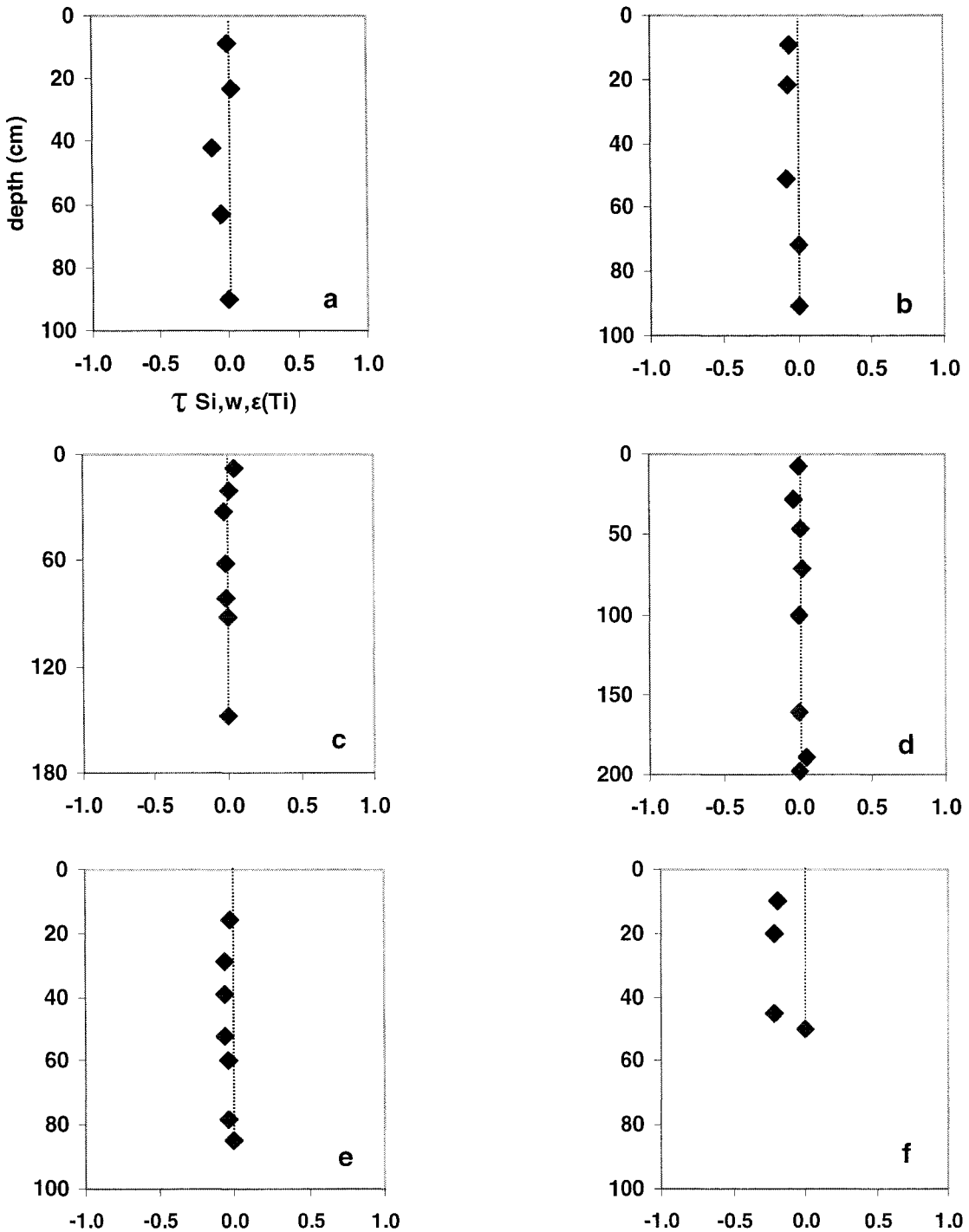

Figure 2.4 – Si mass transport relationships (based on Ti) for climosequence sites, horizons to the right of the dashed line represent an increase in Si relative to the parent material (lowest diamond), horizons to the left represent losses in Si relative to the parent material.
a – SGS, **b** – Arikaree, **c** – Smokey Valley, **d** – Hays, **e** – Konza, **f** – Wah-Kon-Tah.

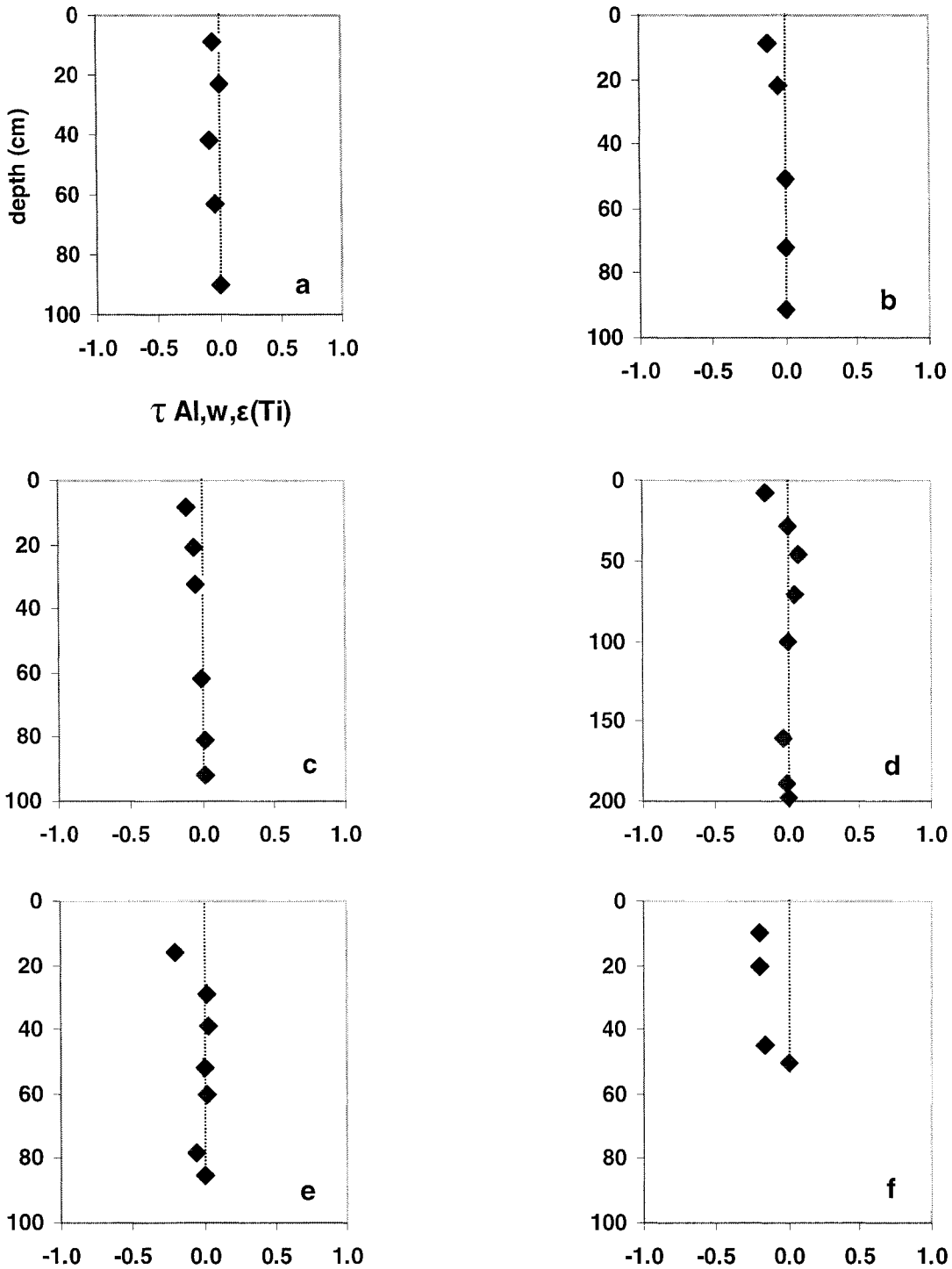

Figure 2.5 – Al mass transport relationships (based on Ti) for climosequence sites, symbols to the right of the dashed line represent an increase in Al for that horizon relative to the parent material (lowest diamond), symbols to the left represent losses in Al relative to the parent material. **a** – SGS, **b** – Arikaree, **c** – Smokey Valley, **d** – Hays, **e** – Konza, **f** – Wah-Kon-Tah.

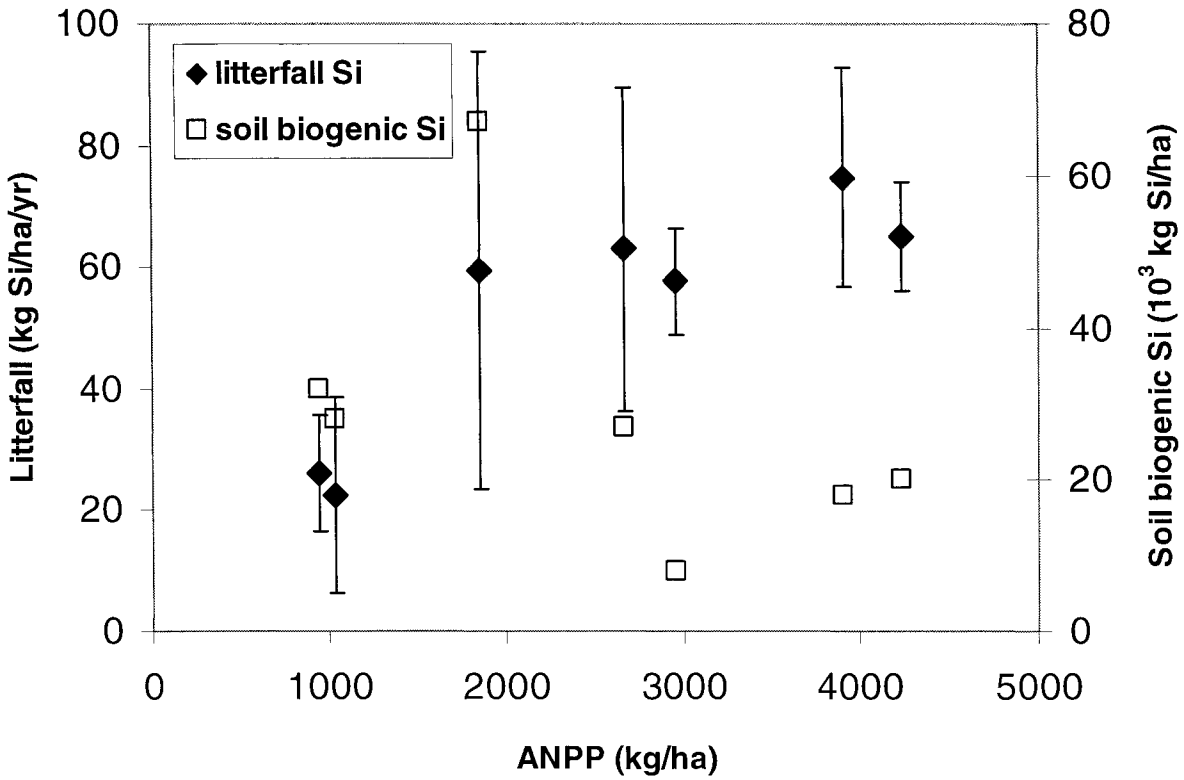

Figure 2.6 – Comparison of annual plant Si input (litterfall) and Si stored in soil phytoliths as a function of primary productivity. Error bars for litter fall input are ± 1 S.E.M.

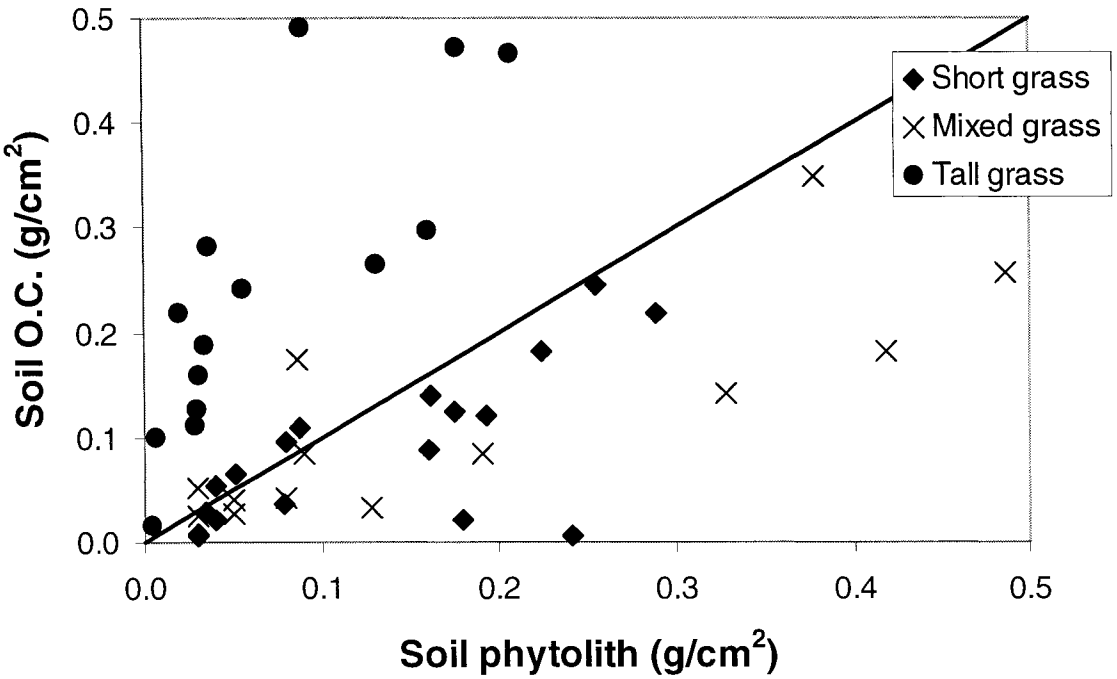

Figure 2.7 – Comparison of two biologically mediated soil constituents, soil organic carbon and soil phytoliths among the grassland systems. The solid line represents a 1:1 ratio.

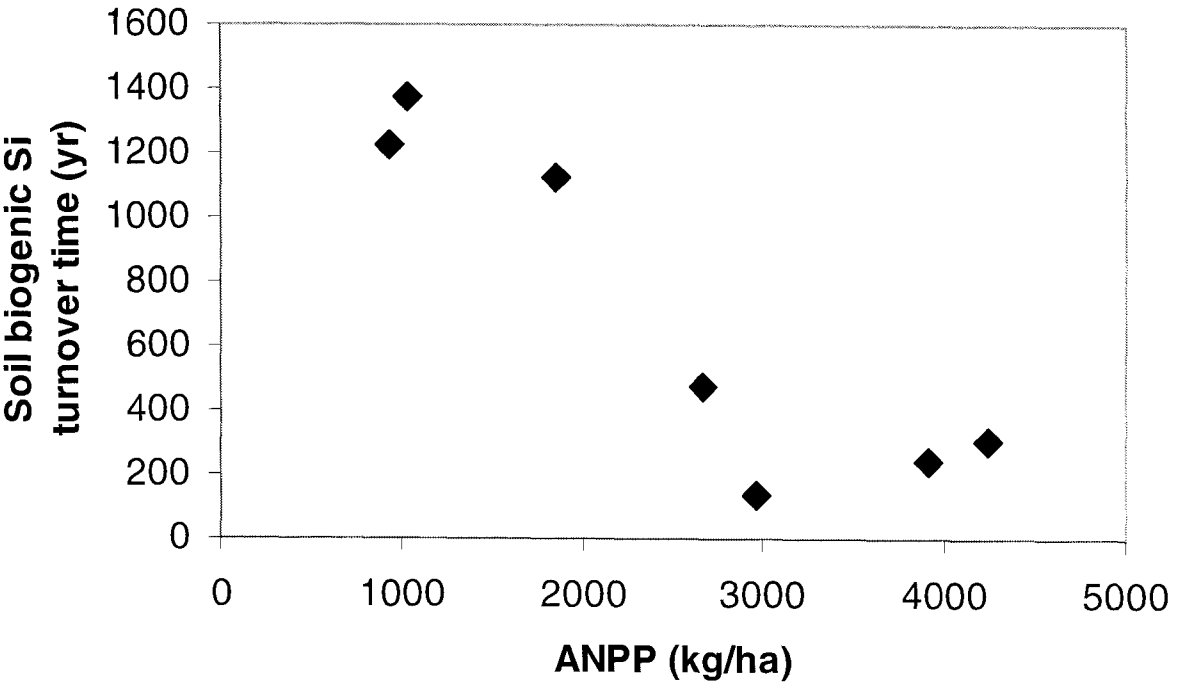

Figure 2.8 – Estimate of soil biogenic Si turnover time as a function of ANPP.

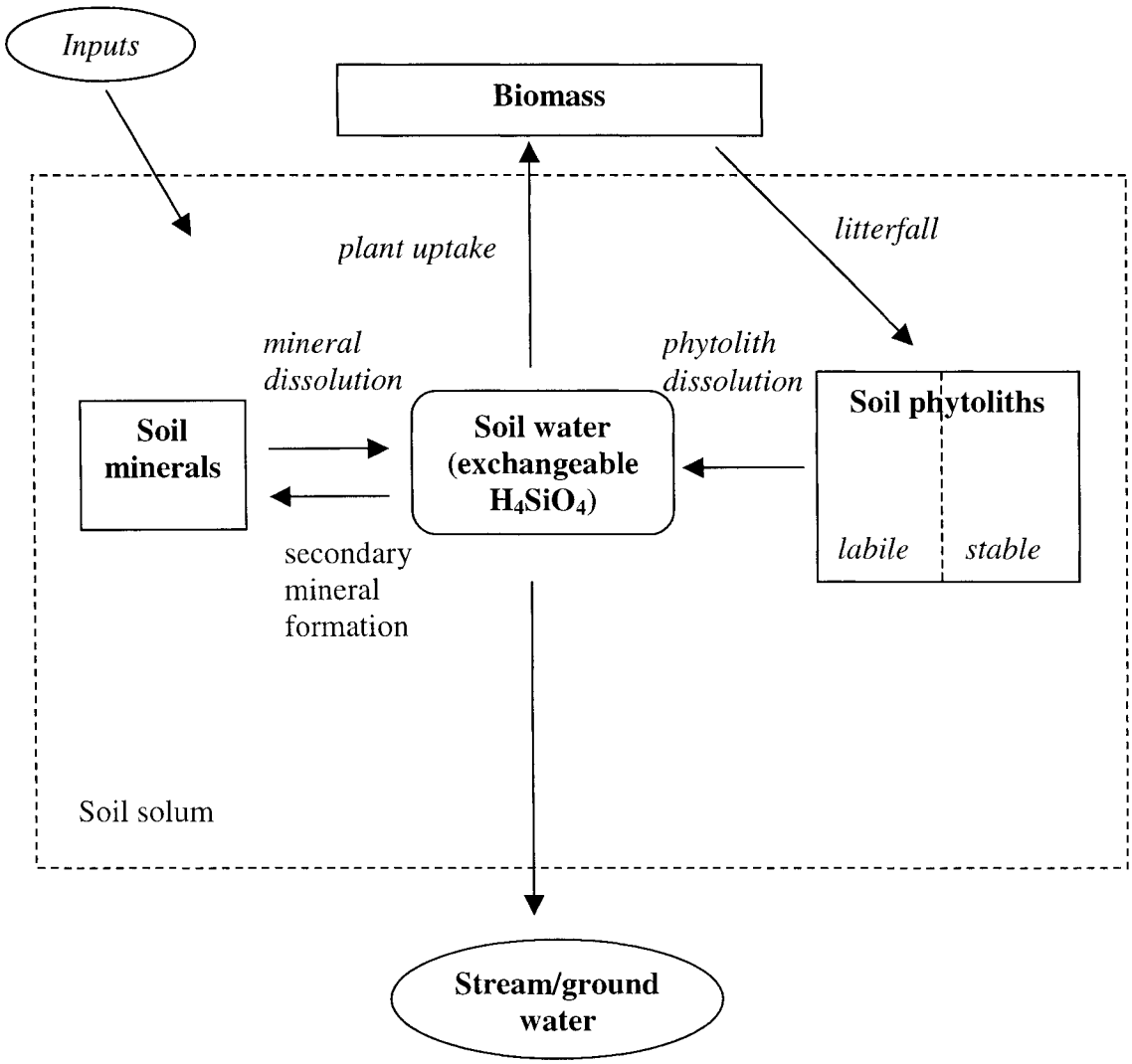

Figure 2.9 - Conceptual model of major pools and fluxes associated with the terrestrial grassland Si cycle. Bold items were directly measured in this study, italicized items were estimated.

References

Alexandre A., Colin F., and Meunier J.D. 1994. Les phytolithes, indicateurs du cycle biogeochimique du silicium en foret equatoriale. C.R. Acad. Sci Paris (II) 319:453-458.

Alexandre A., Meunier J.D., Colin F., and Koud J.M. 1997. Plant impact on the biogeochemical cycle of silicon and related weathering processes. Geochim. Cosmochim. Acta 61:677-682.

Axelrod D.I. 1985. Rise of the grassland biome, Central North America. Botanical Review 51:163.201.

Bartoli F. 1983. The biogechemical cycle of silica in two temperate forest ecosystems. Environ. Biogeochem. Ecol. Bull. 35:469-476.

Bartoli F. 1985. Crystallochemistry and surface properties of biogenic opal. J. Soil Science 36:335-350.

Bartoli F. and Souchier B. 1978. Cycle et role du silicium d'origine vegetale dans les ecosystems forestiers temperes. Ann. Sci. For. 78:187-202.

Bartoli F. and Wilding L.P. 1980. Dissolution of biogenic opal as a function of its physical and chemical properties. Soil Sci. Soc. Am J. 44:873-878.

Berner R.A. 1992. Weathering, plants and the long term carbon cycle. Geochimica Cosmochimica Acta 56:3225-3231.

Berner R.A. 1995. Chemical weathering and its effect on atmospheric CO_2 and climate. *In* White A.F. and Brantley S.L. (eds.), Chemical weathering of the silicate minerals. American Mineralogical Society. Reviews in Mineralogy v.31:565-583.

Blake G.R. and Hartge K.H. 1986. Bulk density. *In* A. Klute (ed.) Methods of soil analysis. Part 1. 2nd ed. Agron. Monograph 9. ASA and SSSA, Madison, WI, p. 363-375.

Blecker S.W., Yonker C.M., Olson, C.G., and Kelly E.F. 1997. Paleopedologic and geomorphic evidence for Holocene climate variation, shortgrass steppe, Colorado, USA. Geoderma 76:113-130.

Blinnikov M., Busacca A., and Whitlock C. 2002. Reconstruction of the late Pleistocene grassland of the Columbia basin, Washington, USA, based on phytolith records in loess. Palaeo. Palaeo. Palaeo. 177:77-101.

Chadwick O.A., Brimhall G.H. and Hendricks D.M. 1990. From a black to a gray box – A mass balance interpretation of pedogenesis. Geomorphology 3:369-390.

Chadwick O.A., Kelly E.F., Merritts D.M., and Amundson R.G. 1994. Carbon dioxide consumption during soil development. Biogeochemistry 24:115-127.

Conley D.J. 2002. Terrestrial ecosystems and the global biogeochemical silica cycle. Global Biogeochemical Cycles 16:681-688.

Dahlgren R.A., Shoji S., and Nanzyo M. 1993. Mineralogical characteristics of valcanic ash soils. *In:* Shoji S., Nanzyo M. and Dahlgren R.A. (eds.) Volcanic ash soils, genesis, properties and utilization. Elsevier, NY. Pp.101-145.

Drees L.R., Wilding L.P., Smeck N.E., and Senkayi A.L. 1989. Silica in soils: quartz and disordered silica polymorphs. In: Dixon J.B. and Weed S.B. (eds.) Minerals in soils environmets. Soil Science Society of America, Madison Wi. pp. 913-974.

Drever J.I. 1994. Effect of plants on chemical weathering rates. Geochimica Cosmochimica Acta 58:2325-2332.

Egli M. and Fitze P. 2000. Formulation of pedologic mass balance based on immobile elements: A revision. Soil Science 165:437-443.

Epstein E. 1994. The anomaly of silicon in plant biology. Proc. Natl. Acad. Sci. USA 91:11-17.

Epstein E. 1999. Silicon. Annu. Rev. Plant Physiol. Plant Mol. Biol. 50:641-664.

Fraysse F., Pokrovsky O.S., Schott J., Meunier J.D. 2004. Surface properties, solubility and dissolution kinetics of phytoliths, from bamboos of Reunion Island. Goldschmidt 2004. Copenhagen, Denmark. Abstract 2.7.P13.

Fredlund G.G., and Tieszen L.L. 1994. Modern phytolith assemblages from the North American Great Plains. J. Biogeogr. 21:321-335.

Gaillardet J., Dupre B., Louvat P., Allegre C.J. 1999. Global silicate weathering and CO_2 consumption rates deduced from the chemistry of large rivers. Chemical Geology 159:3-30.

Gee G.W. and Bauder J.W. 1986. Particle-size analysis. *In* A. Klute (ed.) Methods of soil analysis. Part 1. 2nd ed. Agron. Monograph 9. ASA and SSSA, Madison, WI, p. 383-411.

Hossner L.R. 1996. Dissolution for total elemental analysis. *In* J.M. Bartels (ed.) Methods of soil analysis. Part 3. Chemical Methods. SSSA, Madison, WI, p. 49-64.

Jenny, H. 1941. Factors of soil formation; a system of quantitative pedology. McGraw-Hill, New York. 281p.

Jones L.H.P. and Handreck K.A. 1967. Silica in soils, plants and animals. Adv. Agron. 19:107-149.

Kelly E.F. 1990. Methods for extracting opal phytoliths from soil and plant material. Department of Agronomy. Colorado State University. Fort Collins, Colorado.

Kelly, E. F., B. D. Marino, and C. M. Yonker. 1993. Stable carbon isotope composition of paleosols: an application to the Holocene. Geophysical monograph No. 78. American Geophysical Union. pp. 233-239.

Kelly E.F., Chadwick O.A., and Hilinski T.E. 1998. The effect of plants on mineral weathering. Biogeochemistry 42:21-53.

Lajtha K., Jarrell W.M., Johnson D.W. and Sollins P. 1999. Collection of soil solution. *In* Robertson G.P., Coleman D.C., Bledsoe C. and Sollins P. (eds.) Standard Soil Methods for Long-Term Ecological research Oxford, New York. pp. 166-182.

Likens G.E. and Bormann F.H. 1995. Biogeochemistry of a forested ecosystem. 2nd ed. Springer-Verlag, New York. 162 p.

Lindsay W.L. 1979. Chemical equilibria in soils. John Wiley and Sons, NewYork. 449 pp.

Lovering T.S. 1959. Significance of accumulator plants in rock weathering. Bull. Geol. Soc. Am. 70:781-800.

Lucas Y., Luizao F.J., Chauvel A., Rouiller J., and Nahon D. 1993. The relationship between the biological activity of the rain forest and the mineral composition of the soils. Science 260:521-523.

Ma J.F., Miyake Y., Takahashi E. 2001. Silicon as a beneficial element for crop plants. *In* Datnoff L.E., Snyder G.H., and Korndorfer G.H (eds.) Silicon in Agriculture. Elsevier, New York. pp. 17-40.

Mahowald N., Kohfeld K., Hansson M., Balkanski Y., Harrison S.P., Prentice I.C., Schulz M., Rodhe H. 1999. Dust sources and deposition during the last glacial maximum and current climate: a comparison of model results with paleodata from ice cores and marine sediments. J Geophysical Res. 104:895-916.

Mason J.A., Jacobs P.M., Hanson P.R., Miao X., and Goble R.J. 2003. Sources and paleoclimatic significance of Holocene Bignell loess, central Great Plains, USA. Quaternary Res. 60:330-339.

Meunier J.D., Colin F., and Alarcon C. 1999. Biogenic silica storage in soils. Geology 27:835-838.

Markewitz D. and Richter D.D. 1998. The *bio* in aluminum and silicon geochemistry. Biogeochemistry 42:235-252.

McCulley R.F. and Burke I.C. 2004. Microbial community composition across the Great Plains: landscape versus regional variability. Soil Sci. Soc. Am. J. 68:106-115.

Mortlock R.A. and Froelich P.N. 1989. A simple method for the rapid determination of biogenic opal in pelagic marine sediments. Deep-Sea Res. 36:1415-1426.

Oviatt C.G. 1998. Geomorphology of Konza Prairie. *In* Knapp A.K. et al. (eds.) Grassland dynamics: Long-term ecological research in tallgrass prairie. Oxford University Press, New York. pp.53-47.

Parr J.F. 2002. A comparison of heavy liquid floatation and microwave digestion \ techniques for the extraction of fossil phytoliths from sediments. Review of Palaeobotany and Palynology 120:315-336.

Parr J.F., Lentfer C.J., and Boyd W.E. 2001. A comparative analysis of wet and dry ashing techniques for the extraction of phytoliths from plant material. Journal of Archaeological Science 28:875-886.

Piperno D.R. 1988. Phytolith analysis: An archaeological and geological perspective. Academic Press Inc., New York. 280 pp.

Raven J.A. 1983. The transport and function of silicon in plants. Biological Rev. 58:179-207.

Roberts H.M., Muhs D.R., Wintle A.G., Duller G.A.T., and Bettis III E.A. 2003. Unprecedented last-glacial mass accumulation rates determined by luminescence dating of loess from western Nebraska. Quaternary Res. 59:411-419.

Sangster A.G., and Hodson M.J. 1992. Silica deposition in subterranean organs. In Phytolith systematics. Rapp G. Jr., and Mulholland S.C. Plenum Press, New York. Pp. 239-251.

Sherrod L.A., Dunn G., Peterson G.A., and Kolberg R.L. 2002. Inorganic carbon analysis by modified pressure-calcimeter method. Soil Sci. Soc. Am. Journal 66:299-305.

Soil Survey Staff. 1992. Soil Survey Manual, USDA Handbook 18, Chapter 4. US Government Printing Office, Washington, D.C.

Stromberg C.A.E. 2004. Using phytolith assemblages to reconstruct the origin and spread of grass-dominated habitats in the great plains of North America during the late Eocene to early Miocene. Palaeo. Palaeo. Palaeo. 207:239-275.

Treguer P., Nelson D.M., Van Bennekom A.J., DeMaster D.J. Leynaert A., and Queguiner B. 1995. The silica balance in the world ocean: a reestimate. Science 268:375-379.

U.S. Dept. of Commerce, National Oceanic and Atmospheric Administration, National Climatic Data Center. 2002. U.S. Monthly climate normals 1971-2000. Asheville, N.C. electronic resource.

White A.F., and Blum A.E. 1995. Effects of climate on chemical weathering in watersheds. Geochim. Cosmochim. Acta 59:1729-1747.

White A.F., Blum A.E., Schulz M.S., Vivit D.V., Stonestrom D.A., Larsen M., Murphy S.F., and Eberl D. 1998. Chemical weathering in a tropical watershed, Luquillo Mountains, Puerto Rico: I. Long-term versus short-term weathering fluxes. Geochim. Cosmochim. Acta 62:209-226.

Wilding L.P. and Drees L.R. 1971. Biogenic opal in Ohio soils. Soil Sci. Soc. Am. Proc. 35:1004-1009.

Chapter III. THE RATIO OF GERMANIUM TO SILICON IN PLANT PHYTOLITHS: QUANTIFICATION OF BIOLOGICAL FRACTIONATION UNDER CONTROLLED EXPERIMENTAL CONDITIONS

Introduction

Germanium/silicon (Ge/Si) ratios have been applied in a variety of marine and terrestrial studies. The evident lack of biologic fractionation in marine systems via Si uptake in diatoms (Froelich et al. 1992, Bareille et al. 1998) and their study in marine sediment cores have been used to examine fluctuations of Si inputs and cycling over geologic scales and have been tied directly to diatom productivity (e.g. Froelich et al. 1992). In terrestrial systems, geochemical Ge fractionation pathways have been utilized to examine weathering processes in tropical and temperate ecosystems (Murnane and Stallard 1990, Filippelli et al. 2000, Kurtz et al. 2002, Derry et al. 2005). Little is known however, about the mechanisms responsible for the changes in Ge/Si ratios resulting from biological cycling in higher plants. The low Ge/Si ratios of ferns (*Cybotium* sp.) reported by Derry et al. (2005), suggest fractionation against Ge during plant uptake, but more data is needed to verify the magnitude and direction of this fractionation with higher plants across a variety of ecosystems.

The importance of silica in most higher plants is well understood (Jones and Handreck 1967, Raven 1983), although its inclusion as an essential plant element has only recently

been acknowledged (Epstein 1999, Richmond and Sussman 2003). Though more mechanical than physiological, the many important functions of Si in plants often manifest themselves when the plant is under environmental stress (Ma et al. 2001). Si benefits plants by increasing mechanical strength, yield, enzyme activity, and resistance to disease and pests (Epstein 2001). Salt tolerance, cold hardiness, metal toxicity resistance, and promotion of nodule formation in legumes are also enhanced by silica in the plant (Sangster and Hodson 1992, Epstein 2001). Reduction of transpirational water loss through development of a cuticle Si double layer and improved internal P utilization through enhanced rate of P translocation to the panicle (Ma et al. 2001), further demonstrate some of the many and varied benefits of plant silica.

Plants extract silica from the soil as monosilicic acid (H_4SiO_4), and transport it via the transpiration stream, where it precipitates as amorphous opal (Jones and Handreck 1967, Epstein 1999). Concentrations of monosilicic acid in soil solutions range from about 7-80 mg SiO_2/L depending on various soil properties including pH and mineralogy (Marschner 1986). Epstein (1994) reported a similar range of soil silicic acid concentrations (6-36 mg SiO_2/L), with contributions through mineral dissolution modified in part by plant uptake and mineral formation. Both passive and active transport are believed to operate in silicic acid movement into the plant. Passive uptake involves diffusion across the lipid component of the root cell membrane from higher soil solution concentrations to lower concentrations inside the root (Raven and Edwards 2001). Unlike most other elements taken up by plants, monosilicic acid is uncharged under common soil conditions and is not impacted by electropotential variations in the

rhizosphere. As Si accumulator plants have Si contents greater than those accounted for by transpiration, an active transport mechanism has been deduced. Where Hildebrand et al. (1997) have identified a Na-coupled active silicic acid transportation mechanism in diatoms; the physiology of active Si uptake in plants has yet to be identified (Raven 2001). In the plant, silicic acid polymerizes into amorphous silica bodies that are stored primarily in cell walls, cell luminas, and intercellular spaces near evaporating surfaces (Raven 1983, Sangster and Hodson 1992). Sangster (1977) found that Si was not deposited in photosynthetically active tissue of crabgrass (*Digitaria sanguinalis*). Sangster et al. (2001) have noted variations in Si content between leaves as well as non-uniformity within a single leaf. Commonly known as plant opal or phytoliths, these amorphous silica bodies are present in most plants, ranging in content from 0.5% or less in most dicotyledons, 1-3% in many dryland grasses, and up to 10-15% in some wetland plant species. Species within the latter two groups often actively transpire Si against the concentration gradient (Epstein 1994). This plant or biogenic silica is cycled back into the soil upon death and decomposition of the plants, and can be morphologically diagnostic to the species level, especially those phytoliths associated with epidermal cells (Piperno 1988). Phytolith abundance and distribution in the soil is regulated by the balance between plant production and the degree of chemical weathering (Alexandre et al. 1997), soil mineralogy (Dahlgren et al. 1993), and bioclimatic conditions (Kelly et al. 1998).

Early studies of plants and silica identified the positive relationship among plant Si content and such factors as soil silicic acid concentration and plant age (Jones and

Handreck, 1967). In ensuing decades, detailed studies of Si uptake, transport and deposition, primarily in agricultural plants, have been carried out under controlled greenhouse and field conditions. In a hydroponic study, Van der Vorm (1980) noted an increase in Si absorption among soybean (*Glycine max*), sunflower (*Helianthus* L.), wheat (*Triticum aestivum*), sugarcane (*Saccharum officianarum*), with rice (*Oryza sativa*), showing the greatest absorption, and plants in general taking up proportionally greater amounts of Si at lower external Si concentrations. According to the author, a Si concentration-driven transition from metabolic exclusion to metabolic absorption, both energy-dependent processes, explained the respective lower and greater plant Si contents compared to that expected through simple transpirational Si uptake. Jarvis (1987) attributed 40-70% of Si uptake for ryegrass (*Lolium perenne*) to a combination of passive and active Si uptake. In the same study Jarvis (1987) reported that up to 94% of Si taken up by wheat (*Triticum aestivum* L. cv. Sappo) was transported from roots to shoots, with older leaves containing up to 11.8% Si, evidence that Si is not re-translocated within the plant. Rafi and Epstein (1999) reported similar transfer rates of Si from roots to shoots (90%), allowing for the continual high Si uptake over the life of a wheat (*Triticum aestivum* L.) plant; immobilization in shoots as amorphous Si also short-circuits any feedback to the root to adjust Si uptake, preventing the stabilization of Si uptake over time. In another hydroponic study of wheat (*Triticum aestivum* L.), Sangster et al. (2001) showed rapid root silicification and a transfer up to 95% of the Si to the shoots. Two weeks after Si addition, Ma et al. (1989) reported that roughly 97% of the plant Si in rice (*Oryza sativa*) was in the form of amorphous silica, the remainder existing as colloidal and monomeric silicic acid. Phytolith content was measured at an average of 97% SiO_2

in a pot study of orchard grass (*Dactylis glomerata* L.) and wheat (*Triticum aestivum* L.) by Dietrich et al. (2003), in line with 77% SiO_2 (+ 9% H2O) for fescue (*Festuca silvatica*) measured by Bartoli (1985).

A paucity of data exists regarding the fractionation of Ge from Si during plant uptake. Using ^{68}Ge as a proxy for Si in the study of plant Si uptake, Takahashi et al. (1976) provided an unintended initial look at biologic Ge fractionation in variety of agricultural plants. Though Ge is geochemically similar to Si, and useful in studies of plant Si uptake, varying Ge concentrations in plants refute the claim of Ma et al. (2001) that plant roots can not distinguish Ge from Si in terms of uptake. Work by Derry et al. (2005) has shown lower Ge/Si plant phytolith values compared to concomitant soil solutions for ferns (*Cybotium* sp.) in Hawaii, and a similar trend has been reported in Chapter 4 for grasses of the Great Plains. Though these studies have inferred that plants biologically fractionate against Ge, the magnitude and direction have yet to be quantified under controlled growing conditions. Further isolation of the Ge/Si ratio of the source of Si will provide additional evidence of the magnitude and direction of Ge/Si fractionation by plants. Thus the objective of this study was to examine the magnitude and direction of Ge fractionation in grassland species under controlled conditions in order to clarify the role of vegetation in the terrestrial biogeochemical Si cycle.

Methods

I designed a series of experiments utilizing two growth mediums: 1) hydroponic solutions, and 2) soils, using native plants that are either dominant or co-dominant in the grassland regions of North America, and that possess C_3 and C_4 photosynthetic pathways.

Experiment 1- Hydroponic study

Seeds from western wheatgrass (*Agropyron smithii*), a plant that possesses a C_3 photosynthetic pathway, and little bluestem (*Schizachyrium scoparium*) and big bluestem (*Andropogon gerardii*), two plants that possess a C_4 photosynthetic pathway were germinated in a dilute nutrient solution (Table 3.1) on polypropylene mesh in the dark. Seedlings were transplanted 14 d after germination to 20-L PVC growth tanks aerated with compressed air passed through plastic tubing. The seedlings (approximately 8-10 per tank) were supported by polystyrene disks that floated on the solution surface. Two adjoining greenhouses were used for the study, a 'cooler' greenhouse with an ambient air temperature range of approximately 18-20 °C and a 'warmer' greenhouse with an ambient air temperature range of approximately 24.5-28 °C. For *Agropyron smithii*, three tanks each with concentrations of 10mg Si/L or 50mg Si/L (from $Na_2SiO_3 \cdot 9H_2O$) were set up in both greenhouses. For *Schizachyrium scoparium* and *Andropogon gerardii,* three tanks each with Si levels of 50mg/L were set up in the 'warmer' greenhouse, upon completion of the *Agropyron smithii* experiment. The Si levels were chosen to represent monosilicic acid levels near the lower and higher range of those typically found in soil solution (Lindsay 1979, Marschner 1986, Epstein 1994). Relative humidity levels in both greenhouses were programmed to range between 20-75%. Conductivity and pH levels

were monitored throughout the study using an Orion 105A conductivity meter and an Orion 720A pH meter. Nutrient solutions were changed approximately every 6-7 days in order to maintain adequate nutrient levels and relatively constant Si concentrations, which were monitored throughout the study. Subsamples of nutrient solution were taken throughout the study to measure Ge/Si levels. A slight yellowing of the leaves on most plants, likely indicative of minor nutrient deficiencies, was observed throughout the study. *Agropyron smithii* plants were harvested at 84 d, just as a few of the plants started to set seed. *Schizachyrium scoparium* and *Andropogon gerardii* plants were harvested at 65 d, prior to the plants setting seed. Shoots and roots were separated and oven dried at 60 °C immediately after harvest.

Experiment 2 - Soil study

To further examine the magnitude, direction and variability of biologic Ge fractionation (as earlier hydroponic trials failed to sustain growth of blue grama (*Bouteloua gracilis)*, buffalograss (*Buchloe dactyloides*), and indian ricegrass (*Oryzopsis hymenoide*)), a study using two different soil mediums was initiated. Seeds of *Agropyron smithii*, *Bouteloua gracilis*, *Buchloe dactyloides*, *Oryzopsis hymenoide*, *Schizachyrium scoparium* and *Andropogon gerardii* were planted in two different soils; surface horizon soil from the shortgrass steppe in eastern Colorado (Chapter 2) and potting mix consisting of vermiculite, Canadian sphagnum peat moss, perlite, and dolomitic limestone (Sun Gro Metro-Mix 200, Sun Gro Horticulture, Bellevue, WA). Three replicates of each species were planted in each of the two soils. Soil moisture was maintained approximately at field capacity with a diluted nutrient solution (Table 3.1). Plants were harvested at 60 d,

prior to the plants setting seed. Shoots were separated from roots and oven dried at 60 °C immediately after harvest. Soil water Ge/Si, thought to represent the source of the Ge and Si taken up by the plant, was measured by saturated paste equilibration.

Phytolith extraction

Plant samples from both studies were cleaned to remove soil contamination, dry ashed, then treated to remove non-siliceous material in a method adapted from Piperno (1988), Kelly (1990), and Parr et al. (2001). Oven-dried (55-60 °C) plant material was cut into 2-3 cm lengths, and washed in a mixture of 5% sodium hexametaphosphate, 10% hydrochloric acid and deionized water. After thorough rinsing, the sample was washed in 70% ethanol, and rinsed with deionized water. After drying again at 55-60 °C, a subsample of the cleaned plant material was weighed into a Ni crucible, ashed at 500 °C for 1 hour, allowed to cool in a desiccator and weighed. The ash was washed in warm, 10% hydrochloric acid, rinsed with deionized water, washed in hot 30% hydrogen peroxide, filtered through a 0.20μm filter, and rinsed thoroughly with deionized water. After drying at 55-60 °C, the sample was allowed to cool in a desiccator, weighed, and stored in a plastic vial. Phytolith concentration was calculated gravimetrically (Ma et al. 2001).

Si and Ge analysis

Plant samples were dissolved in 2M NaOH and analyzed for Si content by spectrophotometer at 812 nm using a blue silicomolybdous acid method (Mortlock and Froelich 1989). Aliquots of the dissolved phytolith were neutralized with dilute nitric

acid prior to Ge analysis. Germanium concentrations were measured on sample aliquots by isotope-dilution hydride-generation inductively coupled plasma mass spectrometry (ICP-MS), after spiking dissolved samples with a ^{70}Ge tracer solution and allowing to equilibrate overnight. Si concentrations in the nutrient solution were analyzed using the same silicomolybdous blue method. Germanium concentrations in the nutrient solution were analyzed by isotope-dilution hydride-generation. To dissolve the soils, a mixture of HNO_3-HCl-HF was added to 50 mg of soil in a Teflon container, tightly sealed, and then heated with a microwave digester. After cooling, saturated boric acid was added and the container was again heated in a microwave digester. After cooling, samples were diluted with deionized water. Soil Si was determined by ICP-AES analysis after Li-metaborate fusion and dissolution in nitric acid. Germanium was analyzed by isotope-dilution hydride-generation.

Results

Experiment 1- Hydroponic study

Agropyron smithii

Daily minimum and maximum nutrient solution temperatures over the course of the experiment are presented in Figure 3.1a. For the 'cool' greenhouse, average minimum (16.7 °C), maximum (20.9 °C), and daily average temperatures (18.7 °C) were lower than those of the 'warm' greenhouse (min. 19.2 °C, max. 25.1 °C, daily avg. 22.1 °C; p-value <0.0001). Average relative humidity throughout the experiment was slightly, though not statistically higher (p-value = 0.1132) in the warm greenhouse (42.6%) compared to the cool (38.1%). Humidity fluctuations (Figure 3.1b) reflect the 25-70% range set for both

greenhouses. Nutrient solution pH (Figure 3.2a) and electrical conductivity (Figure 3.2b) were measured approximately weekly for three of the six containers in each greenhouse. The average pH values were statistically similar (p-value = 0.868) ranging from 5.7 to 6.0. The addition of slightly more HCl at the onset of the experiment (used to offset the alkalinity of the sodium metasilicate), likely accounted for the lower pH values. Average electrical conductivity values were slightly lower among the low-Si containers (2.37 dS/m) compared to the high Si-containers (2.66 dS/m; $p < 0.0001$). The higher salinity in the high-Si containers reflects the greater amount of sodium metasilicate.

Figures 3.3a and 3.3b list periodic measurements of Si concentrations for the same subset of containers. The target starting concentration for the low-Si containers was 10 mg Si/L; the actual concentration averaged 10.82 mg Si/L (s.d.= 0.16). The target starting concentration for the high-Si containers was 50 mg Si/L; the actual concentration averaged 53.33 mg Si/L (s.d.= 0.82). In each case, the slightly higher actual values may reflect a different calculated molecular weight than was listed on the container, given the hygroscopic nature of sodium metasilicate. In both the low-Si and high-Si containers, Si content decreased over time (Figures 3.3a and 3.3b), likely due to the increased Si uptake with increased plant growth.

Table 3.2 presents a summary of leaf, stem, and root data for *Agropyron smithii*. C/N ratios for the high-Si leaves were slightly higher (p-value = 0.0448) than the low-Si leaves. On average, the high-Si leaves (approx 6.0 % Si) contained roughly twice as much plant Si as those grown in the low-Si solution (3.1% Si; p-value = 0.0005). Stem

Si concentrations were roughly 2.5 times lower than those of the leaves for plants within the same solution (p-value = 0.0006). Root Si concentration (1.0%) was lower than both leaf and stem concentrations. Molar concentrations of Si and Ge and the Ge/Si ratio are presented in Table 3.2; variability in these concentrations are due to variation in sample weights used in the analysis and do not correlate directly to plant Si concentration. Average low-Si plant nutrient solution Ge/Si values are statistically higher than Ge/Si values for the high-Si plant nutrient solutions (0.53 and 0.48 respectively; p-value = 0.0264). Ge/Si values for high-Si leaves, though slightly higher on average than the Ge/Si values of the low-Si leaves are statistically similar (p-value = 0.1485). Stem Ge/Si values were roughly twice as high as Ge/Si values for leaves (0.12 vs. 0.07 respectively; p-value = 0.0005). The root Ge/Si value for the root sample (0.12) was similar to that of the stems.

Schizachyrium scoparium and Andropogon gerardii

Greenhouse growing conditions are pictured in Figure 3.4a. Though set up in the same 'warm' greenhouse as the *Agropyron smithii*, the water temperatures on average were slightly lower compared to conditions during the *Agropyron smithii* experiment (22.1°C vs. 20.5 °C respectively; p-value <0.0001), as was relative humidity (33.0% vs. 42.6% respectively; p-value 0.0151). Nutrient solution chemistry is depicted in Figure 3.4b. Electrical conductivity values were slightly higher than those of the 50 mg Si/L conductivity values of the *Agropyron smithii* experiment (3.09 dS/m vs. 2.66 dS/m respectively; p-value <0.0001). Average pH values were statistically similar between the *Agropyron smithii* experiment (5.8) and this experiment (5.5; p-value 0.2000). Silicon

contents throughout the course of the experiment followed a similar pattern to those of *Agropyron smithii* experiment, with average initial silicon levels of 52.7 mg Si/L decreasing to an average of 49.4 mg/L as plant growth increased. Table 3.3 presents a summary of plant data. Given the lower total biomass due to the shorter duration of this experiment compared to the *Agropyron smithii* experiment, leaves and stems were combined for analysis. Average plant Si values between *Schizachyrium scoparium* and *Andropogon gerardii* were similar (4.5% vs. 4.2% respectively; p-value = 0.643). Ge/Si values of the leaf/stem tissues of both species were also similar and comparable to *Agropyron smithii.*

Experiment 2 – Soil study

Table 3.4 lists plant data for the soil-grown graminoid Ge/Si uptake experiment. As mentioned previously, a wider variety of range grasses were grown in 2 different soil mediums to compare to the Ge/Si values of those grown hydroponically. On average, the grasses as a group exhibited statistically similar C/N ratios for the field soil compared to the potting soil (15.8 vs. 16.4 respectively; p-value = 0.691). Plant Si values were roughly 2.5 times higher for grasses grown in field soil compared to potting soil (4.8 vs. 1.9%, respectively; p-value = 0.0022). This trend can be partially explained by the higher content of soluble Si associated with the field soil compared to the potting soil (23.8 mg Si/L vs. 17.7 mg Si/L, respectively; p-value 0.0453). Ge/Si values of the soluble Si were greater for the field soil compared to the potting soil (0.33 vs. 0.16 respectively). The Ge/Si values of the plants grown in field soil vs. their counterparts grown in potting soil were also significantly different (0.12 vs. 0.09 respectively; p-value = 0.0020.)

Discussion

A positive correlation between plant Si content and solution Si concentration has been observed by researchers for a variety of plant species (e.g. Van der Vorm 1980, Jarvis 1987, Rafi and Epstein 1999). Though transpiration was not measured in this study, the relatively high plant Si levels of *Agropyron smithii* suggest an active Si uptake mechanism, which is typical of many graminoids (i.e. greater plant Si content than would exist through passive transpirational uptake alone; Van der Vorm 1980, Ma et al. 2001). Despite differences in plant Si content, greenhouse temperature, conductivity, nutrient solution Si content, and the slightly higher Ge/Si value for the low-Si systems compared to the high-Si systems, Ge/Si plant phytolith values for the leaves were statistically similar, ranging from 0.04 to 0.11. The low-Si systems realized a slightly greater degree of fractionation against Ge (88%) compared to 83% for the high-Si systems (Table 3.2 and Figure 3.5). The slightly higher nutrient solution Ge/Si values for the low-Si system (0.53 vs. 0.48 for the high-Si systems) could be a reflection of the greater Ge fractionation by the plants grown in the low-Si solution, creating a nutrient solution slightly more enriched in Ge compared to the high-Si systems. Despite the slight drop in nutrient solution Si content over time for both low- and high-Si systems the Ge/Si values did not drift appreciably over time (i.e. as the plant Si is isolated from the source Si – since the plant discriminates against Ge, the source Ge/Si values should become enriched in Ge over time), implying that weekly replacement of the nutrient solution was adequate to minimize any impact through a Rayleigh distillation type process.

Agropyron smithii stems had less plant Si and higher Ge/Si (i.e. less fractionation against Ge) than the leaves. Though only one composited root sample was measured, the low Si content and Ge/Si value suggests that Ge is excluded at the solution/root interface and not accumulated in the root. Possible fractionation mechanisms are discussed later. A lack of root Si accumulation has been reported in other greenhouse studies (Jarvis 1987, Ma et al. 1989) as the root tends to reach equilibrium Si levels fairly early in growth, while stem and leaf Si contents tend to increase during the growing cycle. In a study of plant Si uptake, Takahashi et al. (1976) reported that removal of roots from rice plants dramatically decreased Ge concentration in the shoots, suggesting a root control of Ge uptake, and that Ge tends to be concentrated in the stem, which was seen in the greater Ge/Si stem values compared to the leaves of *Agropyron smithii*.

Plant Si contents were similar among *Schizachyrium scoparium* and *Andropogon gerardii* and slightly lower than *Agropyron smithii*, which could be both a function of experiment duration (85 days vs.60 days for the former) and species. As differences in conductivity and nutrient solution temperature did not have any impact on Ge discrimination for *Agropyron smithii*, it is likely that the differences in growing conditions among the hydroponic experiments also did not impact Si uptake and Si plant content. Similarities between *Schizachyrium scoparium* and *Andropogon gerardii* in the Ge/Si phytolith values (Table 3.3), and the similarity of these values among the three graminoid species, suggest a similar magnitude and direction of biologic Ge fractionation. Results from Takahashi et al. (1976), in a greenhouse experiment examining the uptake of Si by various plant species also showed biologic fractionation against Ge. Starting with a Ge

spiked nutrient solution (Ge/Si = roughly 39,000 µmol/mol), phytoliths extracted from rice and wheat (the most comparable species to the current study) fractionated against Ge by 53 and 55% respectively compared to Si. While in the current study, taken as a group, *Agropyron smithii*, *Schizachyrium scoparium* and *Andropogon gerardii* fractionated against Ge by an average of 82%. Species differences and the much greater Ge content could account, in part, for the differences in fractionation. Ge fractionation values for the other species in the Takahashi et al. (1976) study (maize (*Zea mays*) 95%, kidney bean (*Phaseolus vulgaris*) 31%, tomato (*Solanum lycpersicum*) - 27%, morning glory (*Ipomoea jaegeri*) 4%, suggest discrimination processes related to species and/or Ge uptake mechanism: passive (*Phaseolus vulgaris*), rejective (*Oryza sativa*, *Triticum aestivum*, *Zea mays*), and active (*Solanum lycpersicum* and *Ipomoea jaegeri*), versus Si uptake mechanisms: passive (*Phaseolus vulgaris*), rejective (*Ipomoea jaegeri* and *Solanum lycpersicum*), active (*Oryza sativa*, *Triticum aestivum*, *Zea mays*).

Though the Si sources in the soil mediums were not isolated to the level of the Si used in the nutrient solution study, comparing Ge/Si phytolith values of different plants grown in the same soil can provide useful information regarding Ge discrimination, assuming the Ge/Si of the soil solution represents the Si source utilized by the plants. Little variability existed among Ge/Si phytolith values for the grass species within each soil medium (potting soil phytolith Ge/Si values averaged 0.09 ± 0.007; field soil average phytolith Ge/Si values averaged 0.12 ± 0.004; Table 3.4), suggesting that species-driven fractionation against Ge, at least among grasses, is not significant. However, differences between the potting soil and field soil Ge/Si values, and differences between the

magnitude of fractionation between the two soils compared with the soil solution Ge/Si, suggest that the different growing conditions and/or Si sources may be impacting Ge speciation or reactivity that in turn impact the degree of fractionation. The three species common to both the nutrient solution and soil studies also showed different degrees of Ge/Si fractionation compared to the source Ge/Si values. *Agropyron smithii*, *Schizachyrium scoparium* and *Andropogon gerardii* grown in nutrient solution showed greater discrimination against Ge than their soil-grown counterparts. Though Si levels between nutrient solution (approximately 10 mg Si/L and 50 mg Si/L), field soil (approximately 23 mg Si/L) and potting soil (approximately 18 mg Si/L) were relatively similar, other differences in growing conditions may have contributed to differences in the magnitude of Ge fractionation. Conditions in the field (i.e. plants grown in soil) are likely closer to equilibrium than conditions present in the nutrient solution (levels of which undergo dramatic replenishment), and may in part explain the nutrient solution conditions producing the greater fractionation seen in the nutrient solution plants. Using carbonate formation as an example, systems far from chemical equilibrium, where reaction rates may be quite fast (and the bicarbonate ion cannot isotopically equilibrate with dissolved CO_2), are likely to produce carbonate minerals with a greater degree of fractionation than those produced under conditions of slower precipitation that are closer to equilibrium.

Biological fractionation of Ge versus Si

A comparison of the greenhouse experimental data to data obtained from field studies (Chapter 4 and Derry et al. 2005) provides another avenue of examining biologic Ge

fractionation. In the greenhouse soil experiments, the Si sources were more homogeneous than those encountered in the field. Though field soil was used as one of the growing mediums in the greenhouse study, it was taken from one "horizon", whereas in the field, soluble Si sources available to the plant contain soluble Si from multiple horizons with potentially different Ge/Si signatures (Chapter 4, Derry et al. 2005). Though greater variability and less certainty of source Ge/Si values exist in the field, similar fractionation mechanisms allow for at least a qualitative comparison. From Chapter 3, soil water Ge/Si values for the surface horizons averaged 0.69, and plant phytolith Ge/Si values averaged 0.31, a fractionation factor against Ge (compared to Si) of roughly 55% as compared to Si. Similar graminoid species grown in the greenhouse in the two different soils exhibited similar fractionation against Ge; field soil soluble-Si Ge/Si values averaged 0.33, plant phytolith Ge/Si values averaged 0.12, for a 62% fractionation against Ge; potting soil soluble-Si averaged 0.16, plant phytolith Ge/Si averaged 0.09, for a 44% fractionation against Ge. Though plant silica content of ferns (Polypodiaceae) varies widely (Piperno 1988, Ma et al. 2001), the relatively low plant-Si content (avg. = 1.0% Si, n=11) of the *Cybotium*, *Dicranopteris* and *Diplazium* genera reported in Derry et al. (2005), would likely classify them as somewhere between passive to rejective Si accumulators. In that study, average soil water Ge/Si values for the surface horizons were 0.34, whereas the average plant Ge/Si values were 0.10;indicating that plants are fractionating against Ge by roughly 60%. Though more study is needed, it appears that degree of Si accumulation does not impact the general mechanisms of plant discrimination of Ge during uptake. Despite the completely different climate and soils associated with Hawaiian ferns vs. Great Plains grasses, both plant groups appear to

discriminate against Ge along the same order of magnitude, when comparing values of $Ge/Si_{phytolith}$ vs. $Ge/Si_{source\text{-}Si}$ (Figure 3.5).

Potential discrimination mechanisms

Toxicity

Ge toxicity to plants, often characterized by brown spots on the leaves, suggests that Ge physiology may differ from Si (Matsumoto et al. 1975). Even low concentrations of Ge were found to inhibit root growth and hypocotyl elongation in a variety of plants in a study by Sankhla and Sankhla (1967). Halperin et al. (1995) hypothesized that weaker Ge-O bonds may disrupt normal function of the cell wall, leading to the leaf necrosis seen in a Ge uptake experiment with hydroponically grown barley. The authors also noted that Ge levels where necrosis occurs were generally greater than those that would normally occur in nature. However, given the ability of Ge to replace boron in certain physiological functions (e.g. maintaining plasma membrane integrity, assisting in cell growth, and complexing phenolics to reduce their toxicity), Ge has been shown to serve a physiological function (Loomis and Durst, 1992; Cakmak et al. 1995), unlike Si, which is still largely assumed to benefit the plant through structural and not physiological means (Epstein 2001). Regardless, physiological discrimination against Ge remains uncertain.

Differences in speciation and reactivity between Ge and Si

Differences in speciation and reactivity between Ge and Si may also help explain of the biologic Ge discrimination. Under a wide range of environmentally common pH conditions, aqueous Si is largely present as monosilicic acid (pK1= 9.7 and pK2 = 11.9),

and is largely unreactive with other compounds (Poulson et al. 1997, Pokrovski and Schott 1998). Though Ge also exists primarily as monogermanic acid under these same conditions (pK1 = 8.5 to 8.8 and pK2 = 12.7: Ingli 1963; Glockling 1969), differences in coordination and dissociation chemistry, could account for differences in availability and uptake. As Ge can enlarge its coordination number from 4 to 6, stable organo-mineral complexes such as Ge-citrate for example, can alter both the size and charge of the ion (Pokrovski and Schott 1998, Pokrovski et al. 2000), whereas Si exhibits a much weaker affinity for aqueous organic ligands due to its strong preference for tetrahedral coordination. Such metal-organic complexes can decrease availability compared to free cations or hydroxide forms in soil-less media; however, chelates can increase micronutrient availability in soils where mobility and concentration are more common (Marschner 1986). The only ligand added to the nutrient solution of this study was Fe-EDDHA, which may have complexed with Ge and impacted Ge uptake; presence of ligands in the soils was not examined. Aqueous inorganic Ge complexes have also been reported; in the presence of phosphate or sulfate ions, $GeO_2(SO_4)^{2-}$ and $HGeO_2(PO_4)^{2-}$ can form (Glockling 1969). However, Kubicki and Heaney (2003) proposed a silica transport and precipitation mechanism via hypercoordinate Si-organic complexes (which may be more prevalent in nature than previously thought; e.g. Pokrovski and Schott 1998, Poulson et al. 1997), which could potentially impact Ge/Si ratios.

Comparison to other biologically mediated isotopes

Kinetic fractionation due to differences in molecular weights between isotopes has been shown to result in preferential uptake of the lighter isotope. The element calcium

presents a reasonably close analogue to Si in terms of biocycling, also lacking reduction-oxidation reactions and gaseous phases that can impact isotopic fractionation as seen in other biologically mediated elements (e.g. C, O, N). Schmitt et al. (2003) reported that beech trees prefer the lighter isotope (^{40}Ca) comparing $\delta^{44}Ca$ plant values ($\delta^{44}Ca$ = -1.63 and -2.46 for leaves and branches respectively) to those of the isotopically heavier source rock ($\delta^{44}Ca$ = -1.48) and soil solution ($\delta^{44}Ca$ = -0.11). This trend of preferential uptake of the lighter isotope (^{40}Ca) was also noticed in an earlier study of date palms by Platzner and Degani (1990), and may drive the difference in Ge versus Si uptake in plants.

Conclusions

Biologic Ge fractionation was observed in studies of grasses grown in both nutrient solution and soil, with the former exhibiting a greater magnitude of Ge fractionation. Discrimination of Ge during uptake likely occurs at the root/solution interface as evidenced by both the lower root and shoot Si contents and slightly higher root and shoot Ge contents. Among the graminoids studied, fractionation appears to be independent of species. Regardless of the fractionation mechanism (e.g. physiological, kinetic), inductively and deductively observed biologic Ge fractionation increases the understanding of terrestrial Ge/Si relationships and the use of Ge/Si as a tracer in terrestrial weathering studies.

Table 3.1 - Nutrient solution composition.

Macronutrients and silicon		Micronutrients[1]	
Compound	Concentration in solution (mM)	Compound	Concentration in solution (μM)
$Ca(NO_3)_2$	4	H_3BO_3	20
KNO_3	6	$MnSO_4 \cdot H_2O$	1.2
$NH_4H_2PO_4$	0.9	$ZnSO_4 \cdot 7H_2O$	1.7
$MgSO_4$	1	$CuSO_4 \cdot H_20$	0.5
Na_2SiO_3[2]	see footnote	H_2MoO_4	0.5
		$Ni(NH_4)_2(SO_4)_2 \cdot 6H_2O$	0.2
		Fe-EDDHA	200

[1] Micronutrients were mixed in a concentrated form in solution then added to the water, producing the final concentration listed. [2] Na_2SiO_3 was added to the water, followed by 1M HCl to adjust pH to approximately 5.5-6.0, then the nutrients.

Table 3.2 - Hydroponic study - *Agropyron Smithii*, selected plant data.

Sample	**C/N**		**[1]Plant Si (%)**		**[2]Si (μmol/g)**		**Ge (pmol/g)**		**[3]Ge/Si x 10^{-6}**	
	leaf	stem	leaf	stem	leaf	stem	leaf	stem	leaf	stem
10C-1	9.6	18.2	3.0	1.1	8.0	6.4	.58	.64	.07	.10
10C-2	9.8		2.7		4.7		.39		.08	
10W-1	9.5		2.7		8.0		.51		.06	
10W-2			3.5	1.5	10.3	7.3	.46	.73	.04	.10
10W-3	9.3		3.6	1.7	7.5	6.3	.46	.73	.06	.12
50C-1		15.3	5.5	2.7	10.9	9.2	.77	1.13	.07	.12
50C-2	10.2		5.6	2.6	7.9	7.9	.68	.95	.09	.12
50C-3			5.6		6.7		.77		.11	
50W-1	11.5	14.6	5.4	2.1	8.1	5.0	.62	.87	.08	.17
50W-2	11.0		7.9		10.7		.72		.07	
50W-3	9.7		7.0	2.6	10.9	8.3	.76	.90	.07	.11
roots[4]	14.7		1.0		4.2		.53		.12	

[1] based on dry weight of plant; [2] based on a subsample of plant Si, but not directly correlated to plant Si (%); [3] Ge/Si values are a molar ratio; [4] roots represent a composite subsample of all the plant samples; empty cells – not determined. 'C' represents containers located in the 'cool' greenhouse; 'W' represents containers located in the 'warm' greenhouse. '10' represents the low Si treatments of 10mg Si/L; '50' represents the high Si treatments of 50mg Si/L; '1', '2', or '3' represent replicates.

Table 3.3 - Hydroponic study - *Schizachyrium scoparium* and *Andropogon gerardii*, selected plant data.

Sample	C/N	Plant Si[1] (%)	Si[2] (µmol/g)	Ge (pmol/g)	Ge/Si x 10^{-6}
Ag-1	14.6	4.2	8.9	.62	.07
Ag-2	13.3	4.4			
Ag-3	14.4	4.1	7.2	.48	.07
Ss-1	12.5	4.8	6.0	.60	.10
Ss-2	12.7	5.4			
Ss-3	13.4	3.4	6.3	.46	.07

[1] – based on dry weight of plant; [2] – based on a subsample of plant Si, but not directly correlated to plant Si (%).

Table 3.4 - Selected plant data for the soil grown graminoids

Sample	C/N		[1]Plant Si (%)		[2]Si (µmol/g)		Ge (pmol/g)		[3]Ge/Si x 10^{-6}	
BOGR	14.3	16.3	7.3	2.4	10.4	6.1	1.29	.49	.12	.08
BUDA	14.7	17.8	5.9	2.0	10.8	8.1	1.48	.93	.14	.11
AGSM	15.3	18.9	2.5	0.9	8.0	6.5	.94	.56	.12	.09
ORHY	12.7	11.1	4.8	1.3	9.0	7.0	1.1	.51	.11	.07
ANGE	19.5	16.9	4.1	2.1	9.8	5.8	1.25	.47	.13	.08
SCSC	18.4	17.7	4.5	2.7	9.9	9.6	1.16	1.06	.12	.11

BOGR = *Bouteloua gracilis*, BUDA = *Buchloe dactyloides*, AGSM = *Agropyron smithii*, ORHY = *Oryzopsis hymenoides*, ANGE = *Andropogon gerardii*, and SCSC = *Schizachyrium scoparium*. For each parameter, the left-hand column represents plants grown in field soil, the right-hand column represents plants grown in potting soil; [1] based on dry weight of plant; [2] based on a subsample of plant Si, but not directly correlated to plant Si (%). [3] Ge/Si values are a molar ratio.

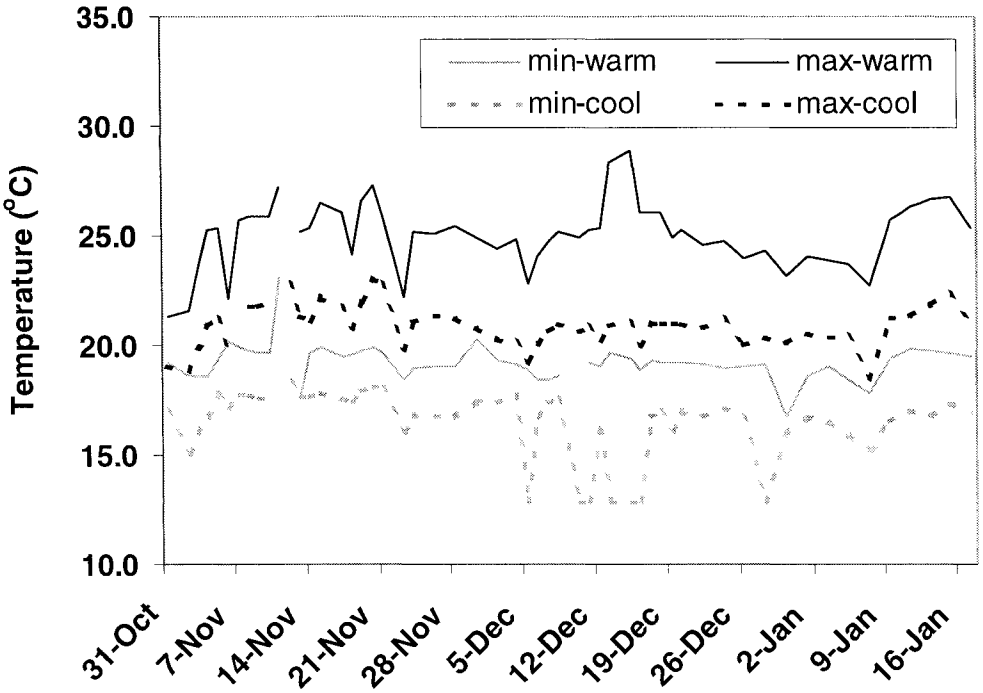

Figure 3.1a - Greenhouse growing conditions (nutrient solution temperature), for *Agropyron smithii* over the course of the experiment; min-warm = daily minimum nutrient solution temperature for the 'warm' greenhouse; max-warm = daily maximum nutrient solution temperature for the 'warm' greenhouse; min-cool = daily minimum nutrient solution temperature for the 'cool' greenhouse; max-cool = daily maximum nutrient solution temperature for the 'cool' greenhouse. Gaps in the data represent days when measurements were not taken.

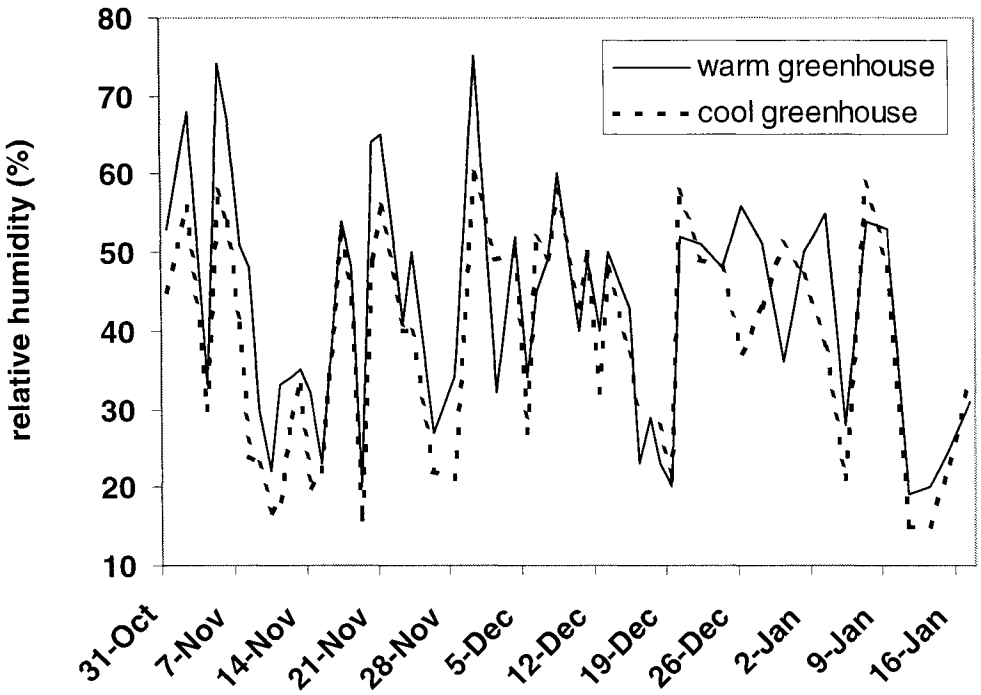

Figure 3.1b - Greenhouse growing conditions (relative humidity), for *Agropyron smithii* over the course of the experiment.

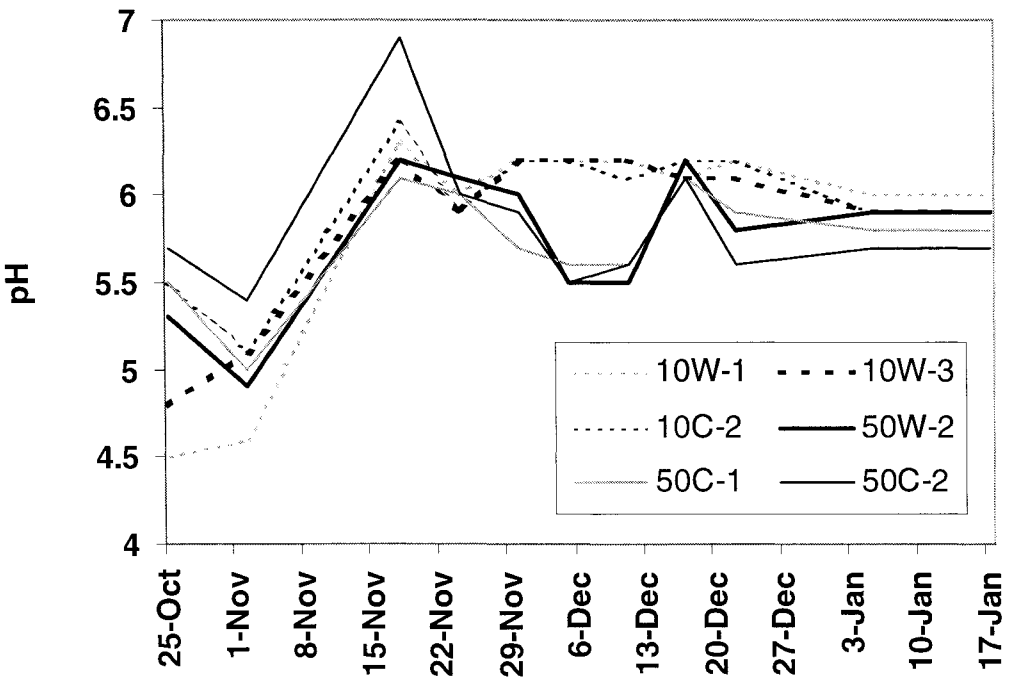

Figure 3.2a - Nutrient solution pH for *Agropyron smithii* over the course of the experiment. '10' represents low-Si containers; '50' represents high-Si containers; 'C' represents containers located in the 'cool' greenhouse; 'W' represents containers located in the 'warm' greenhouse. 1,2,or 3 represent replicates.

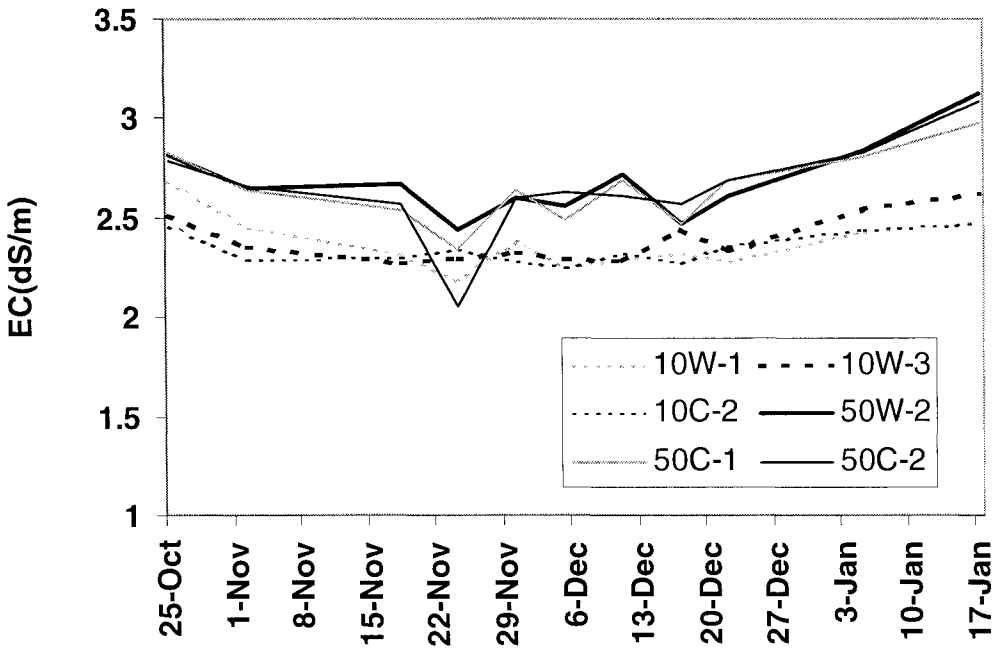

Figure 3.2b - Nutrient solution conductivity (EC) for *Agropyron smithii* over the course of the experiment. '10' represents low-Si containers; '50' represents high-Si containers; 'C' represents containers located in the 'cool' greenhouse; 'W' represents containers located in the 'warm' greenhouse. 1,2,or 3 represent replicates.

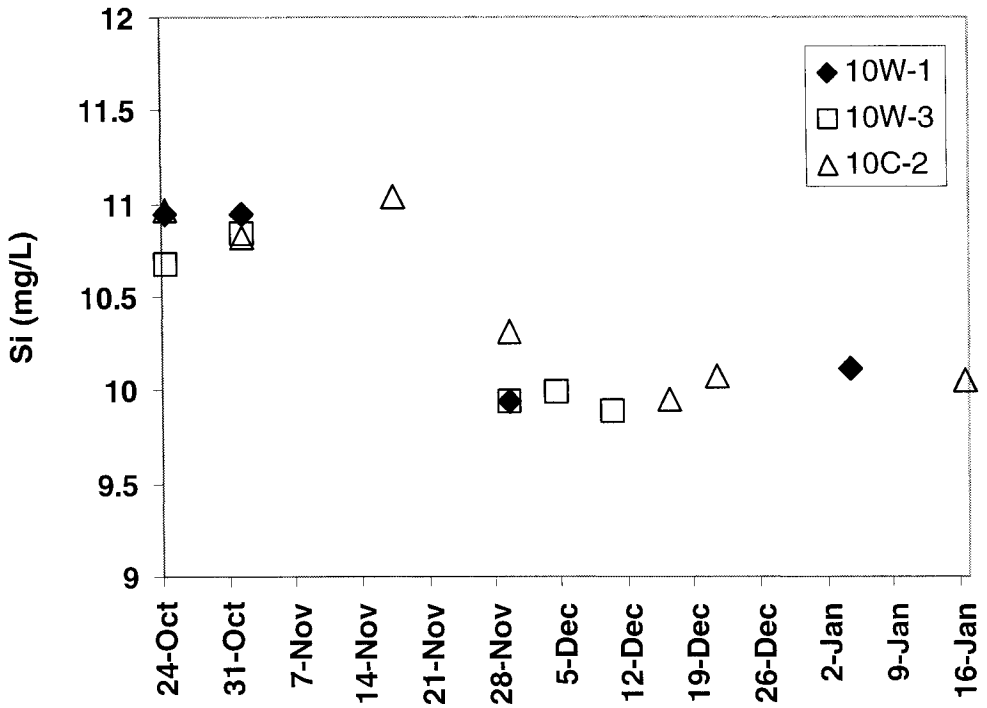

Figure 3.3a - Nutrient solution low Si concentrations for *Agropyron smithii* over the course of the experiment. '10' represents low-Si containers; 'C' represents containers located in the 'cool' greenhouse; 'W' represents containers located in the 'warm' greenhouse. 1,2,or 3 represent replicates.

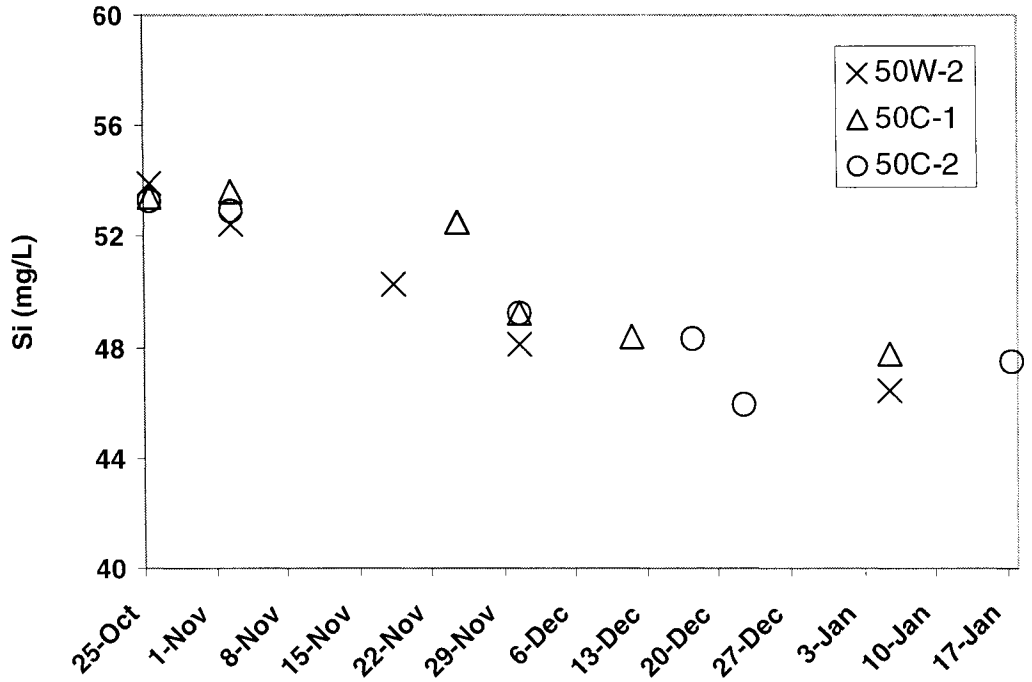

Figure 3.3b - Nutrient solution high Si concentrations for *Agropyron smithii* over the course of the experiment. '50' represents high-Si containers; 'C' represents containers located in the 'cool' greenhouse; 'W' represents containers located in the 'warm' greenhouse. 1,2,or 3 represent replicates.

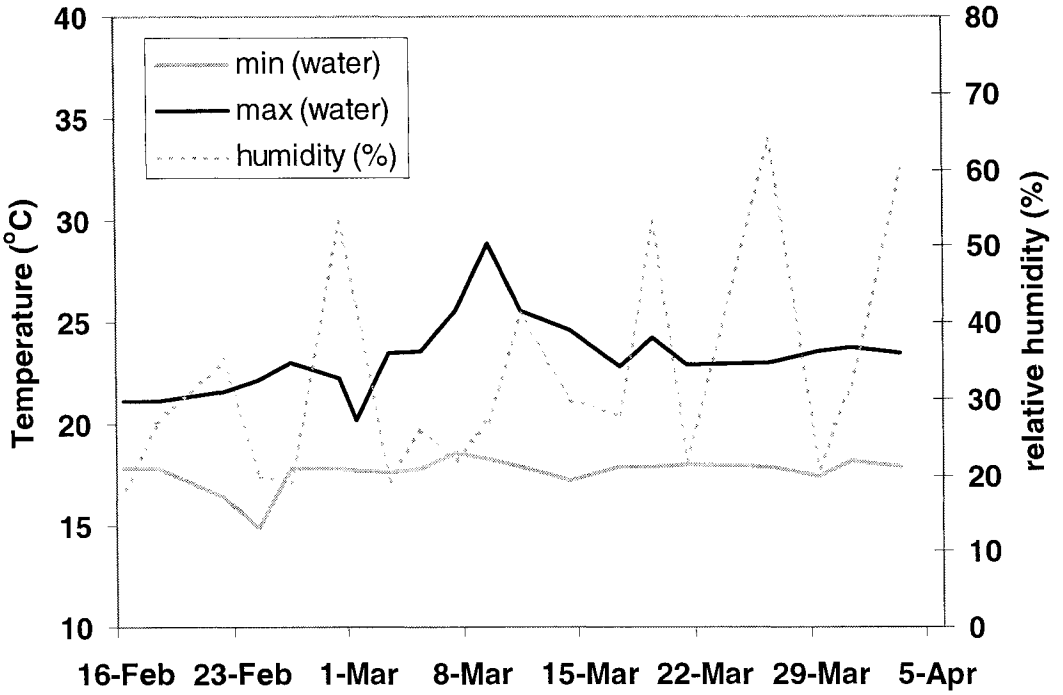

Figure 3.4a - Greenhouse growing conditions (nutrient solution temperature and relative humidity), for *Schizachyrium scoparium* and *Andropogon gerardii* over the course of the experiment.

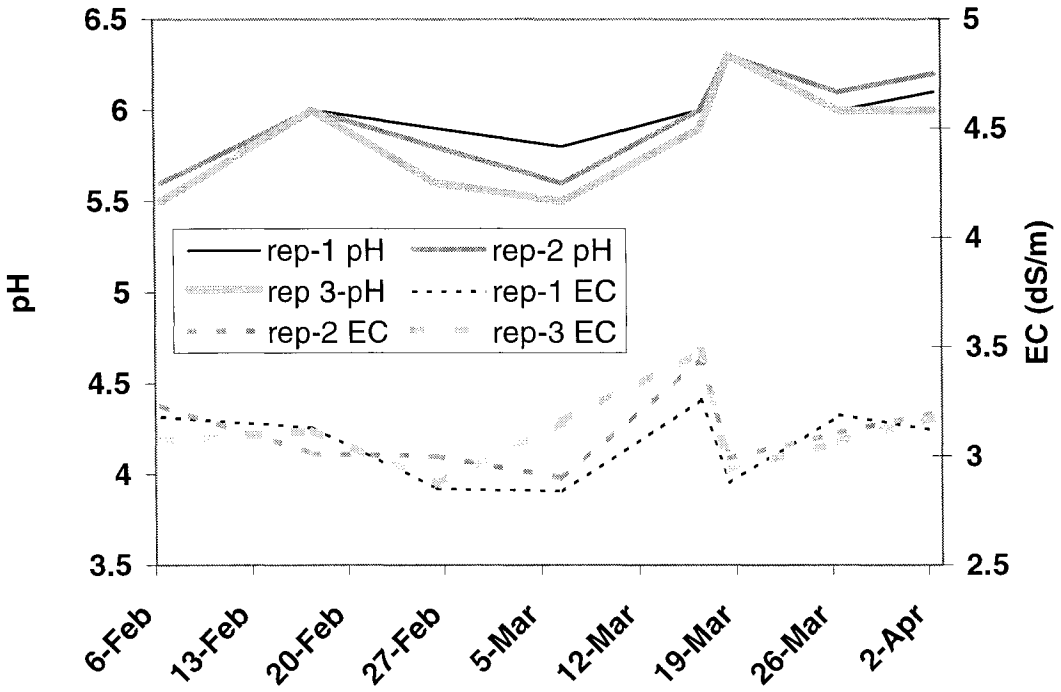

Figure 3.4b - Nutrient solution pH and conductivity (EC) for *Schizachyrium scoparium* and *Andropogon gerardii* over the course of the experiment. 'rep-1, 2 or 3' represent replicates.

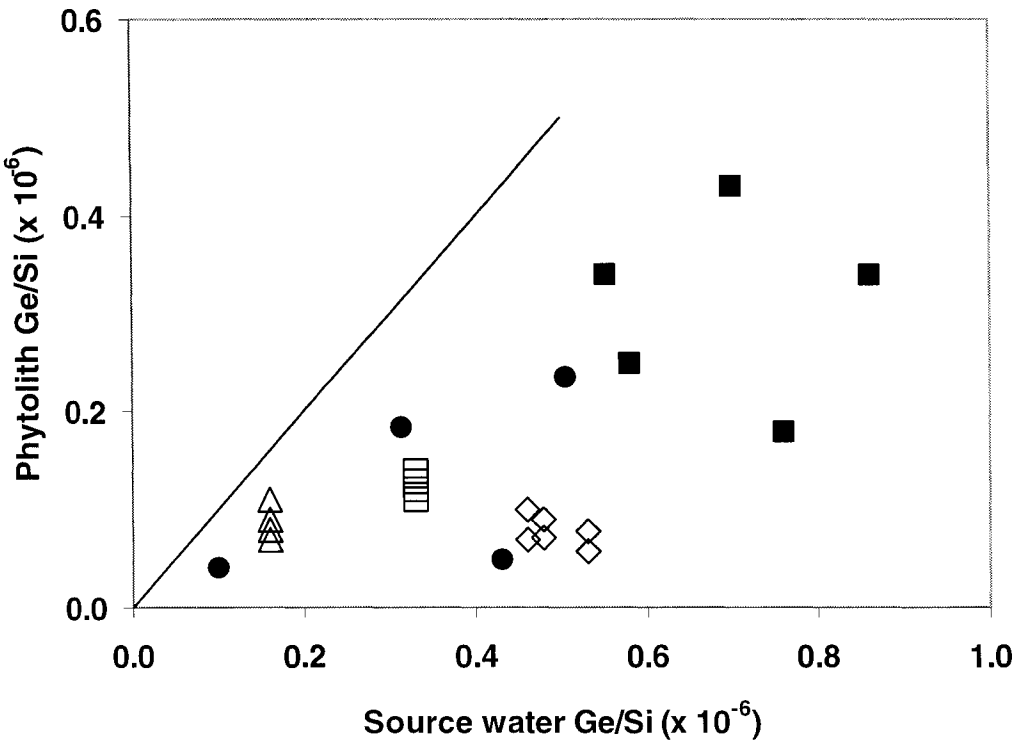

Figure 3.5 – Ge/Si units for both phytolith and source water values are a molar ratio. Open symbols represent samples from the greenhouse study (diamonds = nutrient solution, squares = field soil, triangles = potting soil), closed symbols represent samples from field studies (squares = grasses from Chapter 4, circles = ferns from Derry et al. 2005). The solid line represents a 1:1 relationship between source water and phytolith Ge/Si (i.e. no fractionation).

References

Alexandre A., Meunier J.D., Colin F., and Koud J.M. 1997. Plant impact on the biogeochemical cycle of silicon and related weathering processes. Geochim. Cosmochim. Acta 61:677-682.

Bareille G., Labracherie M., Mortlock R.A., Maier-Reimer E., and Froelich P.N. 1998. A test of $(Ge/Si)_{opal}$ as a paleorecorder of $(Ge/Si)_{seawater}$. Geology 26:179-182.

Bartoli F. 1985. Crystallochemistry and surface properties of biogenic opal. J. of Soil Science 36:335-350.

Cakmak I., Kurz H., and Marschner H. 1995. Short-term effects of boron, germanium and high light-intensity on membrane-permeability in boron deficient leaves of sunflower. Physiologia Plantarum 95:11-18.

Dahlgren R.A., Shoji S., and Nanzyo M. 1993. Mineralogical characteristics of volcanic ash soils. *In:* Shoji S., Nanzyo M. and Dahlgren R.A. (eds.) Volcanic ash soils, genesis, properties and utilization. Elsevier, NY. pp. 101-145.

Derry L.A, Kurtz A.C., Ziegler K. and Chadwick, O.A. 2005. Biological control of terrestrial silica cycling and export fluxes to watersheds. Nature 433:728-730.

Dietrich D., Hinke S., Baumann W., Fehlhaber R., Baucker E., Ruhle G., Wienhaus O., and Marx G. 2003. Silica accumulation in Triticum aestivum L. and Dactylis glomerata L. Anal. Bioanal. Chem. 376:399-404.

Epstein E. 1994. The anomaly of silicon in plant biology. Proc. Nat. Acad. of Sci. 91:11-17.

Epstein E. 1999. Silicon. Ann Rev Plant Physiol. Plant Molec. Biol. 50:641-664.

Epstein E. 2001. Silicon in plants: Facts vs. concepts. *In* Datnoff L.E., Snyder G.H, and Korndorfer G.H. (eds.) Silicon in Agriculture. Elsevier, New York. p. 1-16.

Filippelli G.M., Carnahan J.W., Derry D.A., and Kurtz A. 2000. Terrestrial paleorecords of Ge/Si cycling derived from lake diatoms. Chemical Geology 168:9-26.

Froelich P.N., Blanc V., Mortlock R.A., Chillrud S.N., Dunstan W., Udomkit A., and Peng T.H. 1992. River fluxes of dissolved silica to the ocean were higher during glacials: Ge/Si in diatoms, rivers and oceans. Paleoceanography 7:739-767.

Glockling F. 1969. The chemistry of germanium. Academic Press, New York. 234 p.

Halperin S.J., Barzilay A., Carson M., Roberts C., and Lynch J. 1995. Germanium accumulation and toxicity in barley. J. of Plant Nutr. 18:1417-1426.

Hildebrand M., Volcani B.E., Gossmann W., and Schroeder J. 1997. A gene family of silicon transporters. Nature 385:688-68.

Ingli N. 1963. Equilibrium studies of polyanions 12. Polygermanates in Na(Cl) medium. Acta Chemica Scan. 17:597-616.

Kelly E.F. 1990. Methods for extracting opal phytoliths from soil and plant material. Department of Agronomy. Colorado State University. Fort Collins, Colorado.

Kelly E.F., Chadwick O.A., and Hilinski T.E. 1998. The effect of plants on mineral weathering. Biogeochemistry 42:21-53.

Kubicki J.D. and Heaney P.J. 2003. Molecular orbital modeling of aqueous organosilicon complexes: Implications for silica biomineralization. Geochim. Cosmochim. Acta 67:4113-4121.

Kurtz A.C., Derry L.A., and Chadwick O.A. 2002. Germanium-silicon fractionation in the weathering environment. Geochim. Cosmochim. Acta 66:1525-1537.

Jarvis S.C. 1987. The uptake and transport of silicon by perennial ryegrass and wheat. Plant and Soil 97:429-437.

Jones L.H.P. and Handreck K.A. 1967. Silica in soils, plants and animals. Adv. Agron. 19:107-149.

Lindsay W.L. 1979. Chemical equilibria in soils. John Wiley and Sons, NewYork. 449 pp.

Loomis W.D. and Durst R.W. 1992. Chemistry and biology of boron. Biofactors 3:229-239.

Ma J.F., Miyake Y., Takahashi E. 2001. Silicon as a beneficial element for crop plants. *In* Datnoff L.E., Snyder G.H, and Korndorfer G.H. (eds.) Silicon in Agriculture. Elsevier, New York. p. 17-40.

Ma J.F., Nishimura K., and Takahashi E. 1989. Effect of silicon on the growth of rice plant at different growth stages. Soil Sci. Plant Nutr. 35:347-356.

Matsumoto H., Syo S., and Takahashi E. 1975. Translocation and some forms of germanium in rice plants. Soil Sci. Plant Nutr. 21:273:279.

Marschner H. 1986. Mineral nutrition in higher plants. Academic Press, New York. 674 p.

Mortlock R.A. and Froelich P.N. 1989. A simple method for the rapid determination of biogenic opal in pelagic marine sediments. Deep-Sea Res. 36:1415-1426.

Murnane R.J. and Stallard R.F. 1990. Germanium and silicon in rivers of the Orinoco drainage basin. Nature 344:749-752.

Parr J.F., Lentfer C.J., and Boyd W.E. 2001. A comparative analysis of wet and dry ashing techniques for the extraction of phytoliths from plant material. Journal of Archaeological Science 28:875-886.

Piperno D.R. 1988. Phytolith analysis: An archaeological and geological perspective. Academic Press Inc., New York. 280 pp.

Platzner I. and Degani N. 1990. Fractionation of stable calcium isotopes in tissues of date palm trees. Biomed. Environ. Mass Spectrom. 19:822-824.

Pokrovski G.S., Martin F., Hazemann J.-L., and Schott J. 2000. An X-ray absorption fine structure spectroscopy study of germanium-organic ligand complexes in aqueous solution. Chemical Geol. 163:151-165.

Pokrovski G.S. and Schott J. 1998. Experimental study of the complexation of silicon and germanium with aqueous organic species: Implications for germanium and silicon transport and Ge/Si ratio in natural waters. Geochim. Cosmochim. Acta 62:3413-3428.

Poulson S.R., Drever J.I. and Stillings L.L. 1997. Aqueous Si-oxalate complexing, oxalate adsorption onto quartz, and the effect of oxalate upon quartz dissolution rates. Chem. Geol. 140:1-7.

Rafi M.M., and Epstein E. 1999. Silicon absorption by wheat (*Triticum aestivum* L.). Plant and Soil 211:223-230.

Raven J.A. 1983. The transport and function of silicon in plants. Biol. Rev. 58:179-207.

Raven J.A. and Edwards D. 2001. Roots: Evolutionary origins and biogeochemical significance. J. Exp. Botany 52:381-401.

Richmond K.E. and Sussman M. 2003. Got silicon? The non-essential beneficial plant nutrient. Current Opin. in Plant Biol. 6:268-272.

Sankhla N. and Sankhla D. 1967. Effect of germanium on growth of higher plants. Naturwissenschaften 54:621.

Sangster A.G. 1977. Characteristics of silica deposition in Digitaria sanguinalis (L.) Scop. (Crabgrass). Ann. Bot. 41:341-350.

Sangster A.G., and Hodson M.J. 1992. Silica deposition in subterranean organs. In Phytolith systematics. Rapp G. Jr., and Mulholland S.C. Plenum Press, New York. pp. 239-251.

Sangster A.G, Hodson M.J., and Tubb H.J. 2001. Silicon deposition in higher plants. *In* Datnoff L.E., Snyder G.H, and Korndorfer G.H. (eds.) Silicon in Agriculture. Elsevier, New York. p. 85-114.

Schmitt A.-D., Chabaux F., and Stille P. 2003. The calcium riverine and hydrothermal isotopic fluxes and the oceanic calcium mass balance. Earth and Planetary Science Letters 6731:1-16.

Takahashi E., Matsumoto H., Syo S., and Miyake Y. 1976. Variation in Ge uptake among plant species. Japanese J. Soil Sci Plant Nutr. 74:217-221.

Van der Vorm P.D.J. 1980. Uptake of Si by five plant species, as influenced by variations in Si-supply. Plant and Soil 56: 153-156.

Chapter IV. THE USE OF GERMANIUM TO SILICON RATIOS IN SOILS TO QUANTIFY SI TRANSFORMATIONS IN GRASSLAND ECOSYSTEMS

Introduction

The Ge/Si ratios of diatoms from ocean sediments have been used to study temporal variations in global silica cycling and oceanic productivity. Biogenic marine opal is valuable in this respect, as the vast majority of diatoms do not preferentially take up either Ge or Si from seawater during silicification (Shemesh et al. 1989), and are excellent recorders of temporal changes in continental weathering (Froelich and Andreae 1981, Shemesh et al. 1989, Murnane and Stallard 1990, Mortlock et al. 1991). Study of ocean sediment cores have revealed fluctuations in Ge/Si ratios over time. Lower Ge/Si ratios and greater terrestrial silica flux (16 x 10^{12} mol/yr) are associated with glacial maxima; higher Ge/Si silica ratios and lower terrestrial silica exports (6.6 x 10^{12} mol/yr) are associated with more intensely chemically weathered interglacials (Froelich et al. 1992). Temporal silica fluctuations and subsequent changes in marine NPP (diatoms account for up to 75% and greater marine NPP, Nelson et al. 1995) are also closely tied to global C cycling and temperature regulation.

There is however, little information on the range and variations in Ge/Si ratios in terrestrial ecosystems. Understanding the systematic variations in Ge/Si ratios in terrestrial ecosystems would expand the use of Ge/Si as a potential tracer of silicate

weathering and Si transfers within soils and to aquatic and marine systems. Because Ge and Si atoms have similar ionic sizes, covalent Ge-O and Si-O bond lengths, and identical outer electron structures, Ge can readily substitute for Si in the lattice structure of minerals as well as siliceous structures in plants and animals (Wittman and Hormann 1976, Bernstein 1985). Essentially, Ge behaves as a heavy "pseudo" isotope of Si. Germanium typically occurs in the earth's crust at 1-2 ppm, leading to observed Ge/Si ratios of 1.3 to 2.5 x 10^{-6} in the continental crust and 0.3 to 1.2 x 10^{-6} in uncontaminated rivers (Mortlock and Froelich 1987).

Earlier research identified Ge/Si as a potential tracer in silicate weathering studies, noting that changes in Ge/Si ratios of river water reflect the importance of fractionation mechanisms, lithology, and changes in weathering intensity (Froelich et al. 1985, Mortlock and Froelich 1987, Murnane and Stallard 1990, Froelich et al. 1992). Further examination into Ge/Si fractionation mechanisms led to discoveries of preferential weathering due to changes in climate and differences in mineral stability (Gibbs and Kump 1994, Stallard 1995, Filippelli et al. 2000), and the potential significance of organo-Ge complexes (Pokrovski and Schott 1998) and iron oxide complexation of Ge on Ge/Si ratios (Chillrud et al. 1994, Kurtz et al. 2002). Though terrestrial Ge/Si fractionation was identified in earlier studies, the mechanisms responsible have only recently been examined in detail. A closer look at the mechanisms responsible for Ge/Si fractionation in silicate minerals across well constrained pedological gradients (e.g. Kurtz et al. 2002, Derry et al. 2005) can help increase the utility of Ge/Si ratios in weathering and biogeochemical research. The primary fractionation processes responsible for the

Ge/Si ratios that have been identified in the literature include: 1) formation of secondary clay minerals, 2) precipitation of pedogenic Fe-oxyhydroxides and 3) silica cycling by plants (Kurtz et al. 2002).

In a series of detailed studies of mineral transformations in tropical ecosystems, Kurtz et al. (2002) determined that allophane formation from basalt, rather than allophane to kaolin transformation, was the most critical step in Ge sequestration. Soils derived from dioritic materials in Puerto Rico showed similar fractionation processes, dominated by the production of Ge-enriched kaolinite weathered from plagioclase, whereas other weathering pathways did not appreciably alter Ge/Si ratios, such as biotite to kaolinite, which maintained its relatively high Ge/Si ratio (Kurtz et al. 2002). Given the preliminary identification of these mechanisms, it should be possible to trace silica released from individual reactions with Ge/Si ratios. Analysis of different watershed components by Filippelli et al. (2000) revealed that early preferential weathering of high Ge/Si micas may have contributed to nearby lake diatom Ge/Si values. Basin bedrock and soils revealed little evidence for Ge retention during weathering, however, even though stream Ge/Si values were considerably lower than the soil Ge/Si ratios, a situation likely due to limited weathering of the granite in the relatively dry high alpine system. Regardless of ecosystem or fractionation mechanism, Ge/Si ratios of soil waters tend to be consistently lower than the bulk soil, a finding consistent with Ge enrichment in clay mineral fractions.

Biological processes appear to play a role in determining Ge/Si ratios in soils. Derry et al. (2005) noted that upper organic rich horizons, regardless of age, had higher dissolved Si and lower Ge/Si ratios in soil water than underlying mineral horizons, where phytoliths in the dominant vegetation had low Ge/Si values consistent with the low Ge/Si of the soil water. The cause for this apparent inverted silica profile in these highly weathered soils is similar to that proposed by researchers such as Lucas et al. (1993), biogenic silica cycling. Derry et al. (2005) also provided an initial look into the significance of plant mediated Si in the global Si biogeochemical cycle, concluding that plant mediated Si is a major source of stream water Si in Hawaiian ecosystems where soils are largely depleted in primary minerals. A biogenic origin of dissolved Si in surface soil waters of Puerto Rico granitic soil has also been proposed but not confirmed (Schulz and White 1999). Conley's review (2002) suggested that the quantities of Si fixed by terrestrial plants rivals the quantities of Si stored in phytoplankton of marine systems. Although the Si cycled through marine systems is well quantified, little is known about the compartmentalization, cycling and mobilization of Si in terrestrial ecosystems, particularly ecosystems in arid and semi-arid regions. Because grasslands comprise roughly 40% of the earth's surface, the fate and mobility of Si in these ecosystems may be of critical importance in constraining models of global Si biogeochemistry.

The objectives of this research are: 1) assess the systematic variations of Ge/Si ratios within and among soil of natural grassland environments; 2) examine Ge fractionation relative to Si in weathering systems along a grassland climosequence; and 3) utilize differences in Ge/Si values among the major biogeochemical pools (vegetation, soils,

water) within watersheds along the climosequence to examine the potential link between plant mediated silica and stream water silica.

Methods

Study Area/Sampling Design

A climosequence (Jenny 1941) spanning a precipitation gradient of approximately 350 - 1100 mm (Table 4.1) in the Central Great Plains was sampled in order to utilize estimates of annual net primary production (ANPP) data measured by McCulley and Burke (2004). The climosequence was extended into western Missouri and additional sites within the sequence were sampled in order to further examine variability of Si cycling in grassland ecosystems. Figure 4.1 provides a site location diagram with major grasslands types, and study site abbreviations. Table 4.1 provides a description of basic site characteristics including vegetation, soil, and ownership. Appendix I provides more detailed soils descriptions for the pedons sampled across the climosequence.

To minimize the influence of slope and aspect across the sampling gradient, relatively flat upland sites were selected; two in shortgrass (SGS and ARIK), three in mixedgrass (SV, HAYS and WILSON) and two in tallgrass (KONZA and WKT) communities. Two pedons were sampled at the Shortgrass Steppe LTER in order to examine smaller scale spatial variability (SGS-A and SGS-B). SGS-A is located approximately 1 km from SGS-B, the former having a greater fluvial component (Blecker et al. 1997). Soils are derived from residual sedimentary rock and loess (Mason et al. 2003; Roberts et al. 2003) and range from drier (Aridic Argiustoll) to wetter (Typic Hapludoll) Mollisols across the

gradient. Given the geomorphic history along the gradient and radiocarbon dates, soil ages have been estimated at 10-30 ky (Blecker et al. 1997; Oviatt 1998). Land use was held constant (moderate grazing) and plant communities varied with mean annual precipitation (MAP). In terms of plant species, blue grama (*Bouteloua gracilis*) and buffalograss (*Buchloe dactyloides*) dominate the shortgrass sites (SGS-A, SGS-B, ARIK), *Bouteloua gracilis, Buchloe dactyloides,* fescue (*Festuca sp.*) the drier mixedgrass sites (SVR and HAYS), little bluestem (*Schizachyrium scoparium*) and big bluestem (*Andropogon gerardii*) the wetter mixedgrass site (WILSON), and *Andropogon gerardii* the tall grass sites (KONZA and WKT).

Field Methods

To quantify the degree of chemical weathering along the precipitation gradient, soils were sampled to the C horizon (SGS-A, SGS-B, ARIK, SV, HAYS) or bedrock (WILSON, KONZA, WKT) during the summer of 2003. Pedons were described and sampled by genetic horizon (Soil Survey Staff, 1992). Approximately 1 kg of soil was sampled from each horizon. To examine soil phytolith variability, two additional surface horizon samples were taken in a random direction three meters from each pedon. Where possible, soil peds were taken back to the lab for bulk density analysis. For plant phytolith analysis, samples of the major grass, shrub and forb species were taken adjacent to the soil sampling area. To examine yearly and seasonal variability in plant Si content, live (green) and dead (brown) plant samples from consecutive years (2002-2003) were sampled. The ANPP data was taken from McCulley and Burke (2004), except for the WILSON and WKT sites, where ANPP was measured using $0.25m^2$ quadrats.

Water samples were taken near each sample site periodically from Spring 2003 through Spring 2004 to examine temporal and spatial variability in dissolved Si inputs (precipitation) and outputs (groundwater, stream water). It is important to note that natural water values are dissolved Si and do not include particulate Si. Likens and Bormann (1995) estimated 25% particulate and 75% dissolved Si in stream water measurements within the Hubbard Brook experimental forest, and Treguer et al. (1995) notes that particulate Si comprises only about 5% of the total terrestrial Si load delivered to the oceans. To supplement the water samples, publicly available USGS hydrologic data for discharge and water chemistry was used. Stream, rain, and ground water were collected in acid-rinsed LDPE bottles, filtered through 0.4um polycarbonate filters upon return to the lab and stored in acid-washed LDPE bottles prior to analysis.

Analytical Methods

Soil phytoliths were extracted by heavy liquid floatation from sand and silt fractions, and cleaned with dilute hydrochloric acid, hydrogen peroxide, and deionized water in a method adapted from Piperno (1988), Kelly (1990), and Parr (2002). Oven-dried (105 °C), 2-mm sieved soils were treated with sodium acetate (buffered at pH 5 with acetic acid) to remove carbonates, and 30% hydrogen peroxide to remove organic matter. After rinsing with deionized water, 5% sodium hexametaphosphate was added and the sample is shaken overnight. Sand was separated from the silt and clay fraction by wet sieving through a 53 μm screen. Silt was separated from clay by centrifugation and gravity sedimentation. The sand and silt fractions were then rinsed with deionized water, dried overnight and stored in plastic bottles. To obtain phytoliths, a subsample (2-5g) of either

sand or silt was placed in a 50-ml plastic centrifuge tube along with cadmium iodide/potassium iodide (specific gravity of 2.30 g/cm^3). The samples were thoroughly stirred and then centrifuged at 2000 rpm for 10 min. Phytoliths were removed by pipet from the surface and stored in a separate container. Additional stirring and centrifugation was repeated until negligible yield is obtained. Samples were rinsed of the heavy liquid with deionized water. Small amounts of clay obtained during the separation were removed by shaking the phytolith sample in 5% sodium hexametaphosphate overnight, allowing the phytolith to settle, then siphoning off the suspended clays. Phytoliths were further cleaned in separate steps with 10% hydrochloric acid and 30% hydrogen peroxide. Samples were passed through a 0.2 μm polycarbonate filter, dried overnight and stored in plastic vials. Subsamples of the soil phytoliths were mounted in immersion oil with a refractive index of 1.51 and examined under light microscope as well as a dissecting scope to ensure that sample was not contaminated with other minerals. X-ray diffraction analysis of random phytolith samples corroborated the lack of contamination. The lack of a correlation ($r^2 = 0.001$; $p = 0.79$) between sediment used in the extraction and phytolith recovered also supports the purity of the soil phytoliths. Known amounts of diatomaceous earth (with a density similar to that of phytoliths) were used to check the recovery rates of the procedure, both alone (94% recovery) and spiked with silt-sized material known to contain negligible phytolith (96% recovery), suggesting minimal contamination from non-phytolith material.

Plant samples were cleaned to remove soil contamination, dry ashed, then treated to remove non-siliceous material in a method adapted from Piperno (1988), Kelly (1990),

and Parr et al. (2001). A 5-10 g sample of oven-dried (55-60 °C) plant material was cut into 2-3 cm lengths, washed in a mixture of 5% sodium hexametaphosphate, 10% hydrochloric acid and deionized water. After thorough rinsing, the sample was washed in 70% ethanol, and rinsed again with deionized water. After drying again at 55-60 °C, a subsample of the cleaned plant material was weighed into a Ni crucible. The sample was ashed at 500 °C for 1 hour, allowed to cool in a desiccator and weighed. The ash was washed in warm, 10% hydrochloric acid, rinsed with deionized water, washed in hot 30% hydrogen peroxide, filtered through a pre-weighed 0.20μm filter, and rinsed thoroughly with deionized water. After drying at 55-60 °C, the sample was allowed to cool in a desiccator, weighed, and stored in a plastic vial.

Oven-dried, ball-mill pulverized soil and rock samples were submitted to SGS Mineral Services of Toronto, Canada for total elemental analysis. Samples were ashed at 500°C to remove organic matter, fused with Li-metaborate, dissolved in dilute HNO_3 and analyzed by inductively coupled plasma atomic emission spectroscopy (Hossner 1996). Results are reported on ash-free samples. Internal standards, blind standards and duplicates were analyzed for quality control.

Germanium concentrations were measured by isotope-dilution hydride-generation inductively coupled plasma mass spectrometry (ICP-MS), after spiking dissolved samples with a ^{70}Ge tracer solution. To dissolve the soils, a mixture of HNO_3-HCl-HF was added to 50 mg of soil in a Teflon container, tightly sealed, then heated with a microwave digester. After cooling, saturated boric acid was added and the container was again

heated in a microwave digester. After cooling, samples were diluted with deionized water. An aliquot of the diluted sample was spiked with ^{70}Ge, allowed to equilibrate overnight, then analyzed by hydride generation ICP-MS on a Finnigan Element 2 (Thermo Electron Corp., Waltham, MA) at Cornell University. Accuracy was monitored through analysis of duplicates and USGS rock standard BIR-5. Plant phytolith samples were dissolved in 2M NaOH at room temperature, neutralized with HNO_3, diluted, then treated in a similar manner to the dissolved soil samples.

Soil water samples were prepared by bringing soil samples to near saturation with deionized water (Lajtha et al. 1999). After equilibrating for 72 hr, the samples were filtered through Whatman 40 filter paper and filtered again through a 0.22 μm polycarbonate membrane. Silica concentrations for aqueous samples (both natural waters and soil waters) were analyzed by molybdate-blue method on a spectrophotometer (Mortlock and Froelich 1989). A 0.2ml aliquot of sample was reacted with a molybdate-HCl solution, reduced in a metol-sulfite-oxalic acid-sulfuric acid solution and placed in the dark overnight. The solution was then read at 812 nm on a spectrophotometer. Ge was measured by isotope-dilution hydride-generation ICP-MS.

Sand and clay mineralogy were determined by x-ray diffractometry using a Scintag XDS 2000 Diffractometer (Cupertino, CA). Sand samples were prepared as random packer powder; clays were prepared by filtration slide transfer onto glass disks (Moore and Reynolds 1989) and analyzed air-dried and after exposure to ethylene glycol.

Elemental composition was estimated for handpicked sand-sized grains by electron microprobe analysis using energy dispersive spectroscopy analysis (EMPA-EDS). Samples were placed on carbon coated aluminum stubs and analyzed using a JEOL JSM-6500 Electron Microprobe analyzer (JEOL USA, Inc., Peabody, MA) at an accelerating voltage of 15 keV and a working distance of 10 mm. Secondary electrons were used to collect images and energy dispersive spectroscopy to generate elemental dot maps.

Results

Ge/Si Ratios of Primary Minerals

Total elemental and mineralogical data revealed sand and silt fractions dominated by quartz and feldspar. The corresponding Ge/Si of the sand and silt fractions reflect this composition for the weathering endpoints along the climosequence, SGS and Konza (Table 4.2). Ge/Si values range from 1.0-1.5 for the sand and silt fractions, representing a mixture of quartz (Ge/Si = 0.54, 0.69, 0.76); feldspar (Ge/Si = 2.34, 3.08, 3.79); and lesser amounts of such mafic minerals as biotite and hornblende (Ge/Si = 5.56, 6.18, 6.51). The lower Ge/Si values of the sand and silt fractions of the more highly weathered Konza site are possibly a reflection of the greater proportion of quartz (over feldspar and mafics) at this site compared to the less intensely weathered shortgrass site. The relatively higher amount of quartz at Konza is corroborated by the total elemental data, which shows a higher proportion of SiO_2 in the sand and silt fractions (Tale 3.2).

Ge/Si Ratios of Secondary Minerals

X-ray diffraction analysis showed clay fractions of the soils comprised of smectite, illite, mixed layer smectite/illite and kaolinite. Field morphology, specifically the presence of argillic horizons, supports the presence of secondary clay accumulation throughout the soils of the climosequence. Germanium conservation in secondary clay formation can be seen in the higher Ge/Si of the clay fraction of these soils (Table 4.2). A possible geochemical indicator of the greater weathering intensity associated with the tallgrass sites is seen in the greater magnitude between the sand and silt vs. the clay Ge/Si values of Konza compared to the SGS sites (Table 4.2). With increasing weathering intensity, Si loss and Ge conservation should cause the Ge/Si ratio of the clays to increase relative to parent material values. This trend is apparent when comparing SGS to Konza, the latter having a greater apparent abundance of 1:1 type clays (i.e. kaolinite) based on XRD patterns. Such 1:1 clays would typically have a greater loss of Si and conservation of Ge compared to 2:1 clays. Still, the relative similarity of clay Ge/Si values between surface and argillic horizons across the climosequence indicates limited weathering in these systems compared to regions of greater weathering intensity, such as the tropical ecosystems studied by Kurtz et al. (2002).

Ge/Si ratios of Soil Water

Where lysimeter measures of soil water are generally not practical in semi-arid regions due to sporadic and typically insufficient rainfall, saturated paste extracts can be utilized to estimate soil water chemistry (Lajtha et al. 1999). The solute measured by this technique should represent the fairly labile fraction of ions that are in contact with the

soil minerals. Notable trends in soil water chemistry include decreasing Ge/Si values and fluctuating Si concentrations with depth (Table 4.3). A notable exception is the relative similarity in Ge/Si values and Si content throughout the soil profile of the SGS-A site. Given the complex fluvial history of this site however, a lack of differentiation in these values with depth is not surprising.

As reported in Chapter 2, soil phytolith content decreases both with depth (in a pattern somewhat similar to SOC) and across the climosequence (i.e. greater soil phytolith contents occur in drier sites). Clay content peaks in the subsurface argillic horizon at all sites except Konza. Within the context of the sampling scheme, the deepest horizon represents the least weathered horizon (assuming a lack of groundwater interaction, which is supported by field morphology). For the saturated paste extracts, Ge/Si values tend to decrease with depth, soluble Si contents of the surface and deep horizons tend to be similar, and the lowest soluble Si content occurs in the main argillic horizon (Table 4.3), which typically has the greatest clay content. Plotting clay content (adjusted for bulk density) against soluble Si content along the climosequence gives a negative relationship, with higher clay content for a given horizon having lower soluble Si content (Figure 4.2). The greater amount and lower solubility of secondary clays in a given horizon may partially explain this trend.

Conversely, a positive relationship exists between soil phytolith content and soluble Si (Figure 4.3). This trend may be related to the higher solubility associated with amorphous phytoliths, leading to the higher soluble Si contents found in the surface

horizons. Though a system in equilibrium with amorphous silica (i.e. soil phytoliths) could maintain Si concentrations of up to 1,800 μmol/L (and well above the levels listed in Table 4.3), the low soil phytolith content of the deep horizons discounts this possibility. Since the Ge/Si values are also quite low for the deep horizons of all the sites measured (0.14 to 0.42, x = 0.26, n = 5), a potential mineralogical explanation for these values initially centers on quartz, which has the lowest Ge/Si values of the analyzed minerals. Since these horizons rarely if ever see the water content found in the saturated paste extract, it is possible that fairly rapid dissolution is occurring. However, quartz Ge/Si values and solubility confound this explanation. A quartz Ge/Si value of 0.69 for quartz in horizon 6 of SGS-B does not seem to account for the solute Ge/Si signature of this horizon (0.14). Furthermore, Si concentrations in a system in equilibrium with quartz would only realize levels of 100 μmol/L under typical soil conditions, levels far below those measured in the deep horizons (Table 4.3). Though soil-Si (log K = $10^{-3.1}$; Lindsay 1979) presents a more likely control on the soluble Si levels seen in the saturated paste extracts, such a control does not provide information regarding soluble Si provenance. Further investigation of the deep horizon controls on soluble Si (such as a study of the effect of time and soil moisture content on soluble Si and Ge/Si) are necessary to unravel the relationship between controls on soluble Si and Ge/Si in the deepest soil horizons.

Ge/Si ratios of Plant Phytoliths

Plant phytoliths across the climosequence exhibit fairly low Ge/Si values (0.15-0.44, x = 0.31, n=15; Table 3.4). As these values are lower than those of the corresponding surface soil water Ge/Si, these data corroborate the trend seen in other studies that plants fractionate against Ge at some stage of phytolith formation. Specifically, Derry et al. (2005), report Ge/Si values for Hawaiian ferns (*Cybotium*, *Dicrauopteris*, *Diplazium* sp) of 0.02-0.37, x = 0.10, n=11), that are lower than associated soil water Ge/Si values. Given the grassland root distribution data reported by Leetham and Milchunas (1985), a weighted average of 75% A horizon soil water and 25% argillic horizon soil water was used to calculate an average Ge/Si soil water value taken up by the plants. Though no clear trend exists along the climosequence, the average fractionation of 0.38 Ge/Si is comparable to the fractionation exhibited by the grassland plants grown under controlled greenhouse conditions (Chapter 3). The accuracy of this estimation is limited both by differences in residence time between laboratory conditions and the actual residence time of the soil/water contact in the field, but biologic fractionation against Ge is apparent.

Ge/Si ratios of Stream waters

Stream water Ge/Si values along the grassland climosequence (0.07-1.29, n = 20; Table 4.5) are typical of natural water Ge/Si values (0.7 ± 0.3) found by Froelich et al. (1985). Stream water data is not available for SGS and Smokey Valley, as nearby streams are not present, except for very brief periods following heavy precipitation events. A general trend of decreasing Ge/Si with increasing Si content can be seen in Figure 4.4 for all watersheds except Konza (i.e. lower Si concentrations than one would expect for the

relatively low Ge/Si values). The higher stream water Si and lower Ge/Si associated with the drier watersheds could be a simple function of weathering, as more soluble Si would likely be available in the less intensely weathered systems, or greater contribution of biogenic Si. The case at Konza may be due to the considerable limestone component in this watershed; however, Hays and Wilson, with watersheds underlain by limestone, tend to show the more typical inverse relationship between Ge/Si and Si. The lower Si content associated with limestone is likely reflected in the stream water Si values; however, in other systems such as Hawaii (Derry et al. 2005), lower Si values are more commonly associated with higher Ge/Si. Regardless of the difference between Konza and the rest of the climosequence, further examination of the hydrogeology among these watersheds (e.g. differences in residence time, land use, recharge flow paths) is necessary to resolve these questions.

Ge/Si ratios of Ground water

Well water values, regardless of sampling depth, residence time and geology, are typically higher than those associated with streams of the same drainage at all sites across the climosequence (Table 4.5). No clear trend exists between well water Ge/Si vs. [Si] (Figure 4.5). Increased residence time compared to the water charging the streams, as well as contact with minerals of greater Ge content, could be one explanation for these differences along the climosequence. The one well site of known geologic composition at Konza, is set in a limestone member of the Flint Hills, and helps to account for the low Si content of the water. Higher Ge/Si values associated with two wells from the SGS site

are possibly due to a greater feldspars and mafic mineral content common in this region. Well water from other sites generally follows the trend of the stream water, with higher [Si] associated with the drier sites and possibly more weatherable Si-bearing minerals contributing to the well water composition, when compared to the greater limestone components found in the Hays and Wilson region.

Discussion

Geochemical behavior of Ge

With similar tetrahedral bond lengths between Ge-O (1.75 Å) and Si-O (1.64 Å), and identical outer shell electron structure, Ge acts as a pseudo heavy isotope of Si. Thus, studies of Ge/Si ratios in terrestrial and marine systems have tended to focus on the similarities between Ge and Si (e.g. Mortlock and Froelich 1987, Froelich et al. 1992, Filippelli et al. 2000, Kurtz et al. 2002). However, the geochemical differences between these two elements provide greater insight into the Ge fractionation and differences in Ge/Si ratios among pools in a given ecosystem. Mineral weathering studies have demonstrated that Ge tends to accumulate as Si is lost, a trend that typically becomes more prominent as weathering intensity increases. Given the similarities in electronegativity and size, Ge also behaves similarly to elements such as Al and Fe(III) (e.g. Fe(III)-O = 2.04 Å, Al-O = 1.96 Å, and Ge-O = 1.88 Å; Bernstein and Waychunas 1987). Thus unlike Si, Ge also takes on an octahedral coordination (Bernstein 1985), and in primary minerals Ge has a tendency to concentrate in silicates with few links between silicate tetrahedrae (e.g. olivine, pyroxene) compared to highly polymerized silicates (e.g. quartz, feldspar). Thus the degree of tetrahedral polymerization also controls Ge content

to an extent. It is important to note therefore that initial mineral composition and weathering intensity therefore will tend to drive temporal and spatial relationships of Ge/Si ratios in terrestrial systems.

Model of Ge/Si Fractionation: Tallgrass versus shortgrass ecosystems

Konza (tallgrass system)

Figure 4.6 illustrates the general Si biogeochemical cycle for Konza with Ge/Si values listed for the major pools. Dissected, interbedded limestone (uplands) and shale (hillsides) drainages, and more intense weathering as compared to the shortgrass sites have resulted in soils with a higher clay contents and greater geologic fractionation of Ge/Si, as seen in the greater difference between the primary mineral (sand/silt) fraction compared to the secondary mineral (clay) fraction at Konza. The corresponding fractionation factor Kw, where Kw = $(Ge/Si_{clay})/(Ge/Si_{bedrock})$; Murnane and Stallard (1990) is roughly 2.8, using the Ge/Si of the primary mineral dominated sand and silt fractions as a proxy for the parent material. This value is comparable to that of the Luquillo LTER (Kurtz et al. 2002) and nearly double that of the shortgrass system.

Average stream water Ge/Si values (0.28) are comparable to both plant phytolith (0.43) and deep horizon soil water Ge/Si (0.32) values. Well water Ge/Si values (0.65) are generally higher than the stream water, further clouding the issue of stream water Si provenance. Figure 4.7 provides a look at seasonal stream water dissolved Si values (approximately 11-16 mg/L) and discharge (approximately 0.5-7 cfs) for Kings Creek, taken from public USGS data averaged over a 26-year period from 1980 through 1996.

Overlain on this data are the Ge/Si stream water data for two sites along Kings Creek taken from spring 2003 through spring 2004. Peak stream discharge values in the spring correspond to yearly low dissolved Si content, which may be a dilution effect as seen in other streams (Likens and Bormann 1995). However, this pattern may also reflect the onset on the growing season where plant Si uptake would decrease the amount of silica being released to streams. Stream water Ge/Si values are highest in the spring and decrease slightly throughout the summer and fall. Though overlap of potential steam water Si sources, exacerbated by the complicated hydrogeology in this region (e.g. highly variable hydraulic conductivity; Macpherson 1996), cloud the issue of dissolved Si provenance, the decrease in stream water Ge/Si values in the late summer and fall could reflect an influx of lower plant phytolith derived Si. However, given the general disconnect between soil and stream in this system, direct contribution of plant cycled Si to the stream is questionable. Macpherson and Sophocleuos (2004) reported that recharge pathways in this area are dominated by bedrock fractures, with most of the soil water remaining in the soil lost to evapotranspiration due to the low permeability. More sampling in this and other watersheds in the region may clarify the link between plant mediated and dissolved stream Si. The connection between plant cycled and stream water Si found by Derry et al. (2005) in Hawaii is more difficult to establish at Konza and the other grassland systems.

Arikaree (shortgrass system)

Figure 4.8 illustrates the general Si biogeochemical cycle at Arikaree with the Ge/Si values of the major pools estimated or directly measured. The Ge/Si data for soil

minerals, soil water, plant phytoliths and stream water at Arikaree allows for a closer look at the link between soil-Si and stream-Si in a shortgrass system. Similar parent material and weathering conditions between SGS and Arikaree have resulted in soils of similar mineralogy and development; sand and silt fractions dominated by quartz and feldspar, a fairly well developed argillic horizon, and similar clay mineralogy. Therefore the assumption was made that primary and secondary mineral Ge/Si values (which were not directly measured at Arikaree) and fractionation mechanisms are comparable with those of the SGS shortgrass site; an assumption that is also strengthened by the similarity in total elemental and XRD analyses between the sites. Lower precipitation and less intense weathering have resulted in minimal Ge fractionation when comparing sand and silt fractions to the clays (Kw = 1.3, A horizon; 1.5, argillic horizon). Lower Ge/Si values for the plant phytoliths compared to the surface soil water Ge/Si suggest biologic Ge fractionation. C horizon soil water and stream water are fairly close in Ge/Si, suggesting a possible link between these two water sources, though the complexity of these systems do not allow for a simple Ge/Si explanation of soil-stream Si pathways (i.e. it is difficult to differentiate between plant mediated Si, which also has similar Ge/Si values and mineral Si contributions to stream water Si). Given the general aridity and lack of deep water penetration of shortgrass systems, even though plant Si cycling is occurring, it is difficult to determine if plant mediated Si is a major contributor to stream water Si.

Chemical Weathering in Grassland Ecosystems - Utility of Ge/Si Ratios

In a deeply weathered tropical ecosystem, Murnane and Stallard (1990) reported Ge/Si enrichment in clay of 2.5 times that of the bedrock, resulting in a depleted Ge/Si aqueous component released to stream waters. Kurtz et al. (2002) reported up to a 10-fold Ge enrichment in soils of intensely weathered Hawaiian basalts (where the primary fractionation reaction is the formation of allophone) and less Ge enrichment (approximately 2.8) in the weathering pathway of diorite derived plagioclase to kaolinite in Puerto Rico. The lower degree of enrichment in the latter site is due in part to the presence of low Ge/Si quartz, which maintains a lower Ge/Si in the soil as it weathers. Disparate trends in Ge behavior were noted by Filippelli et al. (2000), in a study in the high Sierra Nevada Mountains of California. Minor Ge enrichment in gneiss-derived soils and apparent Ge depletion in granite-derived soils compared to bedrock were attributed to differences in climate and mineralogy (both of which likely contribute to diminished clay production compared to the previously mentioned studies), though they cautioned that greater sampling intensity was necessary to draw more concrete conclusions regarding Ge/Si behavior in that ecosystem. Data from the current study show Ge enrichment in clay of roughly 1.3 for the shortgrass sites and 2.7 for Konza (tallgrass site) compared to sand and silt of the same horizon (Figure 4.9). Given the likelihood of loess inputs during the formation of these soils (Mason 2001, Muhs and Zarate 2001, Mason et al. 2003), geochemical analysis of regional Bignell (Holocene) and Peoria (late Pleistocene) loess samples have been included (Table 4.2 and Figure 4.9). Though the study transect is outside the region of primary glacial loess deposits (Bettis et al. 2003, Roberts et al. 2003), varying amounts of loess have likely been

incorporated into the soils of these sites, especially in light of the relatively high silt and low coarse fragment contents of the surface horizons throughout the study area. However, without more detailed analyses of the loess contribution to these sites, the similarities in Ge/Si between the relatively pure loess and the soils cannot be expanded on, except that the Ge/Si comparison between the loess and the surface soil horizons of the soils along the climosequence supports the widespread nature of loess deposition in this region.

Soil forming factors are quite different between the tropical forest of the Luquillo LTER (Kurtz et al. 2002) and the grasslands of the Great Plains, but similarities in mineralogy and general weathering pathways provide common ground for comparison. In general, as minerals weather in these systems, Al and Ge are conserved in secondary minerals to a greater extent than Si (Figure 4.10). Both the tropical forest and the grassland soils data fall along the same trend line, suggesting similar fractionation pathways. In general, grassland Ge/Si values cluster nearer the origin than the tropical forest Ge/Si values; the lower Ge/Si and Al/Si values indicative of the lower weathering intensity associated with grasslands compared to tropical rain forests.

Concerning water chemistry, the trend seen in figure 4.4 is similar to that reported by Derry et al. (2005) for Hawaiian streams. The authors attributed higher steam water Si (and corresponding lower Ge/Si values) to greater contributions of plant mediated Si. Along the same line, Schmitt et al. (2003) noted that nutrient biocycling in forested ecosystems can impact stream water chemistry, where up to 80% of the stream water Ca

originates from surface soil horizons during periods of high discharge. Along the grassland climosequence, the streams with the highest Si concentrations (and corresponding lower Ge/Si values) occur in the drier watersheds, suggesting a possible biogenic influence. However, overlap between water, plant and mineral Ge/Si values do not afford a clear explanation for the Ge/Si vs. Si trend of Figure 4.4. Pokrovski and Schott (1998) note that the presence of DOC can considerably effect Ge concentration (via formation of Ge-organic ligand complexes) and increase Ge/Si ratios in organic-rich natural waters. The relatively low DOC amounts associated with the streams in this study and a lack of relationship between Ge/Si and DOC, preclude the importance of this mechanism.

Thus, using Ge/Si as a biogeochemical Si tracer in these less intensely weathered, more geologically complex grassland watersheds will require more intensive study than exists within the constraints of the current study, and even then may not provide a clear indicator of the source of stream water Si given hydrogeological complexity. The data do suggest that stream water Si is not derived entirely from the same source as the ground water, given the differences between ground water and stream water Ge/Si values and a lack of seasonal trends in stream water Ge/Si values. For example, during periods of low flow, where stream flow is supplied primarily through ground water discharge, the Ge/Si would likely be higher (i.e. greater similarity between stream water and ground water Ge/Si values). However, it is important to note that the stream water recharge source and the well water measured in this study are not necessarily the same.

Si biogeochemistry on a global scale - possible link between grasslands and the paleo-marine Si cycle

Beyond the fractionation shown by plants against Ge, plant-mediated Si appears to have an impact on the overall terrestrial Si biogeochemical cycle. Similarities between surface soil water Ge/Si and the Ge/Si of nearby stream water, along with the much higher Ge/Si of subsurface soil waters, led Derry et al. (2005) to conclude that plant cycled Si is a major contributor to exported stream water Si. Though far less straightforward and confounded by unexamined hydrogeologic complexities, Ge/Si values for stream water (0.07-1.29, avg. = 0.39, n = 20), surface soil water (0.22-0.94, avg. = 0.66, n = 6), and subsurface soil water (0.14-0.63, avg. = 0.36, n= 12) along the climosequence, allow for the possibility of a link between plant-mediated Si and stream water Si in these semi-arid ecosystems. Though similarity among Ge/Si values of potential contributors to stream water Si create a more complex picture not readily explainable by a simple mixing model.

In light of the study of terrestrial Ge/Si processes, Shemesh et al. (1989) presented Ge/Si values of marine core diatoms for the past 50 m.y. Fluctuations of marine Ge/Si have been associated with changes in continental weathering rates associated with glacial cycles and variations in riverine Si inputs (Froelich et al. 1992, Shemesh et al. 1989); though it is important to note that other explanations for temporal variations in marine Ge/Si have been proposed (Hammond et al. 2000, King et al. 2000). Nonetheless, the decline in marine Ge/Si values around the time of the global Miocene grassland expansion (roughly 5 to 7 mya to the present), suggest a possible link between these two

global phenomena. However, the concomitant uplift of the Himalayas and impact of subsequent intense weathering in that region, as evidenced by the increase in marine $^{87}Sr/^{86}Sr$ values during that same time period (Raymo and Ruddiman 1992, Galy et al. 1999), allow for other explanations in the decline of marine Ge/Si values. However, if the trend noticed by Derry et al. (2005), whereby plant mediated Si is a significant source of stream derived Si, applies to other ecosystems such as grasslands (which cover roughly 40% of the earth's land surface), the possibility exists that grassland expansion could be at least partially responsible for the general increase in dissolved Si content and the corresponding decrease in Ge/Si values in the oceans over the past 5 to 7 million years.

Conclusions

Geochemical weathering trends of Ge/Si in primary and secondary minerals of grassland ecosystems across the Great Plains follow established trends of Ge conservation in secondary minerals, although to a lesser extent than more weathered silicate systems of tropical rainforests (Kurtz et al 2002). Plants appear to fractionate against Ge at some point during Si uptake and phytolith formation. The trend of decreasing Ge/Si values and increasing Si concentrations with decreasing MAP in streams along the climosequence suggest a possible link between biogenic and stream Si. However, the lesser degree of weathering, more complex mineralogy, and similarity among the major Si pools across the climosequence confound the use of Ge/Si values as a biogeochemical tracer within watersheds of grassland systems. More intensive study of the stoichiometry of major weathering reactions (through more detailed mineralogical examination along with stream and solute ion chemistry) and other means of identifying Si input to streams in

grasslands systems, are necessary to examine the importance of plant cycled Si in these systems. However, the Ge/Si fractionation model first put forth by Froelich et al. (1992), which only accounts for weathering based fractionation, would benefit from inclusion of a biologic fractionation component.

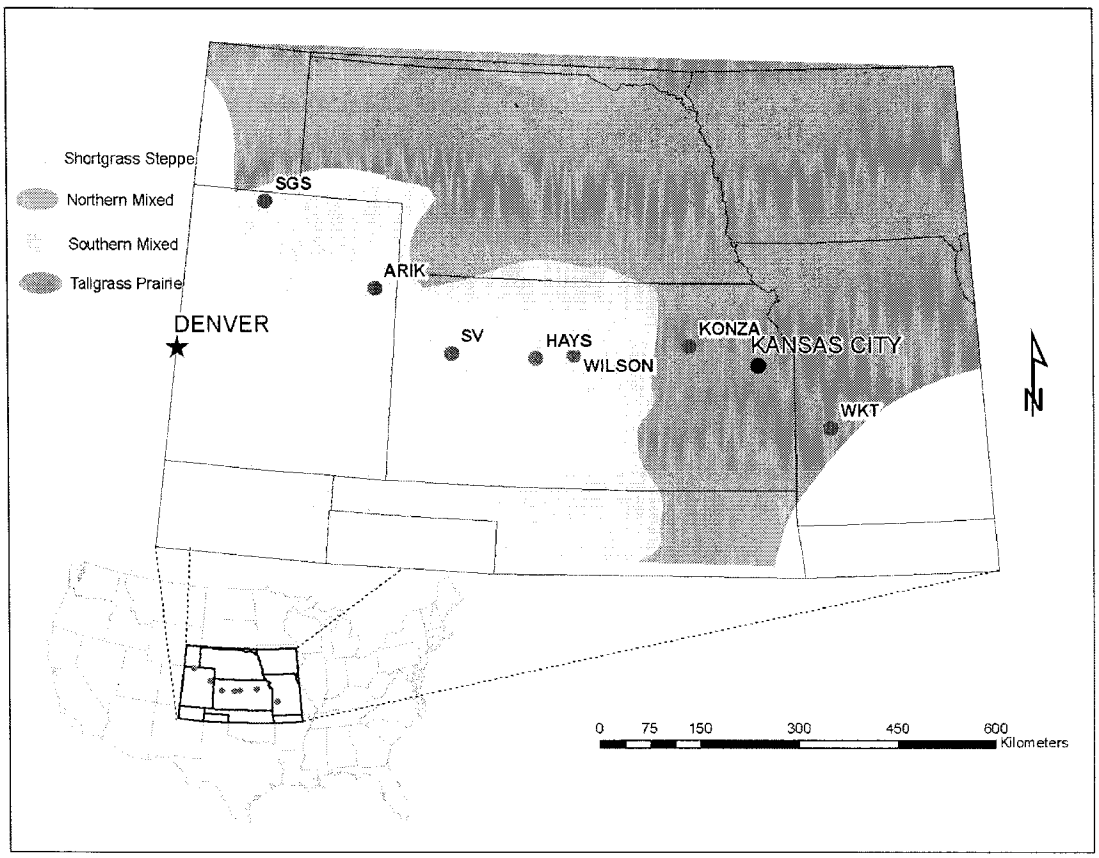

Figure 4.1 - Location map for field sites along the Great Plains climosequence.

Table 4.1 Characteristics for the 7 sites comprising the Great Plains climosequence (SGS – Shortgrass Steppe Long-Term Ecological Research (LTER) site, ARIK – Arikaree River Ranch, owned by The Nature Conservancy (TNC), SV – Smokey Valley River Ranch owned by the TNC, HAYS – Hays Range Area, owned by Ft. Hays State University, WILSON – owned by Wilson Lake State Park, KONZA – Konza Prairie Research Natural Area and LTER site, WKT – Wah-Kon-Tah Natural Area owned by TNC, MAP = mean annual precipitation, MAT = mean annual temperature.

	SGS Shortgrass Steppe - LTER	ARIK Arikaree – TNC	SV Smokey Valley – TNC	HAYS Ft. Hays State Univ.	WILSON Wilson Lake State Park	KONZA Konza Prairie – LTER	WKT Wah-Kon-Tah - TNC
Latitude	40° 51.99 N	39° 45.02 N	38° 53.11 N	38° 52.44 N	38° 56.33 N	39° 05.48 N	37° 53.52 N
Longitude	104° 41.47 W	102° 28.68 W	100° 57.63 W	99° 23.15 W	98° 40.40 W	96° 34.12 W	93° 58.58 W
Elevation (m)	1,650	1,220	879	610	536	406	287
MAP[1] (mm)	344	462	502	575	650	884	1110
MAT[1] (°C)	9.3	9.7	10.8	11.9	12.3	12.7	13.1
Vegetation type	shortgrass steppe	shortgrass steppe	mixedgrass	mixedgrass	mixedgrass	tallgrass	tallgrass
Soil subgroup	Aridic Argiustoll	Aridic Argiustoll	Typic Argiustoll	Typic Argiustoll	Typic Calciustoll	Udic Argiustoll	Typic Hapludoll

[1] U.S. Dept. of Commerce, U.S. Monthly Climate Normals, 1971-2000

Table 4.2 - Selected soil geochemical data from the climosequence endpoints (SGS and Konza).

Site	SiO_2 (wt %)	Al_2O_3 (wt %)	Ge (mg/g)	Ge/Si (μmol/mol)	Ge/Al molar ratio	Al/Si molar ratio
SGS-A (horizon 1)						
bulk soil	60.9	12.0	1.38	1.9	8.1	0.21
Sand	76.7	9.8	1.27	1.4	9.1	0.15
quartz	*98.5*	*1.0*	0.64	0.54	54.8	0.01
heavy fraction	*42*	*22*	2.82	5.56	9.0	0.62
Silt	74.9	10.5	1.28	1.4	8.6	0.16
Clay	39.1	11.7	1.38	2.9	8.3	0.35
SGS-A (horizon 3)						
bulk soil	59.8	14.3	1.69	2.1	8.3	0.27
Sand	74.8	10.7	1.33	1.5	8.7	0.17
Silt	70.3	12.8	1.43	1.7	7.9	0.21
Clay	44.0	12.2	1.69	3.2	9.7	0.33
SGS-B (horizon 1)						
bulk soil	71.3	10.4	1.36	1.6	9.2	0.17
Sand	77.4	9.7	1.27	1.4	9.2	0.15
quartz	*98.5*	*1.0*	0.91	0.76	64.0	0.01
feldspar-1	*53*	*27*	1.50	2.34	3.9	0.60
feldspar-2	*53*	*27*	1.97	3.08	5.1	0.60
heavy fraction	*42*	*22*	3.30	6.51	10.6	0.62
Silt	74.2	10.2	1.33	1.5	9.2	0.16
Clay	25.8	8.5	0.88	2.8	7.2	0.39
SGS-B (horizon 3)						
bulk soil	69.2	11.1	1.34	1.6	8.5	0.19
Sand	77.8	10.1	1.28	1.4	8.9	0.15
Silt	76.2	10.4	1.32	1.4	8.9	0.16
Clay	30.5	11.0	1.07	2.9	6.8	0.43
SGS-B (horizon 6)						
sand - quartz	*98.5*	*1.0*	0.83	0.69	58.0	0.01
sand - feldspar	*53*	*27*	2.42	3.79	6.3	0.60
sand - heavy fraction	*42*	*22*	3.14	6.18	10.0	0.62
Konza (horizon 1)						
bulk soil	65.2	11.4	1.30	1.7	8.0	0.19
Sand	83.8	5.6	1.05	1.0	13.1	0.08
Silt	83.4	6.9	1.19	1.2	12.2	0.10
Clay	37.3	14.3	1.68	3.7	8.3	0.45
Konza (horizon 3)						
bulk soil	61.6	14.0	1.55	2.1	7.8	0.25
Sand	81.3	7.6	1.10	1.1	10.2	0.11
Silt	82.0	6.9	1.18	1.2	12.0	0.10
Clay	36.2	15.2	1.73	4.0	8.0	0.49
Konza (horizon 6)						
bulk soil	62.0	13.0	1.4	1.9	7.6	0.25
clay	37.0	15.0	1.7	3.8	8.0	0.48
Bignell loess	71.8	10.1	1.26	1.45	8.7	0.17
Peoria loess	68.2	10.0	1.32	1.60	9.2	0.17

Italicized values are estimates based on SEM-EDS spectroscopy and ideal mineral formulas.

Table 4.3 - Ge and Si data of soil water from saturated paste extracts.

Site	Si (µmol/L)	Ge (pmol/L)	Ge/Si (pmol/µmol)
SGS A – 1	907	201	0.22
SGS A – 3	961	232	0.24
SGS A – 6	1121	291	0.26
SGS B – 1	765	482	0.63
SGS B – 3	590	243	0.41
SGS B – 6	789	111	0.14
Arikaree – 1	962	561	0.58
Arikaree – 3	289	131	0.45
Arikaree – 7	733	147	0.20
S.V. – 1	885	834	0.94
S.V. – 3	531	334	0.63
S.V. – 9	892	200	0.22
Hays – 1	581	1283	0.81
Hays – 3	290	172	0.59
Hays – 8	368	153	0.42
Konza – 1	455	347	0.76
Konza – 3	288	145	0.50
Konza – 6	204	66	0.32
WKT – 1	210	396	1.88
WKT - 3	236	206	0.87

Table 4.4 – Leaf Si, plant phytolith Ge, and plant phytolith Ge/Si ratios along the climosequence.

Site	Plant	SiO_2 in leaf (wt %)	Ge in opal (pmol/g)	[1]Ge/Si x 10^{-6}
SGS	*Bouteloua gracilis*	5.6	0.48	0.24
	Bouteloua gracilis	5.8	0.57	0.23
	Bouteloua gracilis	6.8	0.47	0.25
	Bouteloua gracilis	6.2	0.60	0.29
	Buchloe dactyloides	9.7	0.53	0.25
Arikaree	*Sporobolus cryptandus*	5.9	0.43	0.44
	Buchloe dactyloides	8.7	0.41	0.23
S.V.	*Aristada* sp.	11.1	0.84	0.39
	Buchloe dactyloides	8.2	0.54	0.29
Hays	*Poa* sp.	9.0	0.28	0.15
	Schizachyrium scoparium	6.1	0.40	0.20
Wilson	*Schizachyrium scoparium*	4.6	0.50	0.30
Konza	*Andropogon gerardii*	5.1	1.00	0.42
	Koeleria sp.	5.0	0.98	0.44
WKT	*Andropogon gerardii*	2.1	2.90	0.36

[1] Ge/Si units are a molar ratio.

Table 4.5 - Ge and Si data from well, stream, and lake, waters along the climosequence.

Site	Collection date	Lat	Lon	Si (mol/L)	Ge (µmol/L)	Ge/Si (µmol/mol)
SGS[1]	6-Oct-03	40 51.347 N	104 41.181 W	312.7	725	2.32
	20-Nov-03	"	"	354.5	981	2.77
	20-Nov-03	40 52.195 N	104 39.533 W	481.8	n.d.	n.d.
	28-Nov-03	"	"	493.5	1653	3.35
	16-May-04	"	"	482.1	1609.9	3.34
Arikaree[1]	19-Aug-03	39 45.293 N	102 28.448 W	978.7	890.6	0.91
	20-Nov-03	"	"	857.3	377.2	0.44
Arikaree[2]	19-Jun-03	39 45.588 N	102 27.847 W	730.0	153.3	0.21
	19-Aug-03	"	"	947.7	66.3	0.07
	20-Nov-03	"	"	876.4	140.2	0.16
	16-May-04	"	"	704.0	123.6	0.18
S.V.[1]	18-Aug-03	38 53.227 N	100 57.469 W	599.9	725.9	1.21
	17-May-04	"	"	367	297.3	0.81
Hays[1]	16-Aug-03	38 52.423 N	99 23.497 W	452.5	190	0.42
Hays[2]	16-Aug-03	38 54.378 N	99 23.488 W	480.9	226.0	0.47
	19-Nov-03	"	"	388.6	116.6	0.30
	17-May-04	"	"	480	144.6	0.30
Wilson[1]	17-Aug-03	38 55.007 N	98 43.466 W	140.2	96.7	0.69
Wilson[2]	17-Aug-03	38 59.042 N	98 43.372 W	179.2	205	1.14
	17-May-04	"	"	252	214.2	0.85
Wilson lake	18-Jul-03	38 54.028 N	98 39.035 W	199.6	123.8	0.62
	17-Aug-03	"	"	242.4	181.8	0.75
	19-Nov-03	"	"	181.8	100.0	0.55
Konza[1]	5-Apr-03	39 05.67 N	96 34.55 W	215.2	146.3	0.68
	10-May-03	"	"	209.5	125.7	0.60
	19-Jun-03	"	"	209.1	102.5	0.49
	6-Sep-03	"	"	190.8	131.7	0.69
	4-Oct-03	"	"	171.6	130.4	0.76
	9-Nov-03	"	"	198.4	134.9	0.68
Konza[2]	10-May-03	39 05.61 N	96 34.86 W	191.9	42.2	0.22
	19-Jun-03	"	"	161.6	53.3	0.33
	2-Aug-03	"	"	232.6	46.5	0.20
	6-Sep-03	"	"	195.7	41.1	0.21
	4-Oct-03	"	"	202.0	28.3	0.14
	5-Apr-03	39 05.57 N	96 34.34 W	226.6	79.3	0.35
	19-Jun-03	"	"	156	68.6	0.44
	2-Aug-03	"	"	225.6	72.2	0.32
	6-Sep-03	"	"	177.3	53.2	0.30
	9-Nov-03	"	"	174.2	55.7	0.32
WKT[2]	19-Jul-03	37 55.803 N	93 57.239 W	172.7	222.8	1.29

n.d. = not determined, [1] = well water, [2] = stream water

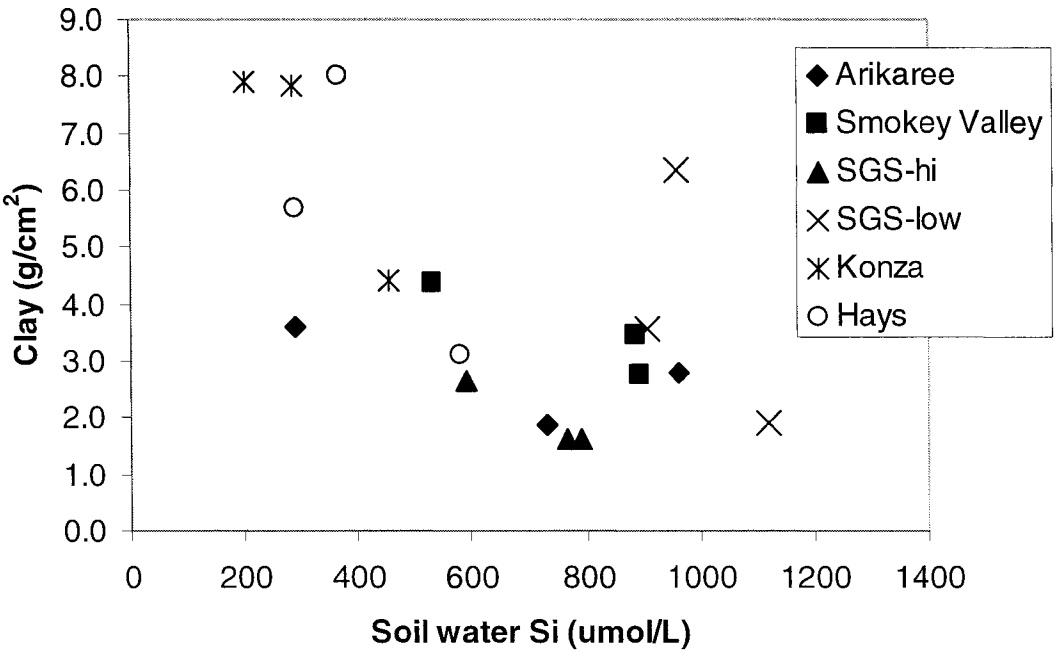

Figure 4.2 - Relationship between clay content and soluble Si across the climosequence, representing the surface, argillic and deepest horizons sampled at each site.
(clay content = -2.9167 ln(soluble Si) + 22.624; $r^2 = 0.444$, $p = 0.002$).

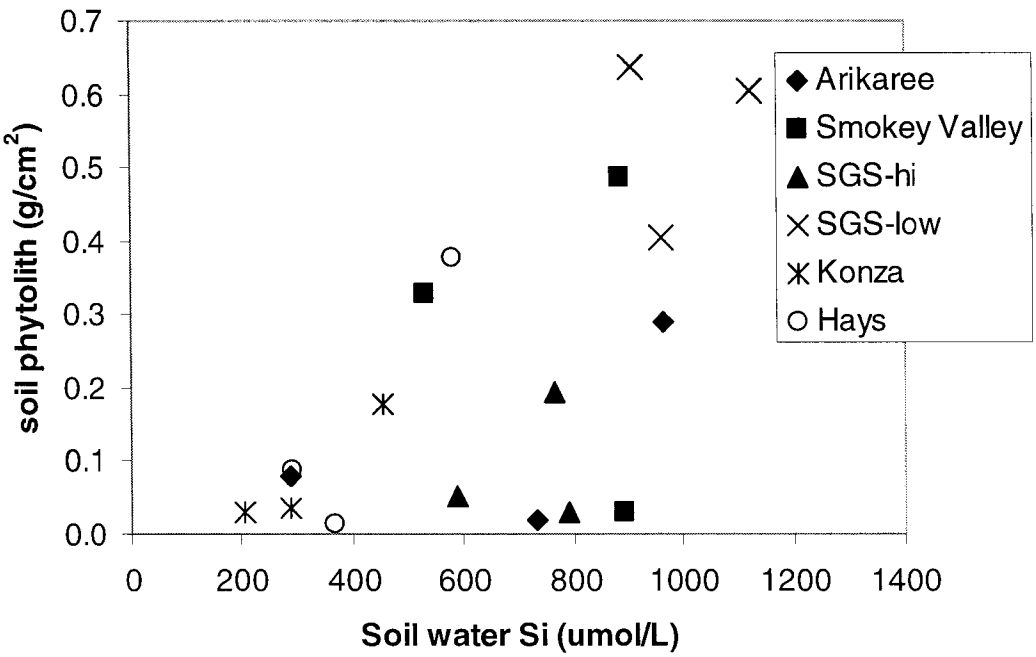

Figure 4.3 - Relationship between soil phytolith content and soluble Si across the climosequence representing the surface, argillic and deepest horizons sampled at each site. (soil phytolith content = 0.0004(soluble Si) – 0.0304; $r^2 = 0.315$, $p = 0.006$).

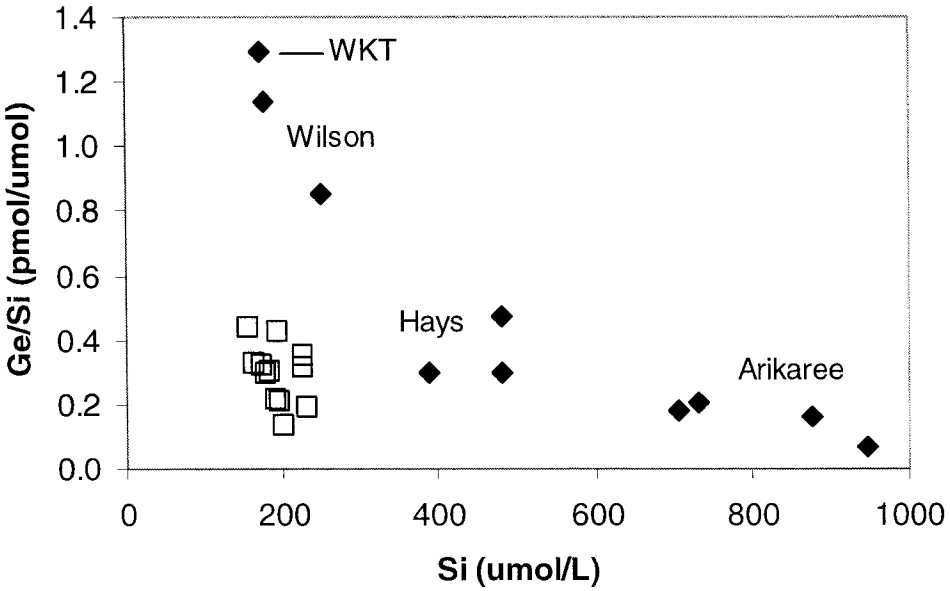

Figure 4.4 - Ge/Si values vs. Si concentrations for stream waters along the climosequence, site names and data taken from Table 5. Open squares are from Konza. Ge/Si units of pmol/umol are comparable to other Ge/Si values in this study, as all the Ge/Si values are10^{-6} molar ratios. (Ge/Si = -0.665 ln(Si) +4.55; $r^2 = 0.897$, $p < 0.0001$; excludes Konza values).

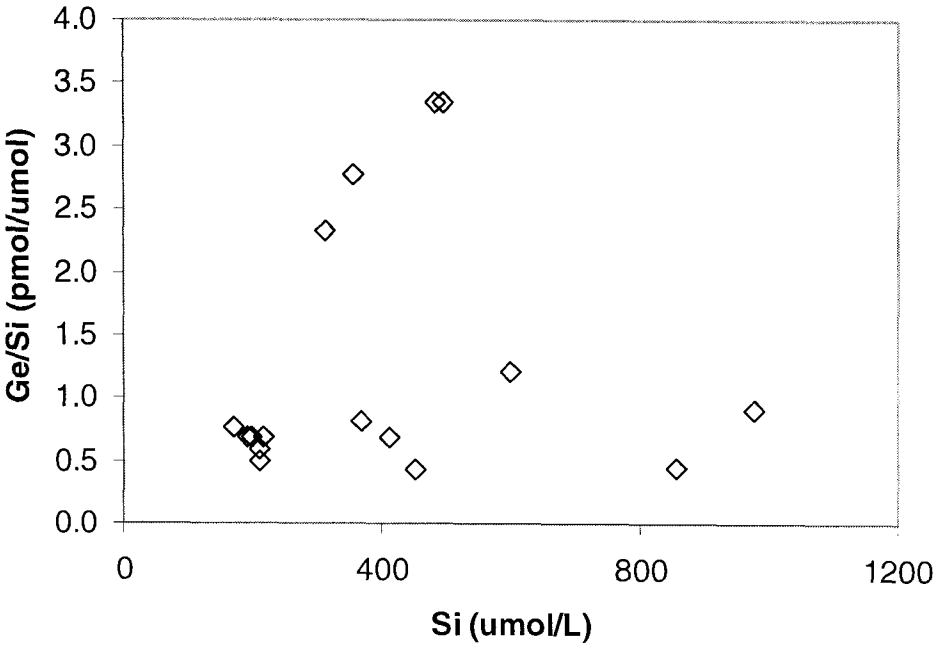

Figure 4.5 - Groundwater Ge/Si values across the climosequence, generated from values located in Table 4.5.

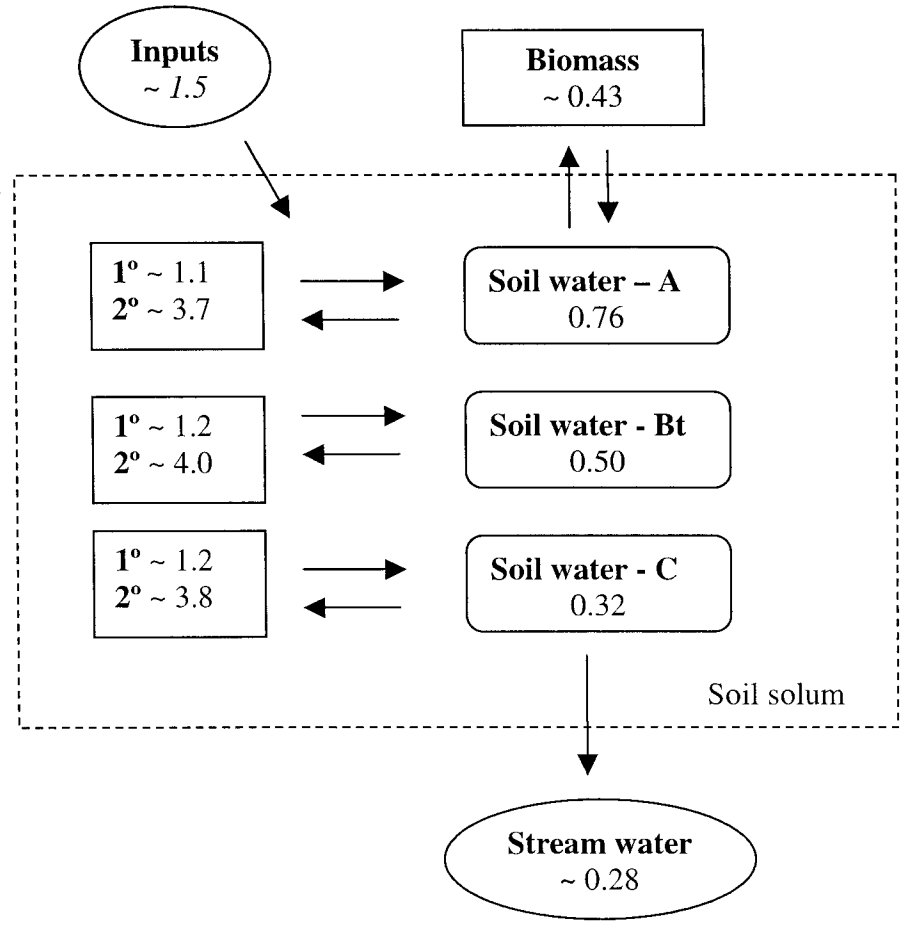

Figure 4.6 - Model of Ge/Si biogeochemistry for the Konza tallgrass system, italicized values are estimates. **1°** - represents the average value of the primary minerals for a given horizon, **2°** - represents the average values of the secondary minerals for a given horizon.

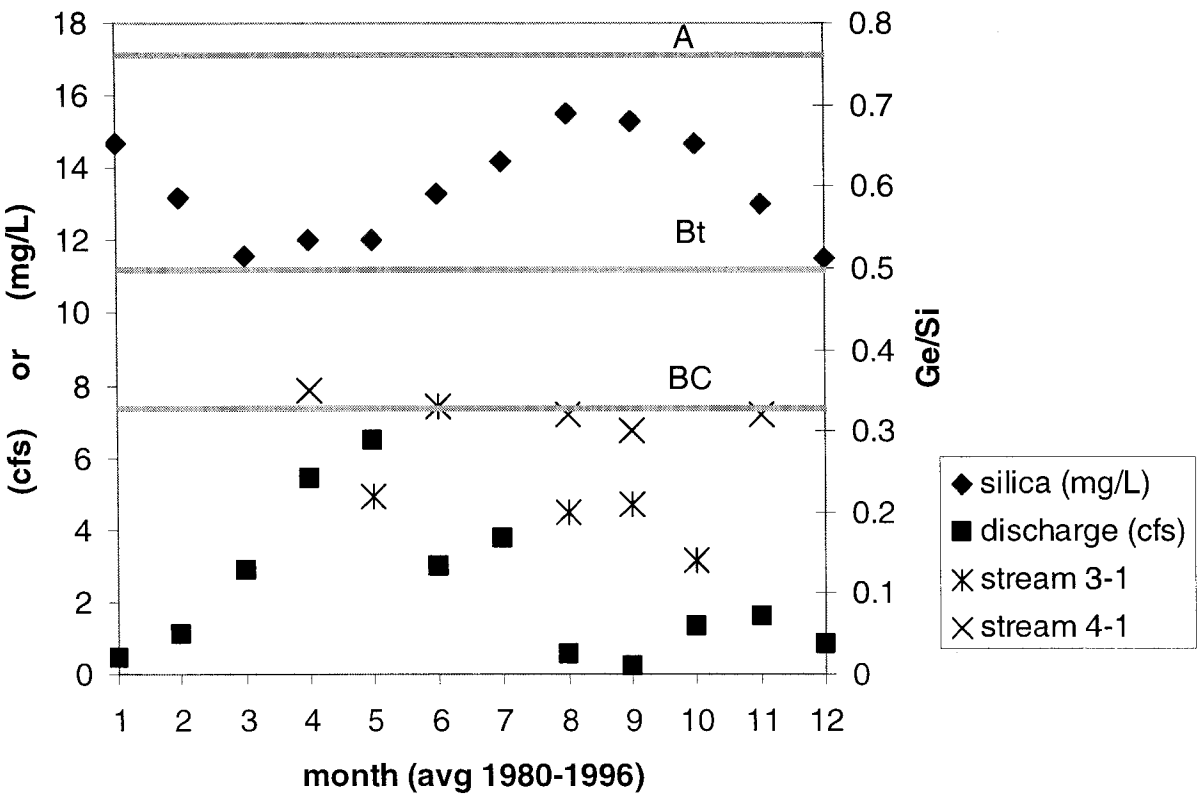

Figure 4.7 - Monthly discharge and stream water dissolved silica values (averaged by month for the years 190 through 1986) for Kings Creek, Konza tallgrass system. Superimposed on this figure are the Ge/Si values of the saturated paste soil water extracts for the A, Bt, and BC horizons (represented by the solid bars), and the Ge/Si stream water values for different reaches of Kings Creek (3-1 is upstream of 4-1).

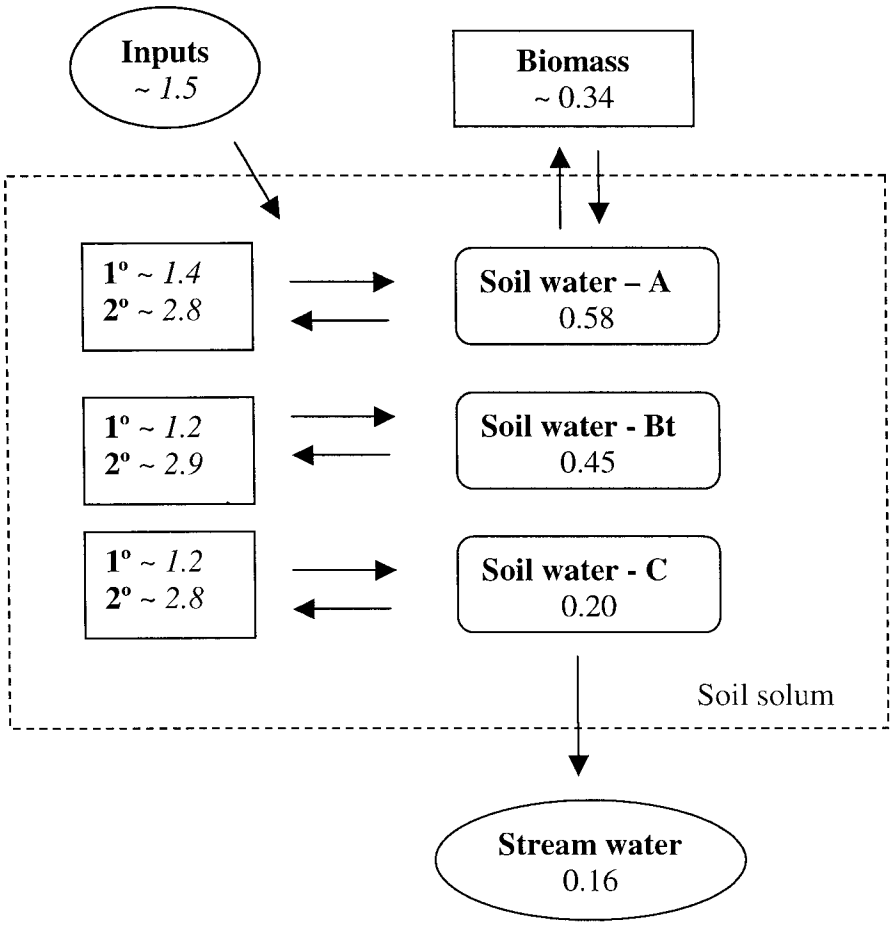

Figure 4.8 - Model of Ge/Si biogeochemistry for the Arikaree shortgrass system, italicized values are estimates. **1°** - represents the average value of the primary minerals for a given horizon, **2°** - represents the average values of the secondary minerals for a given horizon.

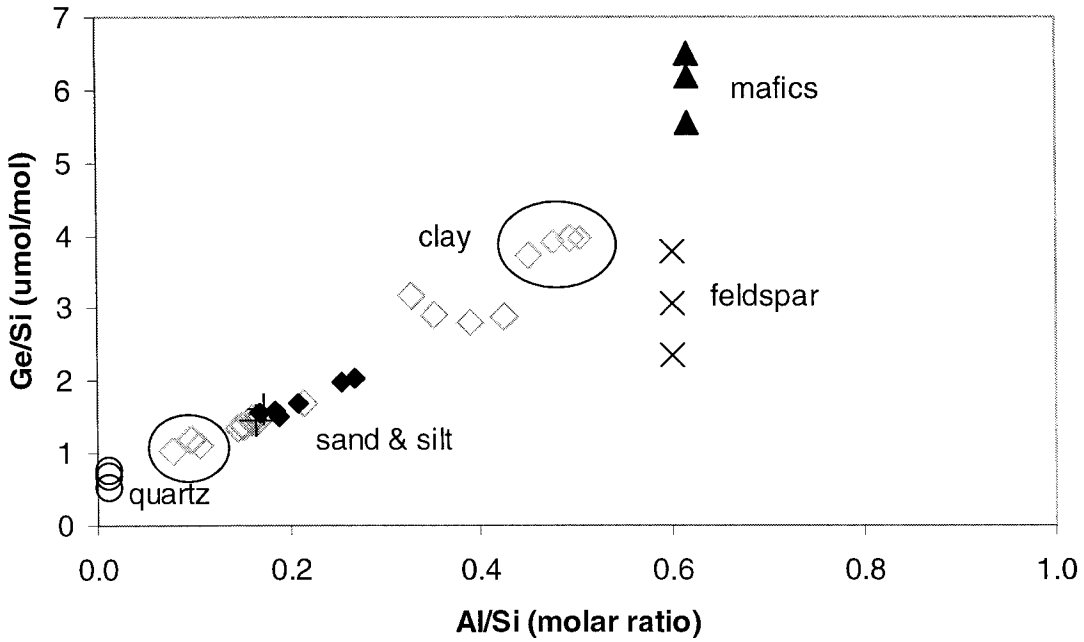

Figure 4.9 - Ge/Si vs. Al/Si for SGS (shortgrass) and Konza (tallgrass). Circled groups represent sand, silt and clay size fractions from Konza. Mineral separates (quartz, feldspar and mafics are from SGS). '+' symbols represent Bignell and Peoria loess.

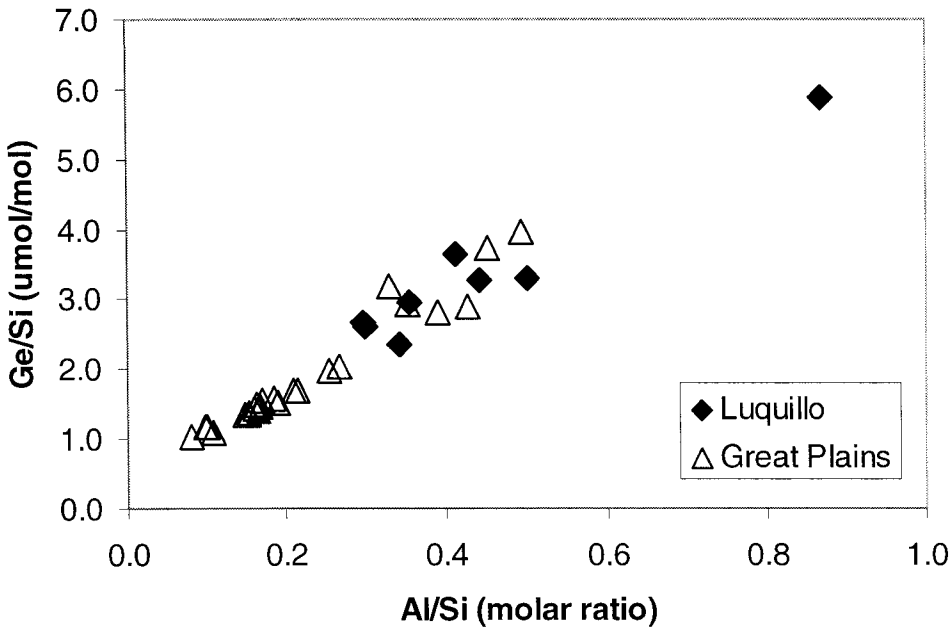

Figure 4.10 - Weathering comparison (in terms of geochemical ratios) between a tropical forest (Luquillo, Puerto Rico – data from Kurtz et al. 2002) and temperate grasslands (Great Plains of North America). Points represent sand, silt, and clay fractions for the Great Plains and bulk soil, saprolite and kaolinite for Luquillo.

References

Bettis E.A., Muhs D.R., Roberts H.M. and Wintle A.G. 2003. Last glacial loess in the conterminous USA. Quaternary Sci. Rev. 22:1907-1946.

Bernstein L.R. 1985. Germanium geochemistry and mineralogy. Geochim. Cosmochim. Acta 49:2409-2422.

Bernstein L.R. and Waychunas G.A. 1987. Germanium crystal-chemistry in hematite and goethite from the Apex mine, Utah, and some new data on germanium in aqueous-solution and in stottite. Geochim. Cosmochim. Acta 51:623-630.

Blecker S.W., Yonker C.M., Olson, C.G., and Kelly E.F. 1997. Paleopedologic and geomorphic evidence for Holocene climate variation, shortgrass steppe, Colorado, USA. Geoderma 76:113-130.

Chillrud S.N., Pedrozo F.L., Temporetti P.F., Planas H.F., and Froelich P.N. 1994. Chemical weathering of phosphate and germanium in glacial meltwater streams: Effects of subglacial pyrite oxidation. Limnol. Oceanogr. 39:1130-1140.

Conley D.J. 2002. Terrestrial ecosystems and the global biogeochemical silica cycle. Global Biogeochemical Cycles 16:681-688.

Derry L.A, Kurtz A.C., Ziegler K. and Chadwick, O.A. 2005. Biological control of terrestrial silica cycling and export fluxes to watersheds. Nature 433:728-730.

Filippelli G.M., Carnahan J.W., Derry D.A., and Kurtz A. 2000. Terrestrial paleorecords of Ge/Si cycling derived from lake diatoms. Chemical Geology 168:9-26.

Froelich P.N. and Andreae M.O. 1981. The marine geochemistry of germanium: Ekasilicon. Science 213:205-207.

Froelich P.N., Hambrick G.A., Andreae M.O., and Mortlock R.A. 1985. The geochemistry of inorganic germanium in natural waters. J. Geophysical Res. 90:1133-1141.

Froelich P.N., Blanc V., Mortlock R.A., Chillrud S.N., Dunstan W., Udomkit A., and Peng T.H. 1992. River fluxes of dissolved silica to the ocean were higher during glacials: Ge/Si in diatoms, rivers and oceans. Paleoceanography 7:739-767.

Galy A., France-Lanord C. and Derry L.A. 1999. The strontium isotopic budget of Himalayan Rivers in Nepal and Bangladesh. Geochim. Cosmochim. Acta 63:1905-1925.

Gibbs M.T., and Kump L.R. 1994. Global chemical erosion during the last glacial maximum and the present: Sensitivity to changes in lithology and hydrology. Paleoceanography 9:529-543.

Hossner L.R. 1996. Dissolution for total elemental analysis. *In* J.M. Bartels (ed.) Methods of soil analysis. Part 3. Chemical Methods. SSSA, Madison, WI, p. 49-64.

Hammond D.E., McManus J., Berelson W.M., Meredith C., Klinkhammer G.P., and Coale K.H. 2000. Diagenetic fractionation of Ge and Si in reducing sediments: The missing Ge sink and a possible mechanism to cause glacial/interglacial variations in oceanic Ge/Si. Geochim. Cosmochim. Acta 64:2453-2465.

Jenny, H. 1941. Factors of soil formation; a system of quantitative pedology. McGraw-Hill, New York. 281p.

Kelly, E.F. 1990. Methods for extracting opal phytoliths from soil and plant material. Department of Agronomy. Colorado State University. Fort Collins, Colorado.

King S.L., Froelich P.N., and Jahnke R.A. 2000. Early diagenesis of germanium in sediments of the Antarctic South Atlantic: In search of the missing Ge sink. Geochim. Cosmochim. Acta 64:1375-1390.

Kurtz A.C., Derry L.A., and Chadwick, O.A. 2002. Germanium-silicon fractionation in the weathering environment. Geochim. Cosmochim. Acta 66:1525-1537.

Lajtha K., Jarrell W.M., Johnson D.W. and Sollins P. 1999. Collection of soil solution. *In* Robertson G.P., Coleman D.C., Bledsoe C. and Sollins P. (eds.) Standard Soil Methods for Long-Term Ecological research Oxford, New York. pp. 166-182.

Leetham J.W. and Milchunas D.G. 1985. The composition and distribution of soil microarthropods in the shortgrass steppe in relation to soil-water, root biomass, and grazing by cattle. Pedobiologia 28:311-325.

Likens G.E. and Bormann F.H. 1995. Biogeochemistry of a forested ecosystem. 2nd ed. Springer-Verlag, New York. 159 p.

Lucas Y., Luizao F.J., Chauvel A., Rouiller J., and Nahon D. 1993. The relationship between the biological activity of the rain forest and the mineral composition of the soils. Science 260:521-523.

Macpherson G.L. 1996. Hydrogeology of thin limestones: The Konza Prairie Long-Term Ecological Research Site, Northeastern Kansas. J. Hydrology 186:191-228.

Macpherson G.L. and Sophocleous M. 2004. Fast ground-water mixing and basal recharge in an unconfined, alluvial aquifer, Konza LTER Site, Northeastern Kansas. J. Hydrology 286:271-299.

Mason J.A. 2001. Transport direction of Peoria loess in Nebraska and Implications for loess sources on the central Great Plains. Quaternary Res. 56:79-86.

Mason J.A., Jacobs P.M., Hanson P.R., Miao X., and Goble R.J. 2003. Sources and paleoclimatic significance of Holocene Bignell loess, central Great Plains, USA. Quaternary Res. 60:330-339.

McCulley R.F. and Burke I.C. 2004. Microbial community composition across the Great Plains: landscape versus regional variability. Soil Sci. Soc. Am. J. 68:106-115.

Muhs D.R. and Zarate M. 2001. Late Quaternary eolian records of the Americas and their paleoclimatic significance. *In* Markgraf V. (ed.) Interhemispheric climate linkages. Academic Press, San Diego. pp.183-216.

Murnane R.J. and Stallard R.F. 1990. Germanium and silicon in rivers of the Orinoco drainage basin. Nature 344:749-752.

Moore D.M. and Reynolds Jr. R.C. 1989. X-Ray diffraction and the identification and analysis of clay minerals. Oxford University Press, New York. 332 p.

Mortlock R.A. and Froelich P.N. 1987. Continental weathering of germanium: Ge/Si in the global river discharge. Geochim. Cosmochim. Acta 51:2075-2082.

Mortlock R.A. and Froelich P.N. 1989. A simple method for the rapid determination of biogenic opal in pelagic marine sediments. Deep-Sea Res. 36:1415-1426.

Mortlock R.A., Charles C.D., Froelich P.N., Zibello M.A., Saltzman J., Hays J.D., and Burckle L.H. 1991. Evidence of lower productivity in the Antarctic Ocean during the last glaciation. Nature 351:220-223.

Nelson D., Treguer M.P., Brzezinski M.A., Leynaert A., and Queguiner B. 1995. Production and dissolution of biogenic silica in the ocean: Revised global estimates, comparison with regional data and relationship to biogenic sedimentation. Global Biogeochem. Cycles 9:359-372.

Oviatt C.G. 1998. Geomorphology of Konza Prairie. *In* Knapp A.K. et al. (eds.) Grassland dynamics: Long-term ecological research in tallgrass prairie. Oxford University Press, New York. pp. 53-47.

Parr, J.F. 2002. A comparison of heavy liquid floatation and microwave digestion \ techniques for the extraction of fossil phytoliths from sediments. Review of Palaeobotany and Palynology 120:315-336.

Parr, J.F., Lentfer, C.J., and Boyd, W.E. 2001. A comparative analysis of wet and dry ashing techniques for the extraction of phytoliths from plant material. Journal of Archaeological Science 28:875-886.

Piperno, D.R. 1988. Phytolith analysis: An archaeological and geological perspective. Academic Press Inc., New York. 280 pp.

Pokrovski G.S., and Schott J. 1998. Experimental study of the complexation of silicon and germanium with aqueous organic species: Implications for germanium and silicon transport and Ge/Si ratio in natural waters. Geochim. Cosmochim. Acta 62: 3413-3428.

Raymo M.E. and Ruddiman W.F. 1992. Tectonic forcing of late Cenozoic climate. Nature 359:117-122.

Roberts H.M., Muhs D.R., Wintle A.G., Duller G.A.T., and Bettis III E.A. 2003. Unprecedented last-glacial mass accumulation rates determined by luminescence dating of loess from western Nebraska. Quaternary Res. 59:411-419.

Schmitt A.-D., Chabaux F., and Stille P. 2003. The calcium riverine and hydrothermal isotopic fluxes and the oceanic calcium mass balance. Earth and Planetary Science Letters 6731:1-16.

Schulz M.S. and White A.F. 1999. Chemical weathering in a tropical watershed, Luquillo Mountains, Puerto Rico III: Quartz dissolution rates. Geochim. Cosmochim. Acta 63:337-350.

Soil Survey Staff. 1992. Soil Survey Manual, USDA Handbook 18, Chapter 4. US Government Printing Office, Washington, D.C.

Shemesh A., Mortlock R.A., and Froelich P.N. 1989. Late Cenozoic Ge/Si records of marine biogenic opal: Implications for variations of riverine fluxes to the ocean. Paleoceanography 4:221-234.

Stallard R.F. 1995. Tectonic, environmental, and human aspects of weathering and erosion: A global review using steady-state perspective. Annual Review of Earth and Planetary Science 23:11-39.

U.S. Dept. of Commerce, National Oceanic and Atmospheric Administration, National Climatic Data Center. 2002. U.S. Monthly climate normals 1971-2000. Asheville, N.C. electronic resource.

Wittman R.A. and Hormann P.K. 1976. Germanium. *In* Wedepohl K.H. (ed.) Handbook of geochemistry. Springer-Verlag, New York. vol 2. pp.32-A-1 through 32-O-9.

Chapter V: SUMMARY AND CONCLUSIONS

Silica mass balance analysis along the grassland climosequence in this study has shown that biogenic Si cycling, though a small portion of the overall Si cycle can be an important pathway of silica flux through grassland ecosystems. Notable trends in plant uptake and storage were observed that are likely due primarily to climatic differences along the gradient. In the drier, less intensely weathered shortgrass systems, higher plant Si contents, slower biogenic cycling and larger soil biogenic Si pools dominate. Conversely, the wetter, more intensely weathered tallgrass systems realize lower plant Si contents, faster biogenic Si cycling and smaller biogenic silica pools. Biogenic cycling of silica through tallgrass ecosystems can approach levels seen in forested ecosystems, which tend to have lower plant silica contents and greater storage in biomass. In both grasslands and forests, biogenic Si cycling tends to have a positive impact on mineral weathering, as the release of Si through phytolith dissolution on an annual basis is not sufficient to meet annual uptake requirements. The omission of plant Si cycling appears to underestimate mineral dissolution (in terms of Si) compared to simple input-output estimates in both grassland and forest ecosystems. Though likely having a positive impact on primary mineral dissolution, the quantitative role of secondary clay formation in these ecosystems remains an unknown variable. More precise measurement of eolian input would also improve the accuracy of the overall estimation of Si flux.

Study of Ge/Si ratios in grassland plants, as demonstrated in several greenhouse experiments, provides more conclusive evidence of the fractionation by plants against Ge, which has thus far only been deduced in the field (Chapter 4 and Derry et al. 2005). Though the actual cause of the fractionation was not determined, several hypotheses were proposed, including differences in reactivity and speciation between Si and Ge, Ge toxicity to plants, and kinetically driven fractionation resulting from differences in molecular weight between Ge and Si. Further examination of Ge fractionation by a greater variety of species under different conditions could further refine the magnitude, direction and variability of biologic Ge fractionation.

Ge/Si signatures of ecosystem pools were used to examine the link between terrestrial and aquatic Si, specifically to determine the importance of plant-mediated Si. Overlap in Ge/Si values among the major pools and the complex hydrology associated with these systems, confounded the utility of this tool in determining stream Si provenance in the present study. Major differences in state factors can result in similar Ge fractionation pathways, as evidenced by the similarity in the Ge/Si of the mineral component of all sites in this study (namely Ge conservation in secondary clays) and the results found by Kurtz et al. (2002) in Puerto Rican diorite. However, Kurtz et al. (2002) in Hawaiian basalt and Filippelli et al. (2000) in Sierra Nevadan gneiss and granite demonstrated that Ge fractionation does not behave the same in all ecosystems, and must be used with caution.

Further Considerations

This research prompted thought into various directions of future study. The spatially extensive nature of this study was designed to provide an initial look at a number of biogeochemical Si processes in a variety of grassland ecosystems. Given the hydrogeological complexities associated with these systems however, my extensive survey did not provide the same degree of clarity as that found in more intensely weathered and better constrained tropical systems studied by Kurtz et al. (2002) and Derry et al. (2005). Along with the hydrogeological complexities, overlap in Ge/Si ratios of the major ecosystem pools confounded the link between terrestrial and aquatic Si as found by Derry et al. (2005) in Hawaiian watersheds. Additional approaches, such as that utilized by Garrels and Mackenzie (1967) for example, where knowledge of parent material, stream water chemistry, and major weathering pathways, may help clarify terrestrial and aquatic linkages on watershed scales. Regardless, greater knowledge of stream Si provenance is necessary to better interpret stream water Ge/Si values and the input of plant-mediated Si.

This study was conducted in relatively undisturbed natural grassland systems, however the vast majority of grasslands in the Great Plains have been converted to agriculture, primarily wheat and corn. As both of these plants accumulate Si in amounts similar to those of other graminoids (Piperno 1998), paired studies of natural and agroecosystems could provide further insight into the importance of biogenic Si cycling. As agricultural plants are typically removed from the ecosystem, disruption of this portion of biogeochemical Si could increase the biogenic impact on soil mineral weathering.

Further, expansion of this type of study to other grassland/savanna systems (which encompass roughly 40% of the earth's land surface) would advance the knowledge of biogeochemical interactions in these ecosystems.

Finally, Conley (2002) mentioned the potential significance of anthropogenic disruption (specifically dams) of terrestrial Si flow to marine systems. Though not presented, analysis of public USGS stream data showed that Si concentration downstream of a dam in central Kansas was significantly lower than the upstream Si concentration. Occurrence of this trend in other ecosystems and more detailed study of sedimentation, Si uptake by lake diatoms and other mechanism in these systems could shed more light on the importance of this process in both grasslands and other ecosystems.

References

Conley D.L. 2002. Terrestrial ecosystems and the global biogeochemical silica cycle. Global Biogeochemical Cycles 16(4):68-1 to 68-8.

Derry L.A, Kurtz A.C., Ziegler K. and Chadwick, O.A. 2005. Biological control of terrestrial silica cycling and export fluxes to watersheds. Nature 433:728-730.

Filippelli G.M., Carnahan J.W., Derry D.A., and Kurtz A. 2000. Terrestrial paleorecords of Ge/Si cycling derived from lake diatoms. Chemical Geology 168:9-26.

Garrels R.M. and Mackenzie F.T. 1967. Origin of the chemical compositions of some springs and lakes. *In* Stumm W. (ed). Equilibrium concepts in natural water systems. Am. Chem. Soc. Adv. Chem. Ser. 76:222-242.

Kurtz A.C., Derry L.A., and Chadwick, O.A. 2002. Germanium-silicon fractionation in the weathering environment. Geochim. Cosmochim. Acta 66:1525-1537.

Piperno D.R. 1988. Phytolith analysis: An archaeological and geological perspective. Academic Press Inc., New York. 280 pp.

APPENDIX I

Soil Pedon Description

Location: **SGS A – lower site** (shortgrass)

Date: 8-6-03

Described by: S. Blecker

Coordinates: 40° 51.989 N, 104° 41.467 W

Elevation: 1650 m

Geomorphic Surface: terrace, 1% slope

Parent Material: loess/alluvium

Depth (cm)	Horizon	Color (Moist/Dry)	Texture	Clay (%)	Gravel (%)	Structure	Effervescence	pH
0-7	A	10YR 3/3 10YR 5/2	cl	31	0	2 m gr	eo	5.9
7-25	Bt	10YR 4/3 10YR 5.5/3	cl	36	0	2 m sbk	eo	6.3
25-38	Btk	10YR 5/3 10YR 5/3.5	c	50	0	2 m & cos sbk	e	7.0
38-65	BCk1	10YR 6/3 10YR 8/2.5	sic	42	5	2 m & cos sbk	es	7.9
65-90	BCk2	10YR 6/3 10YR 8/2.5	sic	40	5	1 m sbk	es+	8.2
90-130+	2BCk3	10YR 6/4 10YR 8/2.5	sil	14	0	sg	es+	8.4

Note: eo – none, e – slight, es – strong, ev – violent

Soil Pedon Description

Location: **SGS B – upper site** (shortgrass)

Date: 8-6-03

Described by: S. Blecker

Coordinates: 40° 51.936 N, 104° 40.801 W

Elevation: 1660m

Geomorphic Surface: footslope, 6% slope

Parent Material: loess/alluvium/colluvium

Depth (cm)	Horizon	Color (Moist/Dry)	Texture	Clay (%)	Gravel (%)	Structure	Effervescence	pH
0-9	A	10YR 3/3 10YR 5/3	sil	10	<5	2 cos gr	eo	5.6
9-23	Bt	10YR 4/3 10YR 5/3	sicl	13	10	2 m sbk	eo	6.5
23-42	Bt2	10YR 4/3.5 10YR 5/3.5	gr sicl	16	15	2 m & cos sbk	eo	7.0
42-63	Bk	10YR 4/4 10YR 6/3	gr sicl	13	15	1 f sbk	e	7.3
63-90	BCk	10YR 6/3 10YR 7/3	sicl	15	5	1 m sbk	es	7.7
90-130+	C	10YR 5/3.5 10YR 6/3	sicl	9	5	sg	es	7.9

Soil Pedon Description

Location: **Arikaree** (shortgrass)

Date: 8-19-03

Described by: S. Blecker

Coordinates: 39° 45.015 N, 102° 28.676 W

Elevation: 1217 m

Geomorphic Surface: terrace, 4% slope

Parent Material: loess/sandstone

Depth (cm)	Horizon	Color (Moist/Dry)	Texture	Clay (%)	Gravel (%)	Structure	Effervescence	pH
0-9	A	10YR 3/2 10YR 4/2	sl	13	0	1 cos gr	eo	5.7
9-22	BAt or Bt1	10YR 3/3 10YR 4/3	scl	20	0	2 m sbk & abk	eo	6.4
22-51	Bt or Bt2	10YR 3/3 10YR 4/3	scl	20	0	2 cos pr	eo	6.7
51-72	Btk	10YR 4/3 10YR 6/3	scl	18	0	1 m sbk	es-	7.8
72-91	BCk	10YR 5/3 10YR 7/3	scl	17	0	1 m sbk	es	8.0
91-184	Ck1	10YR 6/4 10YR 7/4	sl	7	0	sg	es-	8.4
184-221+	Ck2	10YR 6/4 10YR 7/4	ls	6	0	sg	e	8.4

Soil Pedon Description

Location: **Smokey Valley** (mixedgrass)

Date: 8-18-03

Described by: S. Blecker

Coordinates: 38° 53.106 N, 100° 57.633 W

Elevation: 879 m

Geomorphic Surface: terrace, 2% slope

Parent Material: loess/sandstone

Depth (cm)	Horizon	Color (Moist/Dry)	Texture	Clay (%)	Gravel (%)	Structure	Effervescence	pH
0-8	A	10YR 3/2 10YR 4/2	sil	28	0	2 cos gr	eo	5.7
8-21	ABt	10YR 3/.5 10YR 4.5/2	sicl	32	0	2 msbk	eo	6.3
21-32	Bt	10YR 4/2 10YR 5/2	sicl	32	0	1 cos pr	eo	6.4
32-62	Btk1	10YR 5/3 10YR 6&7/3	sicl	33	0	1 cos pr	e	7.5
62-81	BCk1	10YR 6/3 10YR 7/3	sicl	28	0	1 cos pr	es	7.7
81-103	BCk2	10YR 6/3 10YR 7/3	sicl	26	0	massive	es	7.7
103-170	Ck	10YR 5.5/3 10YR 7/3	sil	22	0	sg	es-	7.9
170-215	Ck2	10YR 5.5/3 10YR 7/3	sil	24	0	sg	es-	8.0
215-266+	Ck3	10YR 5.5/3 10YR 7/3	sil	24	0	sg	es-	8.0

Soil Pedon Description

Location: **Hays** (mixedgrass) Date: 8-16-03 Described by: S. Blecker

Coordinates: 38° 52.439 N, 99° 23.151 W Elevation: 610 m

Geomorphic Surface: terrace, 1% slope Parent Material: loess/limestone/shale

Depth (cm)	Horizon	Color (Moist/Dry)	Texture	Clay (%)	Gravel (%)	Structure	Effervescence	pH
0-8	A	10YR 3/2 10YR 5/2	sil	22	0	1 m gr	eo	5.9
8-28	ABt	10YR 3/3 10YR 4.5/2	sicl	32	0	1 f sbk	eo	5.7
28-46	Bt	10YR 4.5/3 10YR 5/3	sicl	34	0	2 m sbk	eo	6.7
46-71	Btk1	10YR 5/4 10YR 6/4	sicl	32	0	1 m sbk	e	8.1
71-101	Btk2	10YR 5/4 10YR 6/4	sicl	36	0	1 cos sbk	e	8.2
101-161	Btk3	10YR 4/4 10YR 5/4	sicl	38	0	1 cos sbk	es-	7.8
161-186	Bk	10YR 4/3 10YR 5/4	cl	31	0	1 cos sbk	es-	7.9
186-198+	BCk	7.5YR 7/4 7.5YR 7/3	sic	57	0	m	es+	8.0

Soil Pedon Description

Location: **Wilson** (mixed/tallgrass) Date: 8-17-03 Described by: S. Blecker

Coordinates: 38° 56.33 N 98° 40.40 W Elevation: 536 m

Geomorphic Surface: terrace/upland, 2% slope Parent Material: loess/limestone/sandstone

Depth (cm)	Horizon	Color (Moist/Dry)	Texture	Clay (%)	Gravel (%)	Structure	Effervescence	pH
1-10	A	10YR 3/2 10YR 5/2	sil	34	5	1cos gr	e+	6.6
10-21	Btk	10YR 4/2 10YR 5/2	sicl	41	5	2 f sbk	es	6.9
21-42	Bk	10YR 4.5/2 10YR 5&6/2	sic	47	10	1 msbk	es+	7.1
42-53	BCk	10YR 5/3 10YR 7/2	gr sic	57	15	1 msbk	ev	7.1
53-75	Cr	10YR 7/4&5 10YR 8/2.5		57	n/a	massive	ev	7.3
75+	R							

Soil Pedon Description

Location: **Konza** (tallgrass)

Date: 8-17-03

Described by: S. Blecker

Coordinates: 39° 05.478 N, 96° 34.122 W

Elevation: 406 m

Geomorphic Surface: terrace/upland, 2% slope

Parent Material: loess/limestone/shale

Depth (cm)	Horizon	Color (Moist/Dry)	Texture	Clay (%)	Gravel (%)	Structure	Effervescence	pH
0-16	A	10YR 3/2 10YR 4/2	sicl	31	0	2 m gr	eo	5.3
16-29	ABt	10YR 3/3.5 10YR 4/3	sic	49	0	1 m sbk	eo	4.9
29-39	Bt1	10YR 4/4 10YR5/4	sic	52	0	2 m sbk	eo	5.1
39-52	Bt2	10YR 4/4 10YR 5/4	sic	48	0	2 m sbk	eo	5.1
52-60	Btg1	10YR 4/4 10YR 5/4	sic	48	10	1 m sbk	eo	5.2
60-81	Btg2	7.5YR 4/4 7.5YR 5/4	gr sic	48	25	1 cos sbk	eo	5.4
81+	R							

Soil Pedon Description

Location: **Wah Kon Tah** (tallgrass)

Date: 7-19-03

Described by: S. Blecker

Coordinates: 37° 53.52 N, 93° 58.58 W

Elevation: 287m

Geomorphic Surface: terrace/upland

Parent Material: loess (?)/sandstone

Depth (cm)	Horizon	Color (Moist/Dry)	Texture	Clay (%)	Gravel (%)	Structure	Effervescence	pH
0-10	A	7.5YR 3/2 7.5YR 4/3	sl	14	<5	2 m gr	eo	5.1
10-20	AB	7.5YR 3/2 7.5YR 4/3	scl	19	<5	2 f sbk	eo	4.3
20-41	Bw or Bt	7.5YR 3/3 7.5 YR 4/4	gr scl	20	15	1 f sbk	eo	4.3
41+	R							